Sustainable Iron-catalyzed direct imine formation by acceptorless dehydrogenative coupling of alcohols with amines

Journal:	*Green Chemistry*
Manuscript ID	GC-COM-02-2016-000565.R2
Article Type:	Communication
Date Submitted by the Author:	18-Apr-2016
Complete List of Authors:	Jaiswal, Garima; CSIR-National Chemical Laboratory, Catalysis Division Landge, Vinod; CSIR-National Chemical Laboratory, Catalysis Division Jagadeesan, Dinesh; CSIR - National Chemical Laboratory, Physical Chemistry and Materials Division Ekambaram, Balaraman; CSIR-National Chemical Laboratory, Catalysis Division

Journal Name

COMMUNICATION

Sustainable Iron-catalyzed direct imine formation by acceptorless dehydrogenative coupling of alcohols with amines†

Received 00th January 20xx,
Accepted 00th January 20xx

DOI: 10.1039/x0xx00000x

www.rsc.org/

Garima Jaiswal,[a,c] Vinod G. Landge, [a,c] Dinesh Jagadeesan,*[b,c] and Ekambaram Balaraman*[a,c]

Acceptorless Dehydrogenative Coupling (ADC) of alcohols with amines is reported using a heterogeneous Fe-catalyst. The reaction operates under mild conditions with the liberation of dihydrogen and water as the byproducts. The developed ADC strategy is simple, efficient, exhibits wide functional group tolerances and can be scaled up. The present catalytic approach possesses a dual role; acting as a catalyst as well as can be magnetically separable. The sustainable reuse of a heterogeneous iron catalyst is also shown.

Introduction

Imine is an exceptionally versatile functional group and is ubiquitous in pharmaceuticals, biologically active heterocycles, and natural products.[1] Traditionally, imine formation was achieved by the condensation reaction of amines with highly reactive carbonyl compounds and often required dehydrating agents as well as Lewis acid catalysts.[2-3] However, direct formation of imine with easily accessible feedstock chemicals is very attractive and highly desirable in organic synthesis.[4] In this context, various methods for imine synthesis have been studied based on oxidative dehydrogenation of amines,[5-6] and oxidative dehydrogenative coupling of alcohols with amines using various oxidants such as dioxygen, TEMPO, quinine, and iodosylbenzene.[7-8] However, several drawbacks remain, for example, the intrinsic self-coupling properties of the substrates, the formation of other side products such as nitrile, amide, azo and a related compound, and the need of stoichiometric amount of oxidants.[6] Although the use of molecular oxygen as a mild oxidant is an attractive strategy, oxidative dehydrogenative coupling accomplished with O_2 might be problematic at the higher pressures (need of special high-pressure equipment) that are usually used on large scales to increase the effective concentration of the oxidant. Thus, the development of an efficient strategy for selective construction of imine scaffolds under the *oxidant-free* condition is a key motivation in the contemporary science.

Recently a direct coupling of alcohols with amines by acceptorless dehydrogenative strategy has been developed as an efficient protocol to construct imine bond (C=N) with the liberation of molecular hydrogen and water as the byproducts, which is a greener and more practical method. Despite several efficient homogeneous catalysts are well-developed for acceptorless dehydrogenation reaction under *oxidant-free* conditions,[9] the major disadvantages such as the use of noble metals, extensive ligand synthesis, sensitivity, handling under the practical conditions, poor recovery and competing *hydrogen atom transfer reaction*[10] (leads to a mixture of amine and imine products) remain unaddressed. However, in a very recent report from Feringa and co-workers, imine was reported as the potential intermediate in the homogeneous Fe-catalyzed direct alkylation of amines with alcohols *via* hydrogen atom transfer reaction.[11] Indeed, heterogeneous catalysts with such activity for the straightforward synthesis of an imine by *oxidant-free*, acceptorless dehydrogenative coupling of alcohols with amines are rare and very limited. Very recently, Pt nanoparticles loaded on TiO_2 was shown to promote direct synthesis of imines from alcohols and amine under UV irradiation,[12] and Pd(0)-immobilized recyclable hydrotalcite catalysts (HT4) for alcohol imination via acceptorless dehydrogenation also reported.[13] Notably, catalysts (both homogeneous and heterogeneous) used for imine synthesis by ADC strategy are extensively based on precious metals. In this regard, the development of novel highly active and selective non-precious metal catalysts; in particular, base metal catalysts is of pivotal importance and a focus point from the perspective of cost, abundance, and sustainable chemistry.[14-15] To best of our knowledge, there are no reusable heterogeneous catalysts based on earth-

[a] *Catalysis Division, Dr. Homi Bhabha Road, CSIR-National Chemical Laboratory (CSIR-NCL), Pune - 411008, India.*
[b] *Physical and Materials Chemistry Division, Dr. Homi Bhabha Road, CSIR-National Chemical Laboratory (CSIR-NCL), Pune - 411008, India.*
[c] *Academy of Scientific and Innovative Research (AcSIR), New Delhi - 110 025, India.*
†Electronic Supplementary Information (ESI) available: [details of experimental procedure, characterization of catalyst, compounds and copy of NMR data]. See DOI:10.1039/x0xx00000x

abundant, economical *'green' metals* for direct imine formation by acceptorless dehydrogenative coupling of alcohols with amines.

During the last decade, N-doped graphene materials have been shown to be an interesting commodity for sustainable catalysis.[16] Inspired by these results, herein we report the preparation of heterogeneous iron-based catalyst (Fe-Phen@C) and describe for the first time environmentally benign dehydrogenative coupling of alcohols and amines to form imines and H_2 (Scheme 1).

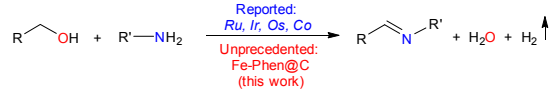

Scheme 1. Overview of the present work and the reusable Fe-based heterogeneous catalyst used in this study.

Results and discussion

The active heterogeneous iron catalyst was prepared by pyrolysis of an *in situ* generated Fe-Phen complex ($Fe(acac)_3$:1,10-phenanthroline = 1:1) on exfoliated graphene oxide support at 800 °C for 4 h under argon atmosphere.[17-18] The complete characterization of the active material (Fe-Phen@C) has been carried out using PXRD, TEM analysis, SEM analysis, XPS, ICP and Raman spectroscopy (see supporting information for characterization data).

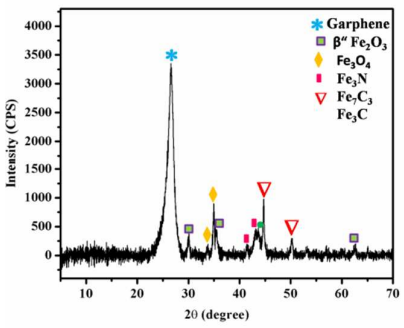

Fig. 1. XRD spectra of Fe-Phen@C material with indices of peaks pattern of β"-Fe_2O_3, Fe_3O_4, Fe_7C_3, Fe_3N, Fe_3C, and graphite.

XRD pattern of Fe-Phen@C sample presented in Fig. 1 shows diffraction peaks confirming the presence of β"-Fe_2O_3 (JCPDS no 40-1139), Fe_3O_4 (JCPDS no 85-1436), Fe_3N (JCPDS no 01-1236) Fe_3C (JCPDS no 85-1317) and Fe_7C_3 (JCPDS no 17-0333). Formation of Fe_3N was probably due to the decomposition of N-containing Fe-phenanthroline complex on exfoliated graphene oxide (EGO). A peak at 2θ = 26.6 degrees corresponding to (002) lattice plane of reduced graphite oxide (RGO) was also observed. The peak is broad suggesting the carbon support was composed of a few layers of graphene sheets. In Fig. 2 (a) TEM image of Fe-Phen@C sample is shown. In the bright field image, one can observe the wrinkles of the thin layers of RGO support as dark lines and Fe-rich nanoparticles as dark spots. It can be observed that the nanoparticles are located only on the RGO sheets. The nanoparticles distributed throughout the graphene sheets varied in size from 8 to 50 nm. However, the majority of particles were in the range of 14-20 nm. FESEM image in Fig. 2 (b) shows the morphology of the as-prepared Fe-Phen@C catalyst. In the dark field, FE-SEM of Fe-Phen@C was taken using secondary electrons in which metal has high surface electrons density appears brighter than RGO. It can be observed that Fe-rich particles are distributed spatially apart on the graphene layers.

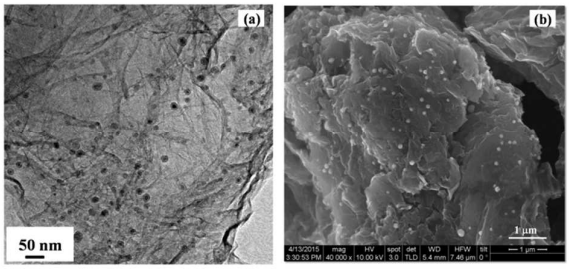

Fig. 2 (a) Microstructural characterization of Fe-Phen@C material TEM image of Fe-Phen@C; Scale bar, 50 nm. **(b)** FESEM image of Fe-Phen@C; scale bar, 1 µm.

A recent unprecedented report from our research group on heterogeneous iron-catalyzed acceptorless dehydrogenation of fundamentally important feedstocks such as alcohols to carbonyl compounds and cyclic amines to *N*-heterocycles[17] prompted us to disclose our first report on a simple, efficient, reusable heterogeneous iron-catalyzed direct imine formation by acceptorless dehydrogenative coupling of alcohols with amines (Scheme 1, Table 1). The present ADC strategy has a broad substrate scope as well as functional group tolerance, and operates under mild conditions with the liberation of hydrogen gas and water as the by-products, thus making the protocol completely environmentally-benign. An ease of separation and reusability of the heterogeneous iron catalyst is also successfully demonstrated.

Table 1. Optimization of the reaction conditions.[a]

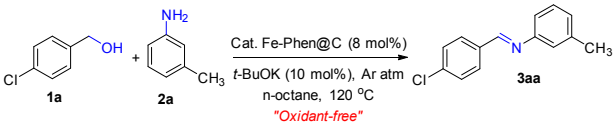

Entry	Cat.	Variation from the initial conditions	Conversion of **1a** (%)[b]	Yield of **3aa** (%)[b]
1	Fe-Phen@C	none	99	97 (93)[c]
2	Fe-Phen@C	closed system	57	40[c]
3	Fe-Phen@C	without *t*-BuOK	17	8
4	Fe-Phen@C	K_2CO_3 instead of *t*-BuOK	35	19
5	Fe-Phen@C	KOH instead of *t*-BuOK	8	0
6	Fe-Phen@C	CH_3CN instead of n-octane	19	15
7	Fe-Phen@C	toluene instead of n-octane	64	46
8	Fe-Phen@C	at 80 °C	40	34[c,d]
9	Fe@C	none	5	0
10	Phen@C	none	0	0
11	---	without Fe-Phen@C	0	0
12[e]	$Fe(acac)_3$/Phen	under homogeneous condition	8	trace
13[e]	$Fe(CO)_5$/Phen	under homogeneous condition	trace	0
14	Fe-Phen@SiO_2	none	31	18
15	Fe-Phen@Al_2O_3	none	17	8
16	Fe-Phen@TiO_2	none	46	31[c]

[a] Reaction conditions: **1a** (0.5 mmol), **2a** (0.55 mmol), cat. Fe-Phen@C (8 mol%), *t*-BuOK

(10 mol%), and n-octane (2 mL) heated at 120 °C (oil-bath temperature) for 24 h under open argon atm. [b] Conversion of **1a** and yield of **3aa** are based on GC using anisole as the internal reference. [c] Isolated yields. [d] after 48 h. [e] Reaction under homogeneous condition using *in situ* generated Fe-catalyst by reacting 1:1 mixture of Fe salt and 1,10-phenanthroline (Phen) followed by treatment with *t*-BuOK (10 mol%).

Optimization studies on Iron-catalyzed direct imine formation by ADC of alcohols with amines are summarized in Table 1. We began our investigation using (4-chlorophenyl)methanol (**1a**) and *m*-toluidine (**2a**) as benchmark substrates in presence of catalytic amount of Fe-Phen@C (8 mol%), and *t*-BuOK (10 mol%) in n-octane heated at 120 °C (bath temperature) under open Ar atm for 24 h to yield **3aa** in 93% isolated yield with the complete conversion of **1a** (Table 1, entry 1). Indeed, the formation of molecular hydrogen was qualitatively analyzed by gas chromatography (GC). Performing reaction under closed condition yielded **3aa** in lower yield (40%) (Table 1, entry 2) and clearly indicating that the constant removal of H_2 gas from the reaction medium is crucial.[9-10,19] Notably, the efficiency of the reaction was significantly affected in the absence of *t*-BuOK (Table 1, entry 3). Other bases like K_2CO_3 and KOH are ineffective under standard reaction conditions (Table 1, entries 4-5).[20-21] The solvent dependency of the same reaction was carried out (Table 1, entries 1, and 6-7) and we found that the reaction proceeds efficiently in n-octane compared to other solvents.[22] By lowering the temperature, we obtained the product in lower yield (Table 1, entry 8) and no reaction was observed in the absence of the Fe-Phen@C catalyst (Table 1, entry 11). Notably, either no imine formation or hydrogen gas was observed under homogeneous conditions (Table 1, entries 12-13).[23] It was worth noting that under the similar experimental conditions, catalysts (Fe-Phen) prepared on other conventional supports such as SiO_2, Al_2O_3 and TiO_2 showed lesser activity in the imine formation (Table 1, entries 14-16).[18,24] These studies show that the special structure of reduced graphene oxide (RGO) may be affected the reactivity in the environmentally-benign dehydrogenative coupling of alcohols and amines to form imines and H_2.

With an optimized catalytic system in hand (Table 1), we set out to probe its versatility in the direct imine synthesis by ADC strategy of various alcohols and amines. Using (4-chlorophenyl)methanol **1a** as the benchmark substrate, a number of different anilines were tested using Fe-Phen@C catalyst under standard conditions. As shown in Table 2, the present heterogeneous Fe-catalysis is compatible with various anilines containing an electron-rich and electron-deficient substituents, affording the desired imines in good to excellent yields (up to 95%) under very mild, eco-benign conditions. Interestingly, the reaction proceeded successfully with both cyclic and acyclic secondary amines and gave the desired imines **3an** (81%), **3ao** (74%), **3ap** (73%), and **3aq** (62%) in good yields. It was noteworthy that benzylamine (**2r**) also affording the corresponding imine in moderate yield (40%), along with the formation of (*E*)-*N*-benzyl-1-phenylmethanimine (26% by GC) by dehydrogenative self-coupling of **2r**. The reaction of benzene-1,3-diamine (**2s**) and **1a** selectively gave the corresponding diimine (**3as**) in 75% isolated yield under our catalytic conditions.

Table 2. Iron-catalyzed direct imine synthesis: Scope of amines.[a,b]

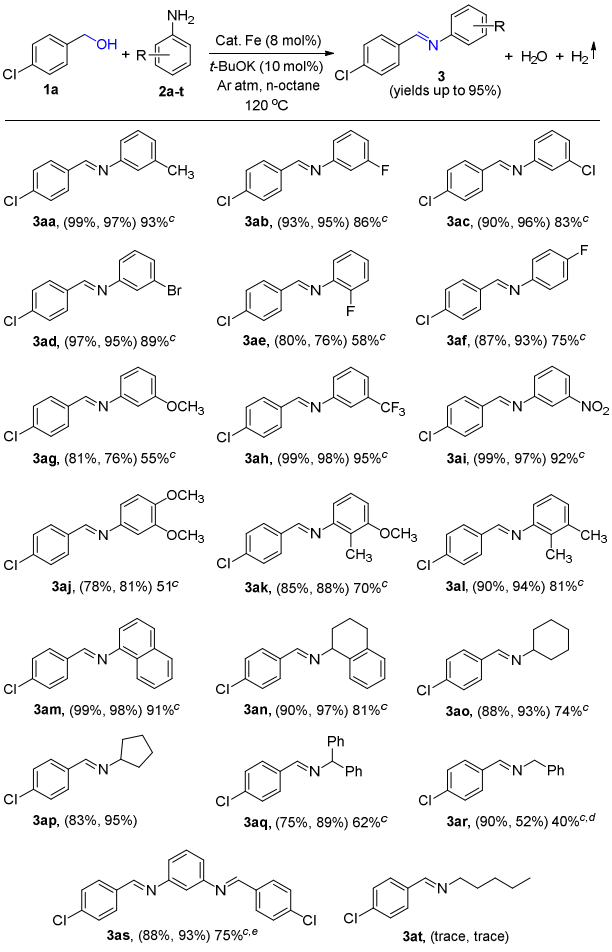

[a] Reaction conditions: **1a** (0.5 mmol), **2a** (0.55 mmol), cat. Fe-Phen@C (8 mol%), *t*-BuOK (10 mol%), and n-octane (2 mL) heated at 120 °C (oil-bath temperature) for 24 h under open argon atm. [b] Yields are in parentheses are based on the conversion of **1a** and selectivity of imines (**3**) respectively and are based on GC using anisole as the internal reference. [c] Isolated yields. [d] Self-dehydrogenative coupling of benzylamine to (*E*)-*N*-benzyl-1-phenylmethanimine was observed as the side reaction. [e] 2 equiv. of **1a**.

Next, the impact of varying the substituents on the alcohol coupling partner was also assessed (Table 3). The straightforward imine formation reaction proceeded in excellent yields with either electron donating (4-methyl, 4-methoxy) or electron withdrawing (4-fluoro, 4-nitro) substituents on the benzyl alcohol. Notably, *ortho*-substituted alcohols yielded the imines (**3bi** and **3bj**) in lower yields, which could be explained by steric effects.[25] To our delight, biomass-derived furfuryl alcohol also gave the corresponding imine in good yield (**3bk** in 76% yield). Less reactive cinnamyl alcohol was also tested for the direct imine formation reaction and efficiently gave the corresponding imine in 66% yield. However, 1-hexanol failed to convert into the corresponding aliphatic imine (**3bm**) under optimized conditions.

Table 3. Iron-catalyzed direct imine synthesis: Scope of alcohols.[a,b]

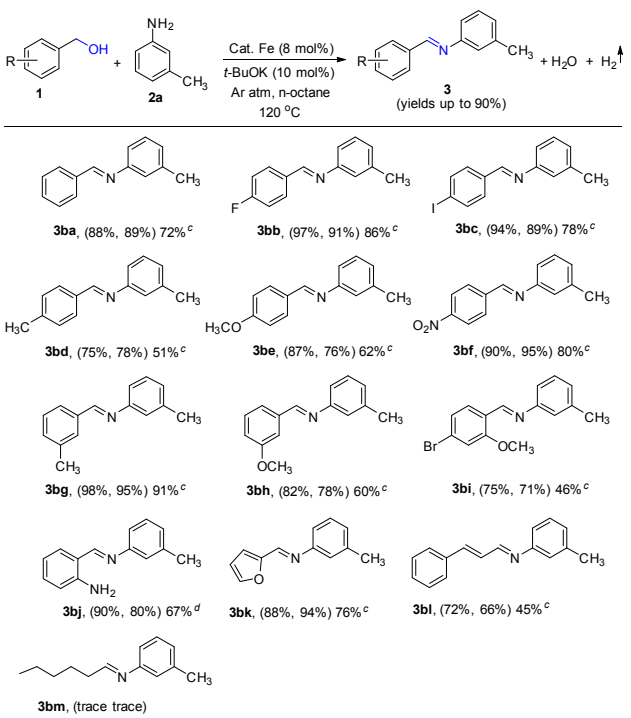

[a] Reaction conditions: **1** (0.5 mmol), **2a** (0.55 mmol), cat. Fe-Phen@C (8 mol%), *t*-BuOK (10 mol%), and n-octane (2 mL) heated at 120 °C (oil-bath temperature) for 24 h under open argon atm. [b] Yields are in parentheses are based on the conversion of alcohol and selectivity of **3** respectively and are based on GC using anisole as the internal reference. [c] Isolated yields. [d] Based on ^{1}H NMR of the crude reaction mixture.

Gram-scale synthesis

We have successfully shown the scalability and particle viability of this catalytic protocol under standard conditions. In this regard, the present iron-catalyzed direct imine synthesis was tested for the gram-scale synthesis of **3aa,** and it worked excellently with an expected imine in 78% isolated yield after 36 h (Scheme 2). The result implies that the heterogeneous Fe-based catalytic system has a potential in the large-scale production of imines under operationally simple, environmentally benign conditions.

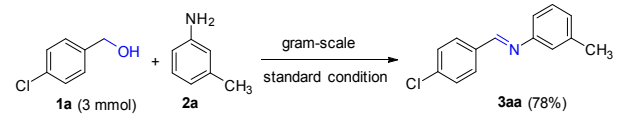

Scheme 2. Gram-scale synthesis of imine (**3aa**).

Time-dependent experiments on direct imine formation by ADC of alcohols with amines were conducted using heterogeneous iron-catalyst to study the reaction kinetics (Fig. 3). Continuous sampling was undertaken with the different time intervals, and the conversion of alcohol (**1a**) and yield of imine (**3aa**) were determined by gas chromatography. Formation of aldehyde intermediate was observed during the reaction pathway, along with the desired imine as the major product.

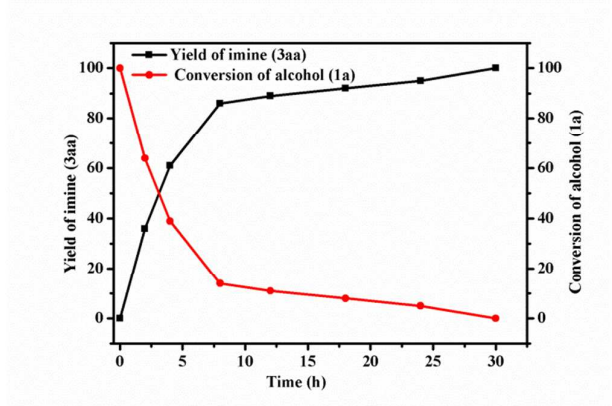

Fig. 3 Reaction profile for the Iron-catalyzed formation of **3aa**. Reaction conditions: **1a** (0.5 mmol), **2a** (0.55 mmol), cat. Fe-Phen@C (8 mol%), *t*-BuOK (10 mol%), and n-octane (2 mL) heated at 120 °C (oil-bath temperature) under open argon atm.

Reusability and Heterogeneity

The significant advantage of heterogeneous catalysts over soluble homogeneous catalysts is its capability for easy separation and recycling. The iron catalyst was easily separated from the reaction medium under the strong magnetic field, as shown in Fig. 4a & 4b. The recovered heterogeneous Fe-Phen@C was reused for direct imine synthesis in at least six cycles without a considerable loss in the yield (Fig. 4c).[18] The results were within the error limits, and indeed, no deactivation of the catalyst was observed. The hot filtration test was carried out, and it was observed that no further imine formation (**3aa**) took place after the catalyst was filtered off at the conversion of **1a** in 67%. Inductively coupled plasma (ICP) analyzes confirmed that the iron concentration in the filtrate was less than 0.22 ppm. Notably, no imine formation was observed in reaction under complete homogeneous condition (Table 1, entries 12-13).[23] All these results clearly demonstrate that the present Fe-catalysis is truly heterogeneous in nature.

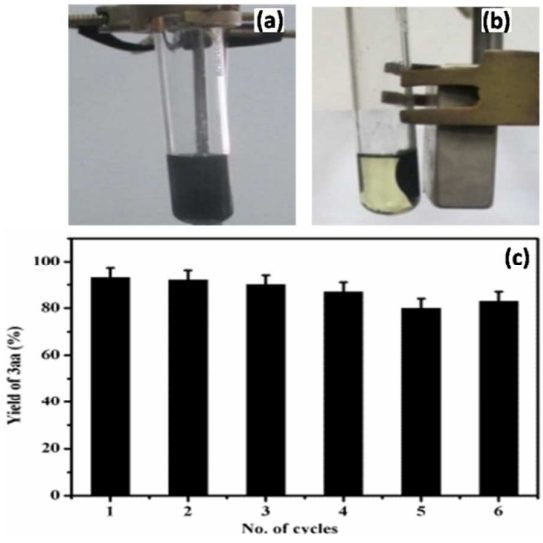

Fig. 4 Separation of the catalyst under strong magnetic field (**a**: reaction mixture; **b**: under magnetic field). **(c)** Recovery and reuse of the Fe-Phen@C catalyst.

Mechanistic Study

The high activity and selectivity of Fe-catalyst in the direct imine formation by acceptorless dehydrogenative coupling of alcohols with amines motivated us to gain insight into the mechanistic details (Scheme 3). In this regard, we performed the acceptorless dehydrogenation of alcohol, **1a** (in the absence of amine) under the identical conditions, and a quantitative yield of the corresponding aldehyde was obtained after 24 h with the liberation of hydrogen gas.[17] The formation of H_2 gas in the Fe-Phen@C catalyzed the direct synthesis of imines from alcohols and amines was qualitatively observed on gas chromatography. We have also endeavored to investigate the effect of the catalyst in the consequent condensation step. It was clearly observed that the rate of condensation of aldehydes and amines was accelerated in the presence of Fe-Phen@C catalyst, which implies the presence of Lewis acid sites on the catalyst.

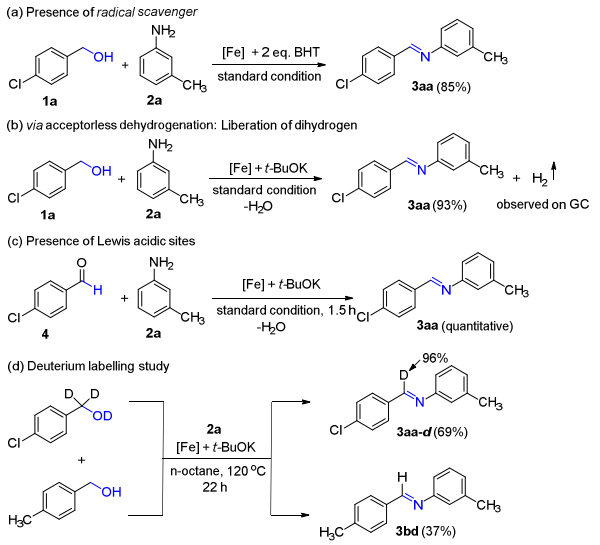

Scheme 3. Mechanistic studies.

To determine if any radical intermediates (e.g. superoxide radical anion, $O^{\cdot-}_2$; due to the presence of residual oxygen/air or to use of *t*-BuOK) were involved in the reaction, we performed the reaction in the presence of a radical scavenger (2,6-di-tert-butyl-4-methylphenol). The scavenger had no effect on the reaction rate in the formation of **3aa**, and thus the effect of residual oxygen or air as an oxidant, and the involvement of radical mechanism can be completely ruled out.[26] Indeed, *t*-BuOK is required to activate alcohols for the initial dehydrogenation reaction. A deuterium labeling experiments unambiguously illustrated that the initial alcohol dehydrogenation step is irreversible. Thus, upon treatment of a 1:1 mixture of 4-methylbenzyl alcohol and α,α-d_2-(4-chlorophenyl)methanol with *m*-toluidine **2a** (1.1 equiv) at 120 °C in n-octane for 22 h with a catalytic amount of Fe-Phen@C catalyst (8 mol%) and *t*-BuOK (10 mol%), 69% of (*E*)-1-(4-chlorophenyl)-*N*-(*m*-tolyl)methanimine-*d* (**3aa-*d***) and 37% of (*E*)-*N*-*m*-tolyl-1-(*p*-tolyl)methanimine (**3bd**) were obtained as reaction products (Scheme 3d). H/D scrambling was not detected in both of the imine products, suggesting that the initial alcohol dehydrogenation step is irreversible.

Conclusions

In summary, a more sustainable Iron-catalyzed direct imine formation by acceptorless dehydrogenative coupling of alcohols with amines under the *oxidant-free* condition is reported for the first time. The reaction operates under very mild and environmentally benign conditions with the liberation of dihydrogen and water as the byproducts. The present catalytic approach possesses a dual role; acting as a catalyst as well as can be magnetically separable. The recyclability experiments showed that the catalytic activity for imination can be retained for at least six cycles. The present strategy has great potential for the straightforward synthesis of imines from feedstock chemicals because it tolerates a wide range of substrates with high yields. Mechanistic studies showed the reaction proceeds in a tandem manner (via aldehyde formation), and deuterium labeling experiments unambiguously illustrated that the initial alcohol dehydrogenation step is irreversible.

Acknowledgements

This research is supported by the SERB (SB/FT/CS-065/2013) and EMR/2015/30 (under Green Chemistry program) and CSIR-NCL. GJ thanks to UGC and VGL thanks to CSIR for fellowships and DJ acknowledges the financial support of DST-Ramanujan Fellowship (RJN-112/2012) and BRNS (37(2)14/21/2015/BRNS). We thank Dr. P. R. Rajamohanan for the NMR facility and Dr. S. P. Borikar for GC-MS analysis. EB thanks to Dr. Abhishek Dey, IACS, Kolkata for providing $Fe(CO)_5$.

Notes and references

1 (a) S. I. Murahashi, *Angew. Chem. Int. Ed. Engl.*, 1995, **34**, 2443-2465; (b) J. P. Adams, *J. Chem. Soc. Perkin Trans. 1* 2000, 125-139; (c) S. Yao, S. Saaby, R. G. Hazell and K. A. Jørgensen, *Chem. -Eur. J.*, 2000, **6**, 2435-2448; (d) S. F. Martin, *Pure Appl. Chem.,* 2009, **81**, 195-204; (e) Z.-Y. Liu, Y.-M. Wang, Z.-R. Li, J.-D. Jiang and D. W. Boykin, *Bioorg. Med. Chem. Lett.* 2009, **19**, 5661-5664.

2 For recent reviews, see (a) R. D. Patil and S. Adimurthy, *Asian J. Org. Chem.*, 2013, **2**, 726-744; (b) R. J. Angelici, *Catal. Sci. Technol.*, 2013, **3**, 279-296; (c) W. Qin, S. Long, M. Panunzio and S. Biondi, *Molecules,* 2013, **18**, 12264-12289.

3 (a) H. Schiff, Justus *Liebigs Ann. Chem.*, 1864, **131**, 118-119; (b) F. Westheimer and K. Taguchi, *J. Org. Chem.*, 1971, **36**, 1570-1572; (c) R. S. Varma, R. Dahiya and S. Kumar, *Tetrahedron Lett.*, 1997, **38**, 2039-2042; (d) G. Liu, D. A. Cogan, T. D. Owens, T. P. Tang and J. A. Ellman, *J. Org. Chem.*, 1999, **64**, 1278-1284; (e) H. Naeimi, F. Salimi and K. Rabiei, *J. Mol. Catal. A: Chem.*, 2006, **260**, 100-104; (f) J. T. Reeves, M. D. Visco, M. A. Marsini, N. Grinberg, C. A. Busacca, A. E. Mattson and C. H. Senanayake, *Org. Lett.*, 2015, **17**, 2442-2445.

4 B. Chen, L. Wang and S. Gao, *ACS Catal.*, 2015, **5**, 5851-5876 and references cited therein.

5 (a) K. Yamaguchi and N. Mizuno, *Angew. Chem. Int. Ed.,* 2003, **42**, 1480-1483; (b) K. Nicolaou, C. J. Mathison and T. Montagnon, *Angew. Chem. Int. Ed.,* 2003, **42**, 4077-4082; (c) K. Nicolaou, C. J. Mathison

and T. Montagnon, *J. Am.Chem. Soc.,* 2004, **126**, 5192-5201; (d) B. Zhu and R. J. Angelici, *Chem. Commun.*, 2007, 2157-2159; (e) M. Largeron, A. Chiaroni and M. B. Fleury, *Chem. -Eur. J.,* 2008, **14**, 996-1003; (f) B. Zhu, M. Lazar, B. G. Trewyn and R. J. Angelici, *J. Catal*., 2008, **260**, 1-6; (g) G. Jiang, J. Chen, J.-S. Huang and C.-M. Che, *Org. Lett*., 2009, **11**, 4568-4571; (h) L. Aschwanden, B. Panella, P. Rossbach, B. Keller and A. Baiker, *ChemCatChem*, 2009, **1**, 111-115; (i) R. D. Patil and S. Adimurthy, *Adv. Synth. Catal.,* 2011, **353**, 1695-1700; (j) S. Furukawa, Y. Ohno, T. Shishido, K. Teramura and T. Tanaka, *ACS Catal*., 2011, **1**, 1150-1153; (k) H. Miyamura, M. Morita, T. Inasaki and S. Kobayashi, *Bull. Chem. Soc. Jpn.,* 2011, **84**, 588-599; (l) X. Lang, H. Ji, C. Chen, W. Ma and J. Zhao, *Angew. Chem. Int. Ed.,* 2011, **50**, 3934-3937; (m) H. Yuan, W.-J. Yoo, H. Miyamura and S. Kobayashi, *J. Am. Chem. Soc*., 2012, **134**, 13970-13973; (n) M. Largeron and M. B. Fleury, *Angew. Chem. Int. Ed*., 2012, **51**, 5409-5412; (o) L. Liu, Z. Wang, X. Fu and C.-H. Yan, *Org. Lett*., 2012, **14**, 5692-5695; (p) A. E. Wendlandt and S. S. Stahl, *Org. Lett*., 2012, **14**, 2850-2853; (q) H. Yuan, W.-J. Yoo, H. Miyamura and S. Kobayashi, *J. Am.Chem. Soc.,* 2012, **134**, 13970-13973; (r) T. Sonobe, K. Oisaki and M. Kanai, *Chem. Sci.,* 2012, **3**,3249-3255; (s) Z. Hu and F. M. Kerton, *Org. Biomol. Chem.,* 2012, **10**, 1618-1624; (t) L. Al-Hmoud and C. W. Jones, *J. Catal*., 2013, **301**, 116-124; (u) N. Li, X. Lang, W. Ma, H. Ji, C. Chen and J. Zhao, *Chem. Commun.* 2013, **49**, 5034-5036; (v) K. N. Tayade and M. Mishra, *J. Mol. Catal. A: Chem.* 2014, **382**, 114-125; (w) A. E. Wendlandt and S. S. Stahl, *J. Am. Chem. Soc*., 2014, **136**, 506-512; (x) A. E. Wendlandt and S. S. Stahl, *J. Am. Chem. Soc*., 2014, **136**, 11910-11913; (y) B. Chen, L.Wang, W. Dai, S. Shang, Y. Lv and S. Gao, *ACS Catal.,* 2015, **5**, 2788-2794; (z) C. Su, R.Tandiana, J. Balapanuru, W. Tang, K. Pareek, C. T. Nai, T.Hayashi, and K. P. Loh, *J. Am. Chem. Soc*. 2015, **137**, 685-690.

6 For selected reviews, see: (a) S.-I. Murahashi, Y. Okano, H. Sato, T. Nakae and N.Komiya, *Synlett,* 2007, 1675-1678; (b) M. T. Schümperli, C. Hammond and I. Hermans, *ACS Catal*., 2012, **2**, 1108-1117; (c) M. Largeron and M. B. Fleury, *Science*, 2013, **339**, 43-44; (d) M. Largeron, *Eur. J. Org. Chem*. 2013, 5225-5235 and references cited therein.

7 (a) L. Blackburn and R. J. Taylor, *Org. Lett*., 2001, **3**, 1637-1639; (b) S. Sithambaram, R. Kumar, Y.-C. Son and S. L. Suib, *J. Catal*., 2008, **253**, 269-277; (c) L. Jiang, L. Jin, H. Tian, X. Yuan, X. Yu and Q. Xu, *Chem. Commun*., 2011, **47**, 10833-10835; (d) J. Xu, R. Zhuang, L. Bao, G. Tang and Y. Zhao, *Green Chem.,* 2012, **14**, 2384-2387; (e) H. Tian, X. Yu, Q. Li, J. Wang and Q. Xu, *Adv. Synth. Catal*., 2012, **354**, 2671-2677; (f) Q. Kang and Y. G. Zhang, *Green Chem.*, 2012, **14**, 1016-1019; (g) E. L. Zhang, H. W. Tian, S. D. Xu, X. C. Yu and Q. Xu, *Org. Lett*., 2013, **15**, 2704-2707; (h) B. Chen, J. Li, W. Dai, L. Wang and S. Gao, *Green Chem*., 2014, **16**, 3328-3334; (i) L. Han, P. Xing and B. Jiang, *Org. Lett*., 2014, **16**, 3428-3431; (j) M. Guan, C. Wang, J. Zhang and Y. Zhao, *RSC Adv,*. 2014, **4**, 48777-48782; (k) M. Tamura and K. Tomishige, *Angew. Chem. Int. Ed.,* 2015, **54**, 864-867; (l) B. Chen, S. Shang, L. Wang, Y. Zhang and S. Gao, *Chem. Commun*., 2016, **52**, 481-484.

8 For supported noble-metal heterogeneous catalysts for oxidative dehydrogenation of alcohols with amines using oxygen as the oxidant, see: (a) M. S. Kwon, S. Kim, S. Park, W. Bosco, R. K. Chidrala and J. Park, *J. Org. Chem*., 2009, **74**, 2877-2879; (b) J. W. Kim, J. He, K. Yamaguchi and N. Mizuno, *Chem. Lett*., 2009, **38**, 920-921; (c) H. Sun, F. Z. Su, J. Ni, Y. Cao, H. Y. He and K. N. Fan, *Angew. Chem. Int. Ed*., 2009, **48**, 4390-4393; (d) S. Kegnæs, J. Mielby, U. V. Mentzel, C. H. Christensen and A. Riisager, *Green Chem*., 2010, **12**, 1437-1441; (e) W. He, L. Wang, C. Sun, K. Wu, S. He, J. Chen, P. Wu and Z. Yu, *Chem. -Eur. J.,* 2011, **17**, 13308-13317; (f) P. Liu, C. Li and E. J. Hensen, *Chem. -Eur. J*., 2012, **18**, 12122-12129; (g) J.-F. Soulé, H. Miyamura and S. Kobayashi, *Chem. Commun*., 2013, **49**, 355-357; (h) T. Zhang, L. Zhang, W. Wang, A.-Q. Wang, Y.-T. Cui, X. Yang, Y. Huang, X. Liu, W. Liu and J.-Y. Son, *Green Chem.,* 2013, **15**, 2680-2684.

9 (a) R. Yamaguchi, C. Ikeda, Y. Takahashi and K.-i. Fujita, *J. Am. Chem. Soc*., 2009, **131**, 8410-8412; (b) B. Gnanaprakasam, J. Zhang and D. Milstein, *Angew. Chem. Int. Ed.,* 2010, **49**, 1468-1471; (c) C. Xu, L. Y. Goh and S. A. Pullarkat, *Organometallics,* 2011, **30**, 6499-6502; (d) H.-A. Ho, K. Manna and A. D. Sadow, *Angew. Chem. Int. Ed.,* 2012, **51**, 8607-8610; (e) A. Maggi and R. Madsen, *Organometallics,* 2012, **31**, 451-455; (f) H. Li, X. Wang, M. Wen and Z.-X. Wang, *Eur. J. Inorg. Chem*., 2012, 5011-5020; (g) J. W. Rigoli, S. A. Moyer, S. D. Pearce and J. M. Schomaker, *Org. Biomol. Chem*., 2012, **10**, 1746-1749; (h) Y. Nakajima, Y. kamoto, Y. H. Chang and F. Ozawa, *Organometallics*, 2013, **32**, 2918-2925; (i) S. Musa, S. Fronton, L. Vaccaro and D. Gelman, *Organometallics*, 2013, **32**, 3069-3073; (j) G. Q. Zhang and S. K. Hanson, *Org. Lett*., 2013, **15**, 650-653; (k) E. Sindhuja and R. Ramesh, *Tetrahedron Lett*., 2014, **55**, 5504-5507; (l) B. Saha, S. M. W. Rahaman, P. Daw, G. Sengupta and J. K. Bera, *Chem. -Eur. J*. 2014, **20**, 6542-6551; (m) E. Balaraman, D. Srimani, Y. Diskin-Posner and D. Milstein, *Catal. Lett*., 2015, **145**, 139-144.

10 For recent review articles on borrowing hydrogen strategy, see: (a) S. Bähn, S. Imm, L. Neubert, M. Zhang, H. Neumann and M. Beller, *ChemCatChem,* 2011, **3**, 1853-1864; (b) C. Gunanathan, D. Milstein, *Science,* 2013, **341**, 1229712; (c) Y. Obora, *ACS Catal*., 2014, **4**, 3972-3981; (d) J. M. Ketcham, I. Shin, T. P. Montgomery and M. J. Krische, *Angew. Chem. Int. Ed*. 2014, **53**, 9142-9150; (d) Q. Yang, Q. Wang and Z. Yu, *Chem. Soc. Rev*. 2015, **44**, 2305-2329; (e) A. Nandakumar, S. P. Midya, V. G. Landge and E. Balaraman, *Angew. Chem. Int. Ed*., 2015, **54**, 11022-11034.

11 T. Yan, B. L. Feringa and K. Barta, *Nat. Commun*., 2014, **5**, 5602-5608.

12 Y. Shiraishi, M. Ikeda, D. Tsukamoto, S. Tanaka and T. Hirai, *Chem. Commun.,* 2011, **47**, 4811-4813.

13 J. Bain, P. Cho and A. V.-Kostal, *Green Chem.,* 2015, **17**, 2271-2280.

14 (a) R. A. Sheldon, *Chem. Soc. Rev.,* 2012, **41**, 1437-1451; (b) I. Delidovich and R. Palkovits, *Green Chem.,* 2016, DOI: 10.1039/c5gc90070k.

15 (a) I. Bauer and H. -J. Knolker, *Chem. Rev*., 2015, **115**, 3170-3387; (b) C. Darcel, J. -B. Sortais, S. Q. Duque, *RSC Green Chemistry* Series 2015, **26**, 67-92.

16 Selected examples: (a) R. V. Jagadeesh, A.-E. Surkus, H. Junge, M.-M. Pohl, J. Radnik, J. Rabeah, H. Huan, V. Schünemann, A. Brückner and M. Beller, *Science*, 2013, **342**, 1073-1076; (b) F. A. Westerhaus, R. V. Jagadeesh, G. Wienhöfer, M.-M. Pohl, J. Radnik, A.-E. Surkus, J. Rabeah, K. Junge, H. Junge, M. Nielsen, A. Brückner and M. Beller, *Nat Chem*, 2013, **5**, 537-543; (c) F. Chen, A.-E. Surkus, L. He, M.-M. Pohl, J. Radnik, C. Topf, K. Junge and M. Beller, *J. Am. Chem. Soc*., 2015, **137**, 11718-11724; (d) A. V. Iosub and S. S. Stahl *Org. Lett*., 2015, **17**, 4404-4407.

17 E. Balaraman, D. Jagadeesan, G. Jaiswal and S. P. Borikar, PCT filled 1494/DEL/2015.

18 See Supporting Information.

19 Interestingly we didn't observe any imine hydrogenated product (*via* borrowing hydrogen strategy), probably Fe-Phen@C is not acting as a hydrogenating catalyst under these conditions.

20 Other bases such as KOAc, CsOAc, Li_2CO_3, Na_2CO_3, K_2CO_3, Cs_2CO_3, Et_3N, DABCO, and DBU proved ineffective and less (~less than 20%), or no formation of **3aa** was observed under optimal conditions.

21 The role of the base (*t*-BuOK) is unclear for the present Fe-catalysis. However, we believe that catalytic amount of base is required to activate the alcoholic substrates.

22 Further screening using a representative set of common solvents, including apolar arenes (*o*-xylene, PhCl, anisole), or polar DMF, DMSO, DMA, and DCE proved ineffective.

23 The reaction was performed under *in situ* generated a soluble Fe-Phen complex by reacting 1:1 mixture of readily available either Fe(III)-acetylacetonate or $Fe(CO)_5$ as a iron precursor and 1,10-phenanthroline as a ligand followed by treatment with a catalytic amount of a base (10 mol% of *t*-BuOK).

24 Formation of molecular hydrogen was not observed on GC.

25 Other by-products (~15% on GC) were also identified in case of **3bj** due *ortho* $-NH_2$ group.

26 X. Cui, Y. Li, S. Bachmann, M. Scalone, A.-E. Surkus, K. Junge, C. Topf and M. Beller, *J. Am. Chem. Soc*., 2015, **137**, 10652-10658.

TOC

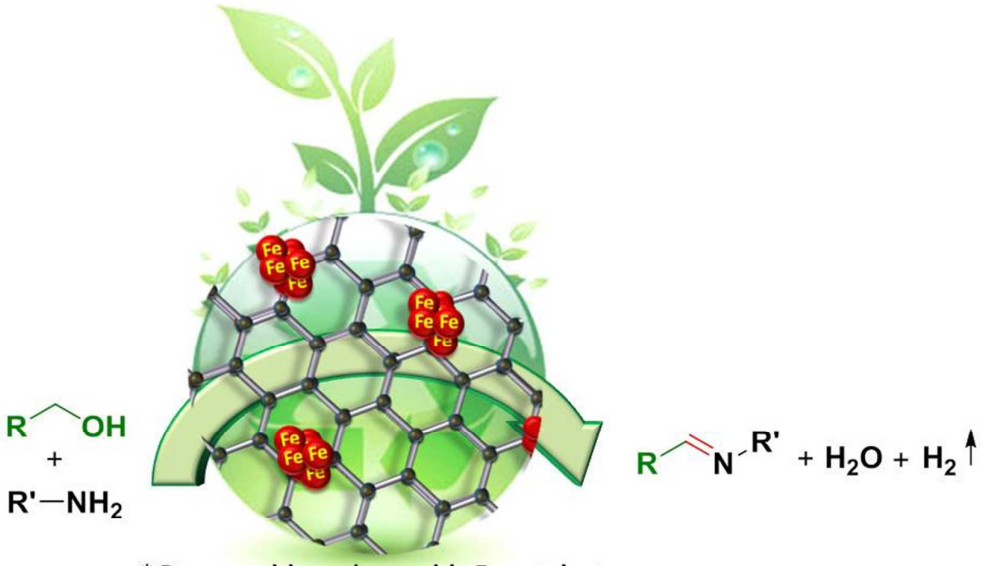

* Recoverable and reusable Fe-catalyst
* Tandem catalytic process
* Oxidant-free strategy
* Broad substrate scope
* Gram-scale synthesis
* Water and H_2 gas as the byproducts

Electronic Supplementary Information (ESI)

Sustainable Iron-catalyzed direct imine formation by acceptorless dehydrogenative coupling of alcohols with amines

Garima Jaiswal,[a,c] Vinod G. Landge,[a,c] Dinesh Jagadeesan,*[b,c] and Ekambaram Balaraman*[a,c]

[a] *Catalysis Division,* [b] *Physical & Material Chemistry Division, CSIR-National Chemical Laboratory, Dr. Homi Bhabha Road, 411008 - Pune, India.* [c] *Academy of Scientific and Innovative Research (AcSIR), New Delhi - 110 025, India.*

Contents

1. General Information	S2
2. Catalyst Synthesis and Characterization	S3-S6
2.1 Synthesis of Supported Catalysts	S3-S4
2.2. Characterization of Catalysts	S4-S6
3. Experimental Section	S7-S8
3.1. General Procedure for the Iron-catalyzed Direct Imine formation	S7
3.2. Gram-scale Synthesis of Imine	S7-S8
3.3. Reusability Procedure	S8
4. Mechanistic Investigation	S8-S12
4.1. Determination of hydrogen gas formation	S8-S9
4.2. Reaction under presence of radical ($\cdot O_2^-$) scavenger	S9-S10
4.3 Hot Filtration Test	S10
4.4. Leaching Test	S10
4.5 Reaction under homogeneous conditions	S11
4.6 Presence of Lewis acid sites	S11
4.7 Deuterium labelling studies	S12
5. Characterization Data	S12-S24
6. References	S24
7. Spectra	S25-S84

1. General Information

All catalytic experiments were carried out using standard Schlenk techniques. All solvents were reagent grade or better. Deuterated solvents were used as received without any additional purification. Most of the chemicals used in catalysis reactions were purified according to standard procedure (or by vacuum distillation/sublimation).[1] Thin layer chromatography (TLC) was performed using silica gel precoated glass plates, which were visualized with visualized with UV light at 254 nm or under iodine. Column chromatography was performed with SiO_2 (Silicycle Siliaflash F60 (230-400 mesh). ^{1}H NMR (400, 200 or 500 MHz), $^{13}C\{^{1}H\}$ NMR (100 MHz) spectra were recorded on the NMR spectrometer. Deuterated chloroform was used as the solvent, and chemical shift values (δ) are reported in parts per million relatives to the residual signals of this solvent [δ 7.27 for ^{1}H (chloroform-d), δ 77.0 for $^{13}C\{^{1}H\}$ (chloroform-d). Abbreviations used in the NMR follow-up experiments: br, broad; s, singlet; d, doublet; t, triplet; q, quartet; m, multiplet. GC analysis was carried out using an HP-5 column (30 m, 0.25 mm, 0.25μ). Mass spectra were obtained on a GCMS-QP 5000 instruments with ionization voltages of 70 eV. High-resolution mass spectra (HRMS) were obtained on a High-resolution mass spectra (HRMS) were obtained by fast atom bombardment (FAB) using a double focusing magnetic sector mass spectrometer and electron impact (EI) ionization technique (magnetic sector-electric sector double focusing mass analyzer). Inductively couple plasma atomic emission spectroscopy (ICP-AES) were acquired for the elemental analysis of absolute iron content within the sample. Analysis performed by SPECTRO analytical instruments GmbH, model ARCOS simultaneous ICP spectrometer, Germany.

2. Catalyst Synthesis and Characterization

2.1 Synthesis of supported catalysts (Fe-Phen@SiO_2, Fe-Phen@TiO_2, and Fe-Phen@Al_2O_3 catalysts)

2.1a Synthesis of Fe-Phen@C catalyst[††]

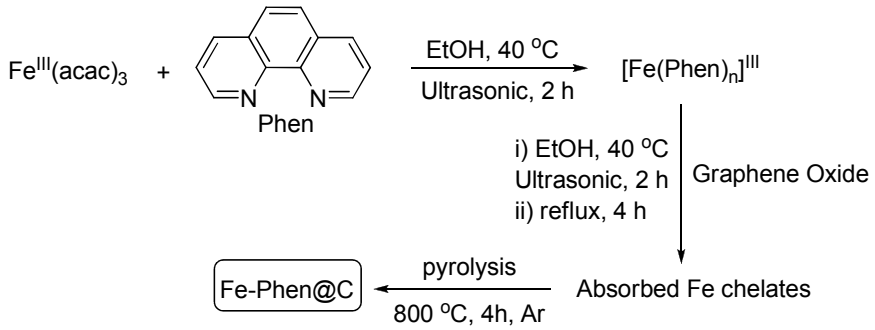

Scheme 1. Synthesis of Fe-Phen@C catalyst

(a) Graphene oxide was prepared from graphite powder by Hummers method as reported in the literature.[2] Graphitic Oxide was heated at 160 °C for 12 h for exfoliation to get exfoliated graphene oxide (EGO).

(b) Fe (III) acetylacetonate 176 mg (0.5 mmol) and 1,10-phenanthroline 90 mg (0.5 mmol) were taken in a beaker containing 30 mL of ethanol and sonicated for 2 h to form Fe-Phenonthroline complex. In another beaker 560 mg of EGO[††] was taken in 70 mL of ethanol and sonicated for 2 h. The EGO suspension and Fe-phenanthroline complex in ethanol were mixed together and further sonicated for 2 h. The suspension was subsequently refluxed for 4 h and ethanol was evaporated using rota-evaporator. After cooling to 30 °C, the ethanol was removed in vacuum and the solid sample obtained was dried at 80 °C for 14 h. Then, it was ground to a fine powder followed by calcination at 800 °C under a stream of argon with the flow rate of 30 mL/min and the heating rate: 25 °C/min for about 4 h to afford a catalyst Fe-

Phen@C. Iron present in the catalyst determined by ICP-AES analysis and was found to be 5.32%.

[††]In the case of other conventional support based catalysts such as Fe-Phen@SiO_2, Fe-Phen@TiO_2 and Fe-Phen@Al_2O_3 catalysts, 560 mg of the respective support (SiO_2, Al_2O_3, and TiO_2) was added and the other steps in the synthesis were identical as described in 2.1a.

2.2. Characterization of catalysts

a) XPS of Fe region of Fe-Phen@C

X-ray photoelectron spectroscopy (XPS) was done on a VG Microtech Multilab ESCA 3000 spectrometer that was equipped with a Mg K_α X-ray source ($h\upsilon$ = 1253.6 eV). The XPS peaks were fitted on XPSPEAK 4.1 having 70% Gaussian and 30% Lorentzian character, after performing a Shirley background subtraction. In the fitting procedure,[3-9] the full width at half-maximum (FWHM) values were fixed 1.5 eV for all the peaks.

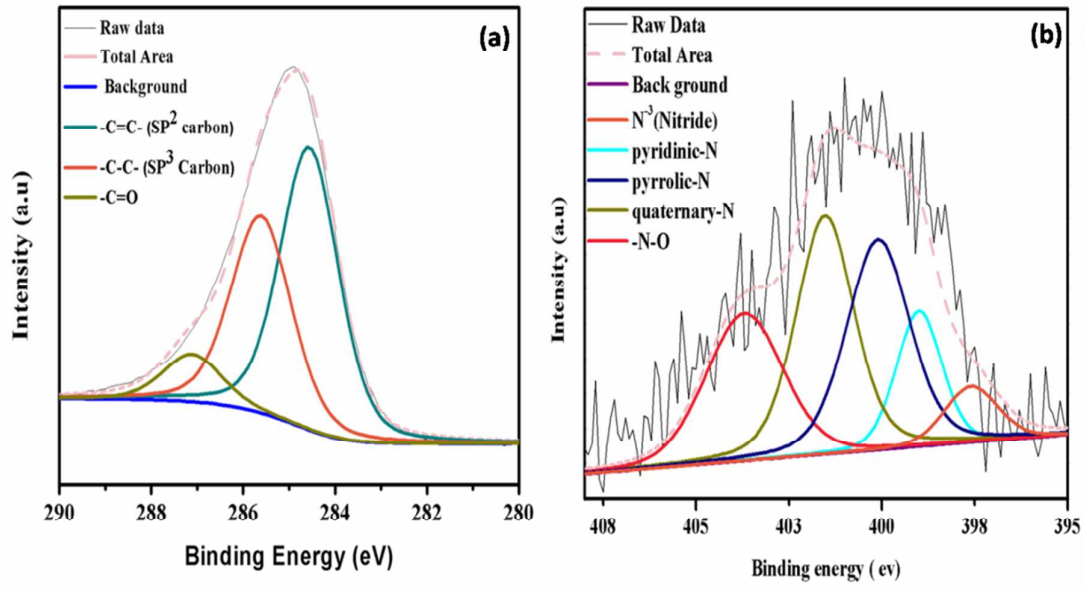

Fig. S1 Deconvoluted XPS spectra of Fe-Phen@C sample: **(a)** C1s region, **(b)** N1s region.

Table showing the peak positions in C1s and N1s XPS spectra and the corresponding chemical species.

C1s Spectra (Fig. S1a)	
Peak Position (eV)	**Inference**
284.5	sp^2 carbon (−C=C−)
285.8	sp^3 carbon such as −C−C− or −C−OH groups
287.3	Carbonyl functional group (C=O).
N1s Spectra (Fig. S1b)	
Peak Position (eV)	**Inference**
397.5	N of Fe_3N
399.1	pyridinic-N/N_{Pyri}
400.1	pyrrolic-N/N_{Pyrr}
401.4	quaternary-N/NR_4^+
403.6	–N–O

b. Raman spectra

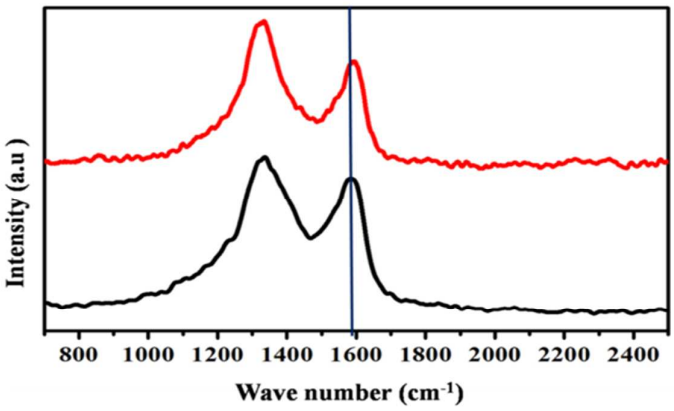

Fig. S2 Raman Spectra of reduced graphitic oxide support (black) and Fe-Phen@C (red).

Fig. S2 shows Raman spectra of Fe-Phen@C (red trace) and reduced graphitic oxide (black trace). The D band due to the vibration mode of A_{1g} symmetry of the sp^2 carbon of graphite lattice located at 1327 cm^{-1} for Fe-Phen@C and 1330 cm^{-1} for reduced graphitic oxide support. The D band mainly characterizes structural defects or edges that can break the symmetry and selection rule. The G band that arises due to the first-order scattering of the E_{2g} mode observed for sp^2 carbon domains was seen at 1595 cm^{-1} for Fe-Phen@C and at 1586 cm^{-1} for reduced graphitic oxide support. G band characterizes the highly ordered graphite

carbon materials. It was observed that deposition of iron in Fe-Phen@C resulted in an increased disorderliness of reduced graphitic oxide, as I_D/I_G increased to 1.36 in Fe-Phen@C compared to I_D/I_G=1.13 in reduced graphitic oxide support. G band showed a blue shift of 9 cm^{-1} in Fe-Phen@C as compared to reduced graphitic oxide support which was mainly due to charge transfer from graphene to iron nanoparticles.[10-11]

C. EDX analysis

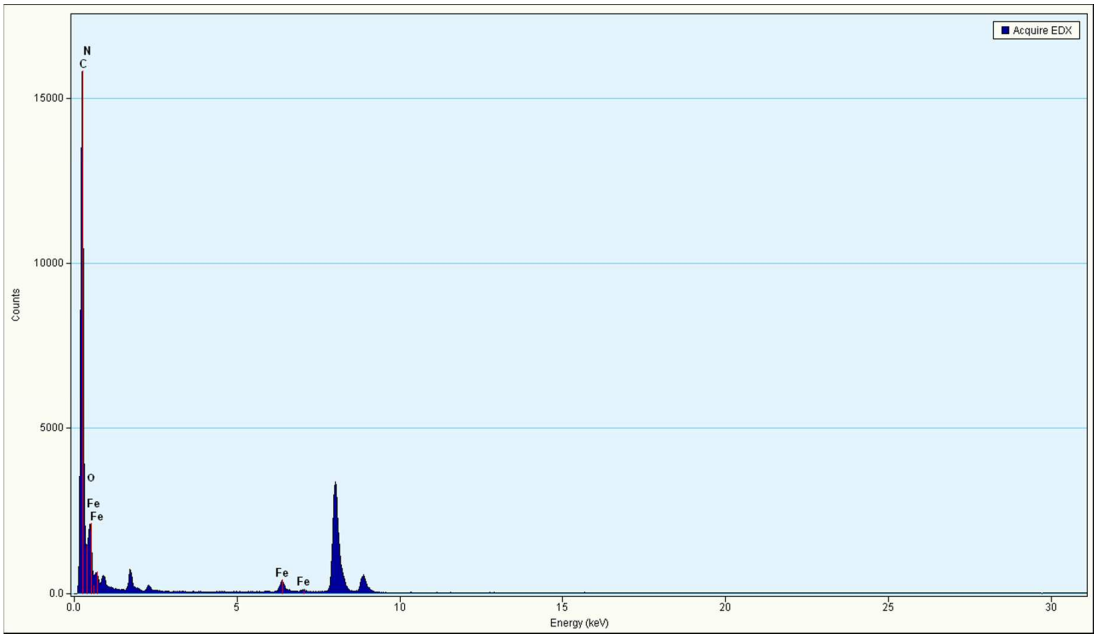

Fig. S3 EDX analysis of Fe-Phen@C.

Table showing the weight percent of different elements in the Fe-Phen@C catalyst.

Element	Weight %	Atomic %	Uncert. %	Correction	k-Factor
C(K)	76.36	83.29	0.41	0.26	3.940
N(K)	9.23	8.64	0.17	0.26	3.826
O(K)	8.02	6.56	0.09	0.49	1.974
Fe(K)	6.37	1.49	0.06	0.99	1.403

3. Experimental Section

3.1 General procedure for the iron-catalyzed direct imine formation

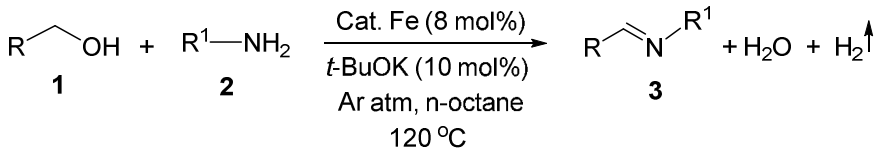

To a 25 mL oven dried schlenk tube, Fe-Phen@C catalyst (43 mg, 8 mol%), *t*-BuOK (10 mol%), alcohol (0.5 mmol), an amine (0.55 mmol), and n-octane (2 mL) were added under argon atmosphere. The schlenk tube was equipped with a reflux condenser, and the solution was heated at 120 ^{o}C (bath temperature) with stirring under open argon flow for 24 h. After cooling to 30 ^{o}C the catalyst was separated from the reaction mixture by an external permanent magnet and the reaction products were analyzed by GC and GC-MS. The supernatant was transferred into another flask, and the catalyst was washed with EtOAc (2 x 4 mL) and the washings were collected. The solvent was evaporated from the reaction mixture, and the crude product was subjected to deactivated silica gel column chromatography using EtOAc : petroleum ether to afford the imine derivatives.

3.2 Gram-scale synthesis of imine

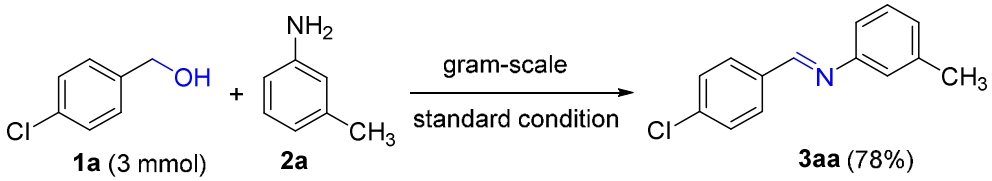

To a 50 mL oven dried schlenk flask, Fe-Phen@C catalyst (258 mg, 8 mol%), *t*-BuOK (34 mg, 10 mol%,), (4-chlorophenyl)methanol (428 mg, 3 mmol), *m*-toluidine (374 mg, 3.5 mmol,), and n-octane (12 mL) were added under argon atmosphere. The schlenk flask was equipped with a reflux condenser, and the solution was heated at 120 ^{o}C (bath temperature)

with stirring under open argon flow for 36 h. After cooling to 30 ^{o}C the reaction mixture was subjected to centrifugation and the supernatant was collected and the obtained solid was washed with EtOAc (3 x 5 mL) and the washings were collected. The collected reaction mixture was concentrated on rotavapor under reduce pressure. The crude product was purified through triethylamine (5 mL triethylamine in 100 ml pet ether/ethyl acetate) neutralized silica-gel column chromatography by using petroleum ether and ethyl acetate as an eluent.

3.3 Reusability procedure

To a 25 mL oven dried schlenk tube, Fe-Phen@C catalyst (86 mg, 8 mol%) *t*-BuOK (11 mg, 10 mol%), (4-chlorophenyl)methanol (143 mg, 1 mmol), *m*-toluidine (125 mg, 1.1 mmol), and n-octane (4 mL) were added under argon atmosphere. The schlenk tube was equipped with a reflux condenser, and the solution was heated at 120 ^{o}C (bath temperature) with stirring under open argon flow for 24 h. After cooling to 30 ^{o}C, the catalyst was separated from the reaction mixture by an external permanent magnet, washed with EtOAc several times and dried under vacuum at 60 °C for 4 h. Then the catalyst was reused for the next cycle. All yields are averages from at least 2 runs.

4. Mechanistic Investigation

4.1 Determination of hydrogen gas formation

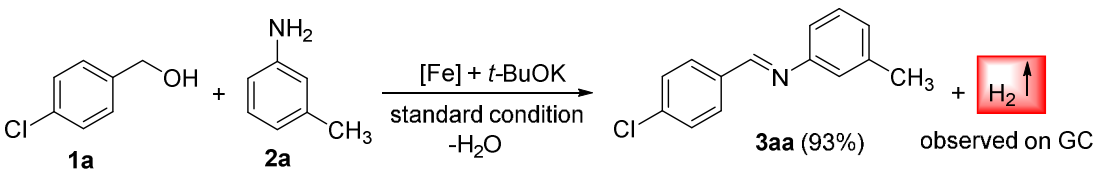

To an oven dried 20 mL screw-capped septa vial, Fe-Phen@C catalyst (86 mg, 8 mol%), *t*-BuOK (11 mg, 10 mol%), (4-chlorophenyl)methanol **1a** (143 mg, 1 mmol), *m*-toluidine **2a** (125 mg, 1.1 mmol), and n-octane (4 mL) were added under argon atmosphere. The vial was heated at 120 ^{o}C for 4 h. After cooling to room temperature, the gaseous mixture (formation of hydrogen gas) was qualitatively analyzed by GC-TCD with a Carbon plot capillary column.

Area % Report

Data File: C:\Users\Dr. E. BALARAMAN\Desktop\garima 030915.dat
Method: D:\E BALARAMAN\MANOJ\Method\untitled.met
Acquired: 9/3/2015 5:12:11 PM (GMT Unknown)
Printed: 9/7/2015 6:08:42 PM (GMT -07:00)

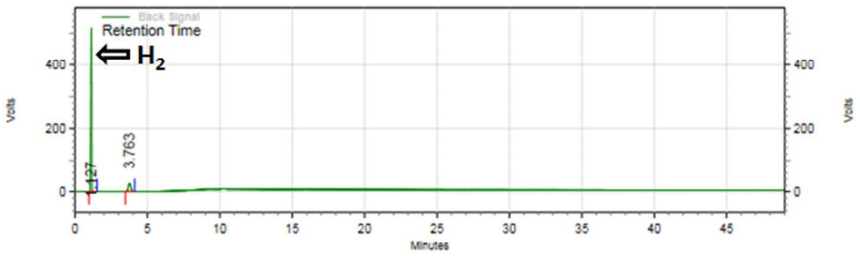

Back Signal Results

Retention Time	Area	Area %	Height	Height %
1.127	16555386	87.39	3957450	95.22
3.763	2389762	12.61	198546	4.78
Totals	18945148	100.00	4155996	100.00

4.2 Reaction under presence of radical ($O^{\cdot -}_2$) scavenger

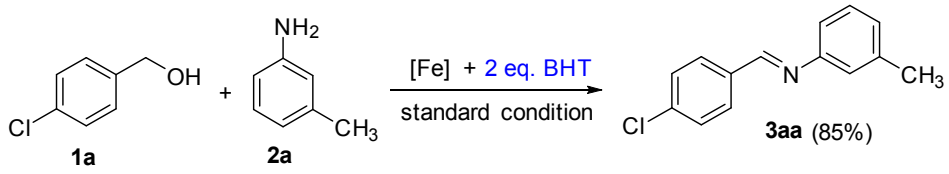

To a 25 mL oven dried schlenk tube, Fe-Phen@C catalyst (43 mg, 8 mol%), *t*-BuOK (6 mg, 10 mol%), (4-chlorophenyl)methanol (71 mg, 0.5 mmol), *m*-toluidine (62 mg, 0.55 mmol), 2,6-di-tert-butyl-4-methylphenol (BHT) (242 mg, 1.1 mmol), and n-octane (2 mL) were added under argon atmosphere. The schlenk tube was equipped with a reflux condenser and the solution was refluxed under argon atmosphere for 24 h. After cooling to 30 ^{o}C the

reaction mixture was subjected to centrifugation and the supernatant was collected and the obtained solid was washed with EtOAc (2 x 4 mL) and the washings were collected. The collected reaction mixture was concentrated on rotavapor under reduce pressure. The crude product was purified (deactivated silica gel column chromatography and the eluvent is a mixture of petroleum ether and ethyl acetate) and the yield of (*E*)-1-(4-chlorophenyl)-*N*-(*m*-tolyl)methanimine (**3aa**) is 85%.

4.3. Hot Filtration Test

To a 25 mL oven dried schlenk tube, Fe-Phen@C catalyst (43 mg, 8 mol%), *t*-BuOK (6 mg, 10 mol%), (4-chlorophenyl)methanol **1a** (71 mg, 0.5 mmol), *m*-toluidine **2a** (62 mg, 0.55 mmol), and n-octane (2 mL) were added under argon atmosphere. The schlenk tube was equipped with a reflux condenser, and the solution was heated at 120 ^{o}C (bath temperature) with stirring under open argon flow for 8 h. After cooling to 30 ^{o}C the catalyst was separated from the reaction mixture by an external permanent magnet (at this stage the crude reaction mixture was analyzed by GC (67% of **3aa**)). Then, the reaction mixture was transferred into another 25 mL oven dried schlenk tube under an argon atmosphere and was equipped with a reflux condenser, and the solution was heated at 120 ^{o}C (bath temperature) with stirring under open argon flow for 24 h. After cooling to room temperature, the crude reaction mixture was quantitatively analyzed by GC and observed that no change in the yield of **3aa**.

4.4 Leaching Test

To crude sample (after removal the catalyst) were added sulfuric acid and aqua regia then the volume of the residue was adjusted to 50 mL using water to give a sample for Inductively coupled plasma (ICP) for the measurement of the leaching of Iron and the analyses confirmed that the iron concentration in the filtrate was less than 0.22 ppm.

4.5 Reaction under homogeneous conditions

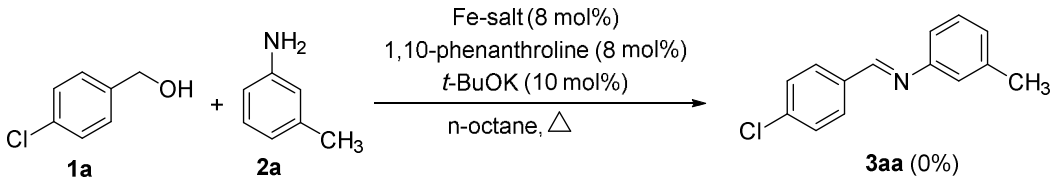

1a **2a** **3aa** (0%)

To a 25 mL oven dried schlenk tube, 8 mol% of Fe salt (iron(III) acetylacetonate or $Fe(CO)_5$) and 1,10-phenanthroline (7 mg, 8 mol%) and n-octane (2 mL) were added under argon atmosphere. The schlenk tube was equipped with a reflux condenser, and the solution was heated at 80 ^oC under argon atmosphere for 1 h. To the pre-formed Fe-complex, (4-chlorophenyl)methanol (71 mg, 0.5 mmol), *m*-toluidine (62 mg, 0.55 mmol), and *t*-BuOK (6 mg, 10 mol%) were added under argon atm and heated at 120 ^oC (bath temperature) for 24 h. After cooling to room temperature, the crude reaction mixture was analyzed by GC and observed no formation imine.

4.6 Presence of Lewis acid sites

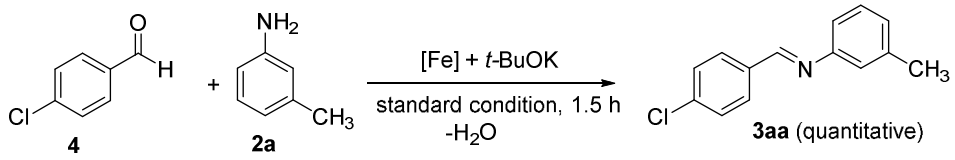

4 **2a** **3aa** (quantitative)

To a 25 mL oven dried schlenk tube, Fe-Phen@C catalyst (43 mg, 8 mol%), *t*-BuOK (6 mg, 10 mol%), 4-chlorobenzaldehyde **4** (71 mg, 0.5 mmol), *m*-toluidine **2a** (62 mg, 0.55 mmol), and n-octane (2 mL) were added under argon atmosphere. The schlenk tube was equipped with a reflux condenser and the solution was refluxed under argon atmosphere for 1.5 h. After cooling to 30 ^oC, the crude reaction mixture was analyzed by ^1H NMR and observed the quantitative formation of **3aa**. The same result was observed in the absence of *t*-BuOK.

4.7 Deuterium labelling studies

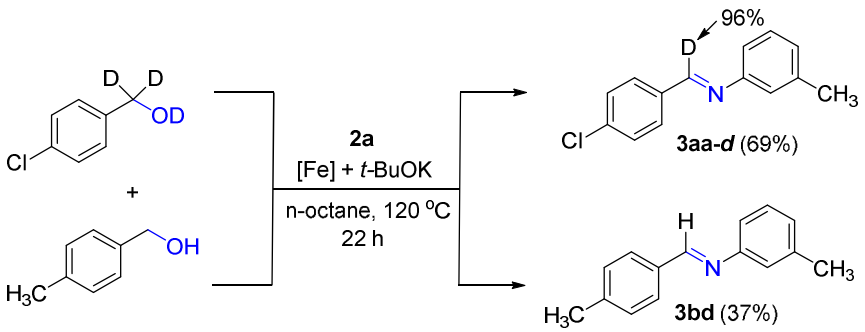

To a 25 mL oven dried schlenk tube, Fe-Phen@C catalyst (86 mg, 8 mol%), *t*-BuOK (11 mg, 10 mol%), *p*-tolylmethanol (62 mg, 0.5 mmol), (4-chlorophenyl)methan-d_2-ol-*d* (73 mg, 0.5 mmol),[12] and *m*-toluidine (138 mg, 1.1 mmol), and n-octane (4 mL) were added under argon atmosphere. The schlenk tube was equipped with a reflux condenser and the solution was refluxed under argon atmosphere for 22 h. After cooling to 30 °C the reaction mixture was subjected to centrifugation and the supernatant was collected and the obtained solid was washed with EtOAc (2 x 4 mL) and the washings were collected. The collected reaction mixture was concentrated under reduce pressure. The crude product was purified, and the yield of (*E*)-1-(4-chlorophenyl)-*N*-(*m*-tolyl)methanimine-*d* and (*E*)-*N*-*m*-tolyl-1-(*p*-tolyl)methanimine are 69% and 37% respectively.

5. Characterization Data

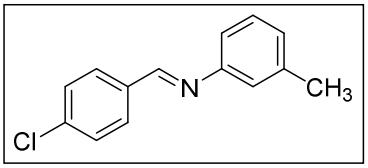

(E)-N-(4-chlorobenzylidene)-3-methylaniline **(3aa)**

106 mg, 93% isolated yield. ^{1}H NMR ($CDCl_3$, 500 MHz) δ 8.43 (s, 1H), 7.85 (d, *J* = 8.4 Hz, 2H), 7.46 (d, *J* = 8.4 Hz, 2H), 7.30 (t, *J* = 7.5 Hz, 1H), 7.08 (d, *J* = 7.2 Hz, 1H), 7.04-7.02 (m,

2H), 2.41 (s, 3H). ^{13}C NMR ($CDCl_3$, 125 MHz) δ 158.61, 151.62, 139.02, 137.25, 134.69, 129.89, 129.02(d, J = 4.8 Hz), 126.95, 121.58, 117.79, 21.38; HRMS Calcd for $C_{14}H_{12}NCl$ $[M+H]^+$: 230.0731; Found: 230.0734.

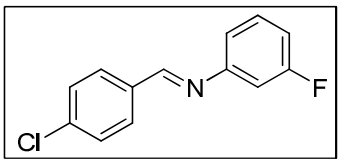

N-(4-chlorobenzylidene)-3-fluoroaniline **(3ab)**

100 mg, 86% isolated yield. ^{1}H NMR ($CDCl_3$, 200 MHz) δ 8.29 (s, 1H), 7.74 (d, *J* = 8.5 Hz, 2H), 7.36 (d, *J* = 8.4 Hz, 2H), 7.23-7.16 (m, 1H), 6.90-6.81 (m, 3H). ^{13}C NMR ($CDCl_3$, 125 MHz) δ 164.23, 162.27, 159.58, 153.48, 153.40, 130.32, 130.05, 129.08, 116.66, 116.64, 112.88, 112.70, 108.09, 107.91; HRMS Calcd for $C_{13}H_9NClF$ $[M+H]^+$: 234.0480; Found: 234.0482.

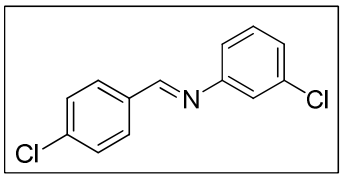

(E)-3-chloro-N-(4-chlorobenzylidene)aniline **(3ac)**

103 mg, 83% isolated yield. ^{1}H NMR ($CDCl_3$, 200 MHz) δ 8.29 (s, 1H), 7.74 (d, *J* = 8.6 Hz, 2H), 7.36 (d, *J* = 8.5 Hz, 2H), 7.23-7.10 (m, 3H), 6.98 (d, *J* = 7.91, 1H)**.** ^{13}C NMR ($CDCl_3$, 50 MHz) δ 159.76, 152.95, 137.81, 134.78, 134.31, 130.89, 130.18, 130.09, 129.46, 129.15, 126.05, 120.87, 119.36; HRMS Calcd for $C_{13}H_9NCl_2$ $[M+H]^+$: 250.0185; Found: 250.0187.

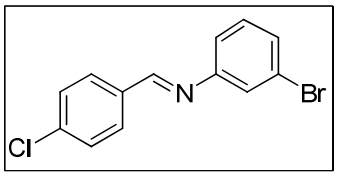

(E)-3-bromo-N-(4-chlorobenzylidene)aniline **(3ad)**

130 mg, 89% isolated yield. ^{1}H NMR ($CDCl_3$, 500 MHz) δ 8.31 (s, 1H), 7.76 (d, *J* = 8.3 Hz, 2H), 7.38 (d, *J* = 8.3 Hz, 2H), 7.31–7.14 (m, 3H), 7.06 (d, *J* = 7.8 Hz, 1H); ^{13}C NMR ($CDCl_3$, 125 MHz) δ 159.76, 153.01, 137.77, 134.23, 130.85, 130.54, 130.44, 130.07, 129.41, 129.11, 128.92, 123.64, 119.90; HRMS Calcd for $C_{13}H_9NBrCl$ $[M+H]^+$: 293.9680; Found: 293.9684.

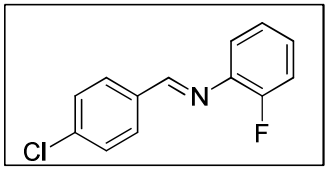

(E)-N-(4-chlorobenzylidene)-2-fluoroaniline **(3ae)**

68 mg, 58% isolated yield. ^{1}H NMR ($CDCl_3$, 500 MHz) δ 8.50 (s, 1H), 7.87 (d, *J* = 8.6 Hz, 2H), 7.46 (d, *J* = 8.6 Hz, 2H), 7.27 - 7.15 (m, 4H). ^{13}C NMR ($CDCl_3$, 125 MHz) δ 161.33, 156.15, 154.16, 139.61, 139.53, 137.77, 134.50, 130.08, 129.06, 126.94, 126.88, 124.50, 124.47, 122.02, 116.37, 116.21; HRMS Calcd for $C_{13}H_9NClF$ $[M+H]^+$: 234.0480; Found: 234.0482.

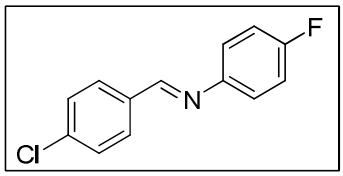

(E)-N-(4-chlorobenzylidene)-4-fluoroaniline **(3af)**

87 mg, 75% isolated yield. ^{1}H NMR ($CDCl_3$, 200 MHz) δ 8.41 (s, 1H), 7.85 (d, *J* = 8.7 Hz, 2H), 7.47 (d, *J* = 8.7 Hz, 2H), 7.37 (d, *J* = 8.5 Hz, 2H), 7.15 (d, *J* = 8.7 Hz, 2H). ^{13}C NMR

($CDCl_3$, 125 MHz) δ 159.12, 150.10, 137.65, 134.44, 131.75, 130.90, 130.01, 129.46, 129.29, 129.14, 122.17; HRMS Calcd for $C_{13}H_9NClF$ $[M+H]^+$: 234.0480; Found: 234.0482.

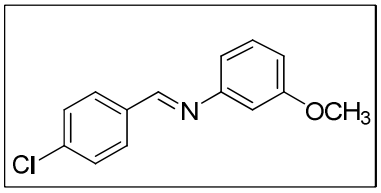

(E)-N-(4-chlorobenzylidene)-3-methoxyaniline **(3ag)**

68 mg, 55% isolated yield. ^1H NMR ($CDCl_3$, 500 MHz) δ 8.43 (s, 1H), 7.85 (d, J = 8.6 Hz, 2H), 7.46 (d, J = 8.2 Hz, 2H), 7.31 (t, J = 8.2 Hz, 1H), 6.82 - 6.78 (m, 3H), 3.85 (s, 3H). ^{13}C NMR ($CDCl_3$, 125 MHz) δ 160.31, 159.01, 153.08, 137.42, 134.56, 129.97, 129.94, 129.08, 112.79, 112.02, 106.62, 55.33; HRMS Calcd for $C_{14}H_{12}NClO$ $[M+H]^+$: 246.0680; Found: 246.0683.

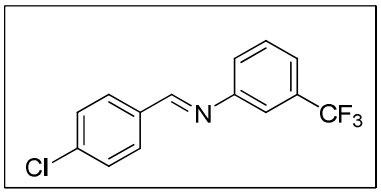

(E)-N-(4-chlorobenzylidene)-3-(trifluoromethyl)aniline **(3ah)**

134 mg. 95% isolated yield. ^1H NMR ($CDCl_3$, 500 MHz) δ 8.44 (s, 1H), 7.87 (d, J = 8.6 Hz, 2H), 7.53-7.45 (m, 4H), 7.39 - 7.37 (m, 2H). ^{13}C NMR ($CDCl_3$, 125 MHz) δ 160.24, 152.12, 137.96, 134.19, 130.14, 129.73, 129.20, 128.32, 124.15, 122.66, 117.71; HRMS Calcd for $C_{14}H_9NClF_3$ $[M+H]^+$: 284.0448; Found: 284.0450.

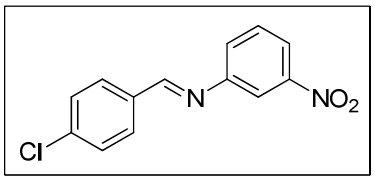

(E)-N-(4-chlorobenzylidene)-3-nitroaniline **(3ai)**

120 mg, 92% isolated yield. ^{1}H NMR ($CDCl_3$, 500 MHz) δ 8.47 (s,1H), 8.11 (dt, *J* = 8.2, 2.2 Hz, 1H), 8.05 (t, *J* = 2.2 Hz, 1H), 7.88 (d, *J* = 8.5 Hz, 2H), 7.58 (t, *J* = 7.7 Hz, 1H), 7.54 (dt, *J* = 8.5, 1.6 Hz, 1H), 7.50 (d, *J* = 8.5 Hz, 2H). ^{13}C NMR ($CDCl_3$, 125 MHz) δ 161.08, 152.75, 138.33, 133.88, 130.29, 129.96, 129.27, 129.11, 127.62, 120.67, 115.31; HRMS Calcd for $C_{13}H_9N_2O_2$ $[M+H]^+$: 261.0425; Found: 261.0733.

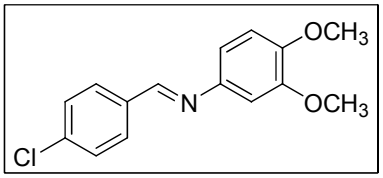

(E)-N-(4-chlorobenzylidene)-3,4-dimethoxyaniline (**3aj)**

71 mg, 51% isolated yield. ^{1}H NMR ($CDCl_3$, 400 MHz) δ 8.44 (s, 1H), 7.81 (d, *J* = 8.6 Hz, 2H), 7.42 (d, *J* = 8.6 Hz, 2H), 6.89-6.87 (m, 2H), 6.82 (dd, *J* = 8.2, 2.3 Hz, 1H), 3.92 (s, 3H), 3.90 (s, 3H). ^{13}C NMR ($CDCl_3$, 100 MHz) δ 156.80, 149.26, 147.83, 144.74, 136.92, 134.73, 129.64, 128.93, 112.12, 111.30, 105.51, 55.99, 55.80; HRMS Calcd for $C_{15}H_{15}NO_2Cl$ $[M+H]^+$: 276.0786; Found: 276.0787.

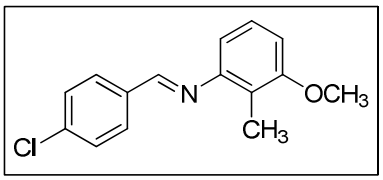

(E)-N-(4-chlorobenzylidene)-3-methoxy-2-methylaniline **(3ak)**

91 mg, 70% isolated yield. ^{1}H NMR ($CDCl_3$, 500 MHz) δ 8.33 (s, 1H), 7.87 (d, *J* = 7.4 Hz, 2H), 7.46 (d, *J* = 8.1 Hz, 2H), 7.18 (t, *J* = 7.5 Hz, 1H), 6.77 (d, *J* = 7.3 Hz, 1H), 6.60 (d, *J* = 7.7 Hz), 3.88 (s, 3H), 2.25 (s, 3H). ^{13}C NMR ($CDCl_3$, 125 MHz) δ 158.13, 151.62, 137.20, 134.98, 129.86, 129.01, 126.56, 120.40, 110.50, 107.79, 55.68, 10.32; HRMS Calcd for $C_{15}H_{14}ONCl$ $[M+H]^+$: 260.0764; Found: 260.0837.

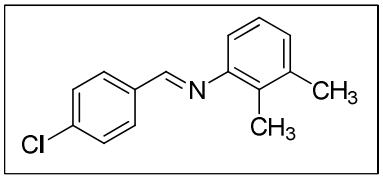

(*E*)-*N*-(4-chlorobenzylidene)-2,3-dimethylaniline **(3al)**

97 mg, 81% isolated yield. ^{1}H NMR ($CDCl_3$, 200 MHz) δ 8.32 (s, 1H), 7.87 (d, *J* = 8.7 Hz, 2H), 7.46 (d, *J*= 8.2 Hz, 2H), 7.17 - 7.04 (m, 2H), 6.79 (d, *J* = 7.2 Hz, 1H), 2.33 (s, 3H), 2.30 (s, 3H). ^{13}C NMR ($CDCl_3$, 50 MHz) δ 157.69, 150.67, 137.51, 137.05, 135.01, 130.47, 129.80, 128.98, 127.46, 126.02, 115.33, 20.09, 13.79; HRMS Calcd for $C_{15}H_{14}NCl$ $[M+H]^+$: 244.0888; Found: 244.0890.

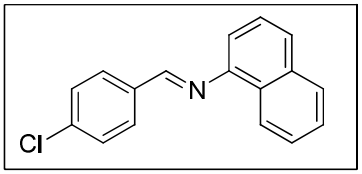

(E)-N-(4-chlorobenzylidene) naphthalen-1-amine **(3am)**

121 mg, 91% isolated yield. ^{1}H NMR ($CDCl_3$, 500 MHz) δ 8.6 (s, 1H), 7.91-7.86 (m, 5H), 7.62 (s, 1H), 7.53 - 7.45 (m, 5H). ^{13}C NMR ($CDCl_3$, 125 MHz) δ 158.92, 149.16, 137.38, 134.66, 134.00, 132.05, 129.97, 129.08, 129.00, 127.92, 127.71, 126.45, 125.47, 120.89, 117.93; HRMS Calcd for $C_{17}H_{12}NCl$ $[M+H]^+$: 266.0731; Found: 266.0733.

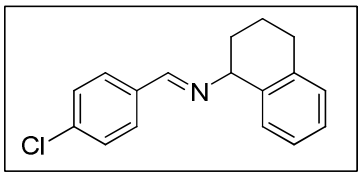

(E)-N-(4-chlorobenzylidene)-1,2,3,4-tetrahydronaphthalen-1-amine **(3an)**

109 mg, 81% isolated yield. ^{1}H NMR ($CDCl_3$, 500 MHz) δ 8.4 (s, 1H), 7.74 (d, *J* = 8.2 Hz, 2H), 7.40 (d, *J* = 8.9 Hz, 2H), 7.19 - 7.14 (m, 3H), 7.02 (2, *J* = 8.2 Hz, 1H), 4.54 (t, *J* = 7 Hz, 1H), 2.96 – 2.84 (m, 2H), 2.13 - 2.02 (m, 3H), 1.91 - 1.84 (m, 1H). ^{13}C NMR ($CDCl_3$, 125 MHz) δ 159.15 137.15, 136.96, 136.56, 134.80, 129.56, 129.25, 128.84, 128.58, 127.01, 125.83, 68.52, 31.52, 29.49, 20.10; HRMS Calcd for $C_{17}H_{16}NCl$ $[M+H]^+$: 270.1044; Found: 270.1042.

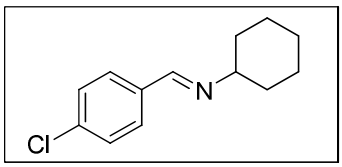

(E)-N-(4-chlorobenzylidene)cyclohexanamine **(3ao)**

82 mg, 74% isolated yield. ^{1}H NMR ($CDCl_3$, 500 MHz) δ 8.27 (s, 1H), 7.67 (d, *J* = 7.7 Hz, 2H), 7.37 (d, *J* = 7.7 Hz, 2H), 3.19 (s, 1H), 1.85 - 1.82 (m, 2H), 1.74 - 1.67 (m, 3H), 1.62 - 1.55 (m, 2H), 1.40 - 1.33 (m, 2H), 1.30 - 1.25 (m, 1H). ^{13}C NMR ($CDCl_3$, 125 MHz) δ 157.25, 136.16, 135.01, 129.20, 128.72, 69.92, 34.25, 25.55, 24.71; HRMS Calcd for $C_{13}H_{16}NCl$ $[M+H]^+$: 222.1044; Found: 222.1042.

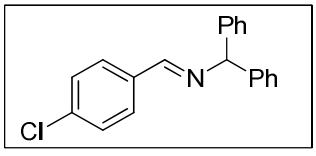

(E)-N-(4-chlorobenzylidene)-1,1-diphenylmethanamine **(3aq)**

94 mg, 62% isolated yield. ^{1}H NMR ($CDCl_3$, 500 MHz) δ 8.40 (s, 1H), 7.80 (d, *J* = 8.5 Hz, 2H), 7.42 – 7.30 (m, 11H), 7.26 – 7.20 (m, 1H), 5.62 (s, 1H). ^{13}C NMR ($CDCl_3$, 125 MHz) δ

159.44, 143.65, 136.70, 134.74, 129.62, 128.79, 128.46, 127.60, 127.05, 77.84; HRMS Calcd for $C_{20}H_{16}NCl$ $[M+H]^+$: 306.1044; Found: 306.1042.

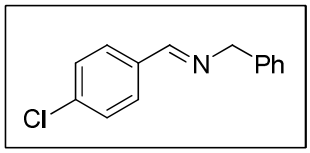

(E)-N-(4-chlorobenzylidene)-1-phenylmethanamine **(3ar)**

46 mg, 40% isolated yield. ^{1}H NMR ($CDCl_3$, 200 MHz) δ 8.25 (s, 1H), 7.63 (d, J = 8.5 Hz, 2H), 7.31 – 7.21 (m, 7H), 4.73 (d, J = 1.1 Hz, 1H). ^{13}C NMR ($CDCl_3$, 50 MHz) δ 160.47, 139.01, 136.66, 134.60, 129.41, 128.83, 128.50, 127.95, 127.04, 64.94; HRMS Calcd for $C_{14}H_{12}NCl$ $[M+H]^+$: 230.0731; Found: 230.0730.

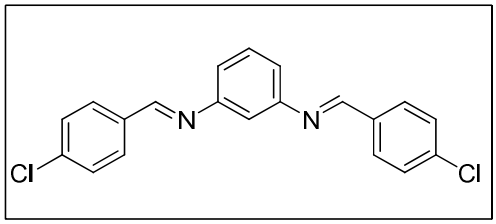

(E,E)-N^1,N^3-bis(4-chlorobenzylidene)benzene-1,3-diamine **(3as)**

132 mg, 75% isolated yield. ^{1}H NMR ($CDCl_3$, 500 MHz) δ 8.48 (s, 2H), 7.86 (d, J = 8.5 Hz, 4H), 7.47 (d, J = 8.5 Hz, 4H), 7.42 (t, J = 8.1 Hz, 1H), 7.11 (dd, J = 7.6, 1.8 Hz, 2H), 7.06 (s, 1H). ^{13}C NMR ($CDCl_3$, 125 MHz) δ 159.25, 152.64, 137.52, 134.53, 129.99, 129.86, 129.10, 129.01, 118.77, 113.04; HRMS Calcd for $C_{20}H_{14}N_2Cl_2$ $[M+H]^+$: 353.0607; Found: 353.0603.

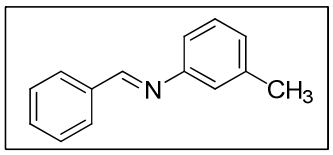

(E)-N-benzylidene-3-methylaniline **(3ba)**

70 mg, 72% isolated yield. ^{1}H NMR ($CDCl_3$, 200 MHz) δ 8.47 (s, 1H), 7.94 – 7.89 (m, 2H), 7.50–7.47 (m, 3H), 7.33 – 7.29 (m, 1H), 7.09 – 7.01 (m, 3H), 2.41 (s, 3H). ^{13}C NMR ($CDCl_3$,

50 MHz) δ ppm 160.25, 131.35, 129.79, 129.01, 128.80, 126.75, 121.66, 117.87, 21.45; HRMS Calcd for $C_{14}H_{13}N$ $[M+H]^+$: 196.1121; Found: 196.1121.

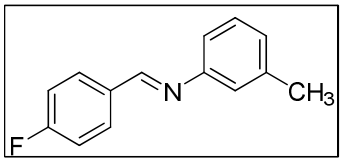

(E)-N-(4-fluorobenzylidene)-3-methylaniline **(3bb)**

92 mg, 86% isolated yield. ^{1}H NMR ($CDCl_3$, 200 MHz) δ 8.31 (s, 1H), 7.79 (d, *J* = 8.1 Hz, 2H), 7.23 - 6.90 (m, 6H), 2.30 (s, 3H). ^{13}C NMR ($CDCl_3$, 50 MHz) δ 167.12, 162.12, 158.52, 151.81, 138.96, 132.58, 130.77, 130.60, 128.95, 126.75, 121.55, 117.76, 116.07, 115.63, 21.34; HRMS Calcd for $C_{14}H_{12}NF$ $[M+H]^+$: 214.1027; Found: 214.1027.

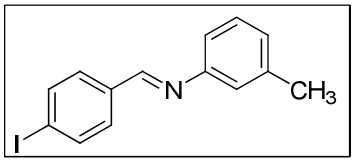

(E)-N-(4-iodobenzylidene)-3-methylaniline **(3bc)**

125 mg, 78% isolated yield. ^{1}H NMR ($CDCl_3$, 400 MHz) δ 8.37 (s, 1H), 7.81 (d, *J* = 8.2 Hz, 2H), 7.61 (d, *J* = 8.2 Hz, 2H), 7.26 (s, 1H), 7.06-6.99 (m, 1H), 2.38 (s, 3H); ^{13}C NMR ($CDCl_3$, 100 MHz) δ 158.91, 151.62, 139.04, 137.97, 135.70, 130.14, 129.01, 127.00, 121.57, 117.79, 98.09, 21.38; HRMS Calcd for $C_{14}H_{12}NI$ $[M+H]^+$: 322.0087; Found: 322.0086.

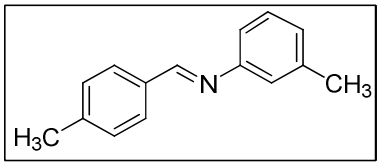

(E)-3-methyl-N-(4-methylbenzylidene)aniline **(3bd)**

53 mg, 51% isolated yield. ^{1}H NMR ($CDCl_3$, 200 MHz) δ 8.32 (s, 1H), 7.70 (d, *J* = 8.8 Hz, 2H), 7.20-7.15 (m, 3H), 6.97-6.91 (m, 3H), 2.33 (s, 3H), 2.30 (s, 3H). ^{13}C NMR ($CDCl_3$, 50

MHz) δ 160.07, 152.22, 141.72, 138.87, 133.71, 129.45, 128.90, 128.74, 126.47, 121.60, 117.81, 21.56, 21.36; HRMS Calcd for $C_{15}H_{15}N$ $[M+H]^+$: 210.1277; Found: 210.1277.

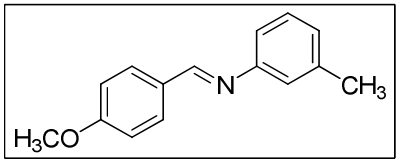

(*E)-N-(4-methoxybenzylidene)-3-methylaniline* **(3be)**

70 mg, 62% isolated yield. ^{1}H NMR ($CDCl_3$, 200 MHz) δ 8.38 (s, 1H), 7.84 (d, *J* = 8.9 Hz, 2H), 7.31-7.23 (m, 1H), 7.04 - 6.96 (m, 5H), 3.87 (s, 3H), 2.38 (s, 3H). ^{13}C NMR ($CDCl_3$, 125 MHz) δ 162.15, 159.53, 152.30, 138.90, 130.44, 129.25, 128.91, 126.31, 121.61, 117.81, 114.13, 55.41, 21.40.

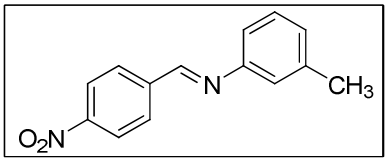

(E)-3-methyl-N-(4-nitrobenzylidene)aniline **(3bf)**

96 mg, 80% isolated yield. ^{1}H NMR ($CDCl_3$, 400 MHz) δ 8.56 (s, 1H), 8.34 (d, *J* = 8.7 Hz, 2H), 8.08 (d, *J* = 8.7 Hz, 2H), 7.33 (t, *J* = 7.3 Hz, 1H), 7.14-7.07 (m, 3H), 2.42 (s, 3H). ^{13}C NMR ($CDCl_3$, 100 MHz)) δ 157.19, 151.01, 149.34, 141.74, 139.32, 129.43, 129.23, 127.93, 124.09, 121.78, 118.00, 77.08, 21.47; HRMS Calcd for $C_{14}H_{12}O_2N_2$ $[M+H]^+$: 241.0972; Found: 241.0972.

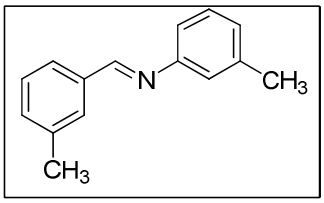

(E)-3-methyl-N-(3-methylbenzylidene)aniline **(3bg)**

95 mg, 91% isolated yield. ^{1}H NMR ($CDCl_3$, 200 MHz) δ 8.33 (s, 1H), 7.67 (s, 1H), 7.56 (d, *J* = 7.8 Hz, 1H), 7.22-7.15 (m, 3H), 6.97-6.90 (m, 3H), 2.33 (s, 3H), 2.30 (s, 3H). ^{13}C NMR

($CDCl_3$, 50 MHz) δ 160.42, 152.16, 138.94, 138.52, 136.23, 132.15, 128.93, 128.62, 126.62, 126.37, 121.61, 117.81, 21.38, 21.28; HRMS Calcd for $C_{15}H_{15}N$ $[M+H]^+$: 210.1277; Found: 210.1279.

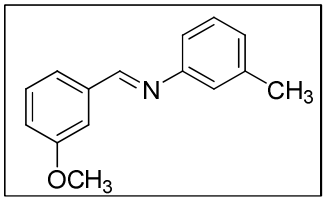

(E)-N-(3-methoxybenzylidene)-3-methylaniline **(3bh)**

67 mg, 60% isolated yield. ^1H NMR ($CDCl_3$, 200 MHz) δ 8.37 (s, 1H), 7.47-7.31 (m, 3H), 7.23-7.19 (dd, J = 7.3, 2.6 Hz, 1H), 7.02-6.69 (m, 4H), 3.84 (s, 3H), 2.34 (s, 3H). ^{13}C NMR ($CDCl_3$, 125 MHz) δ 162.15, 159.53, 152.30, 138.90, 130.44, 129.25, 128.91, 126.31, 121.61, 117.81, 114.13, 55.41, 21.40; HRMS Calcd for $C_{15}H_{15}NO$ $[M+H]^+$: 226.1226; Found: 226.1227.

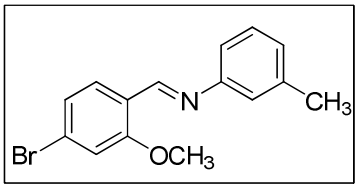

(E)-N-(4-bromo-2-methoxybenzylidene)-3-methylaniline **(3bi)**

70 mg, 46% isolated yield. ^1H NMR ($CDCl_3$, 500 MHz) δ 8.78 (s, 1H), 7.97 (d, J = 8.2 Hz, 1H), 7.23-6.96 (m, 6H), 3.86 (s, 3H), 2.35 (s, 3H). ^{13}C NMR ($CDCl_3$, 125 MHz) δ 159.66, 155.14, 152.33, 138.90, 128.89, 128.65, 126.67, 126.46, 124.15, 123.79, 121.71, 118.01, 115.33, 114.69, 55.83, 21.38; HRMS Calcd for $C_{15}H_{14}ONBr$ $[M+H]^+$: 304.0332; Found: 304.0333.

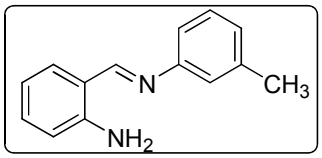

(E)-N-(2-aminobenzylidene)-3-methylaniline **(3bj)**

70 mg, 67% isolated yield. ^{1}H NMR ($CDCl_3$, 500 MHz) δ 8.53 (s, 1H), 7.35 (d, *J* = 8.0 Hz, 1H), 7.20 (d, *J* = 8.0 Hz, 1 H), 7.06-6.99 (m, 3H), 6.77-6.70 (m, 3H), 6.53(s, 1H), 2.40 (s, 3H). HRMS Calcd for $C_{14}H_{14}N_2$ $[M+H]^+$: 211.1230; Found: 211.1230.

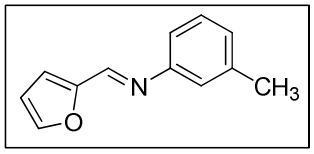

(E)-N-(furan-2-ylmethylene)-3-methylaniline **(3bk)**

70 mg, 76% isolated yield. ^{1}H NMR ($CDCl_3$, 200 MHz) δ 8.24 (s, 1H), 7.57 (s, 1H), 7.24-7.19 (m, 1H), 7.03-6.99 (m, 3H), 6.90 (d, *J* = 3.5 Hz, 1H), 6.52-6.50 (m, 1H), 2.34 (s, 3H). ^{13}C NMR ($CDCl_3$, 100 MHz) δ 152.10, 151.32, 147.49, 145.52, 138.94, 128.93, 126.97, 121.65, 118.02, 116.04, 112.08, 21.35; HRMS Calcd for $C_{12}H_{11}ON$ $[M+H]^+$: 186.0913; Found: 186.0914.

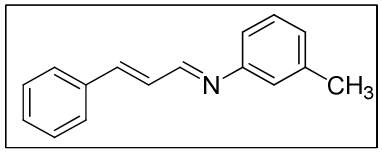

(E)-3-methyl-N-((E)-3-phenylallylidene)aniline **(3bl)**

50 mg, 45% Isolated yield. ^{1}H NMR ($CDCl_3$, 500 MHz) δ 8.26 (d, *J* = 7.5 Hz, 1H), 7.53 (d, *J* = 7.5 Hz, 1H), 7.40-7.34 (m, 3H), 7.25 (d, *J* = 6.5Hz, 1H), 7.16-6.97 (m, 3H), 2.37 (s, 3H). ^{13}C NMR ($CDCl_3$, 125 MHz) δ 161.44, 151.71, 143.83, 138.99, 135.62, 129.54, 128.98, 128.91, 128.65, 127.47, 126.89, 121.61, 117.95, 21.39; HRMS Calcd for $C_{16}H_{15}N$ $[M+H]^+$: 222.1277; Found: 222.1277.

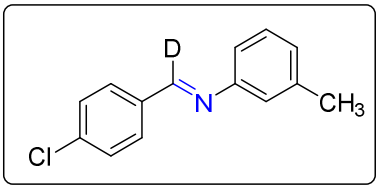

(E)-1-(4-chlorophenyl)-N-(m-tolyl)methanimine-d **(3aa-*d*)**

^{1}H NMR ($CDCl_3$, 500 MHz) δ 7.85 (d, J = 8.4 Hz, 2H), 7.46 (d, J = 8.4 Hz, 2H), 7.29 (t, J = 7.2 Hz, 1H), 7.08-7.02 (m, 3H), 2.40 (s, 3H); HRMS Calcd for $C_{14}H_{11}NClD$ $[M+H]^+$: 231.0794; Found: 231.0794.

6. References

[1] Armarego, W. L. F. & Perrin, D. D. Purification of Laboratory Chemicals (Pergamon Press, Oxford, 1988) ed 3.

[2] D. C. Marcano, D. V. Kosynkin, J. M. Berlin, A. Sinitskii, Z. Sun, A. Slesarev, L. B. Alemany, W. Lu and J. M. Tour *ACS Nano,* 2010, **8**, 4806-4814.

[3] A. Ganguly, S. Sharma, P. Papakonstantinou and J. Hamilton, *J. Phys. Chem. C*, 2011, **115**, 17009-17019.

[4] S. Stankovich, D. A. Dikin, R. D. Piner, K. A. Kohlhaas, A. Kleinhammes, Y. Jia, Y. Wu, S. T. Nguyen and R. S. Ruoff, *Carbon*, 2007, **45**, 1558-1565.

[5] H.-K. Jeong, Y. P. Lee, R. J. W. E. Lahaye, M.-H. Park, K. H. An, I. J. Kim, C.-W. Yang, C. Y. Park, R. S. Ruoff and Y. H. Lee, *J. Am. Chem. Soc*., 2008, **130**, 1362-1366.

[6] D. Yang, A. Velamakanni, G. Bozoklu, S. Park, M. Stoller, R. D. Piner, S. Stankovich, I. Jung, D. A. Field, C. A. Ventrice Jr and R. S. Ruoff, *Carbon*, 2009, **47**, 145-152.

[7] J. W. Jang, C. E. Lee, S. C. Lyu, T. J. Lee and C. J. Lee, *Appl. Phys. Lett*., 2004, **84**, 2877-2879.

[8] J. R. Pels, F. Kapteijn, J. A. Moulijn, Q. Zhu and K. M. Thomas, *Carbon*, 1995, **33**, 1641-1653.

[9] R. V. Jagadeesh, H. Junge, M.-M. Pohl, J. Radnik, A. Brückner and M. Beller, *J. Am. Chem. Soc*., 2013, **135**, 10776-10782.

[10] R. McCann, S. S. Roy, P. Papakonstantinou, J. A. McLaughlin and S. C. Ray, *J. Appl. Phys*., 2005, **97**, 073522.

[11] J. Zhou, H. Song, L. Ma and X. Chen, *RSC Adv*., 2011, **1**, 782-791.

[12] E. Khaskin and D. Milstein, *ACS Catal.*, 2013, **3**, 448-452.

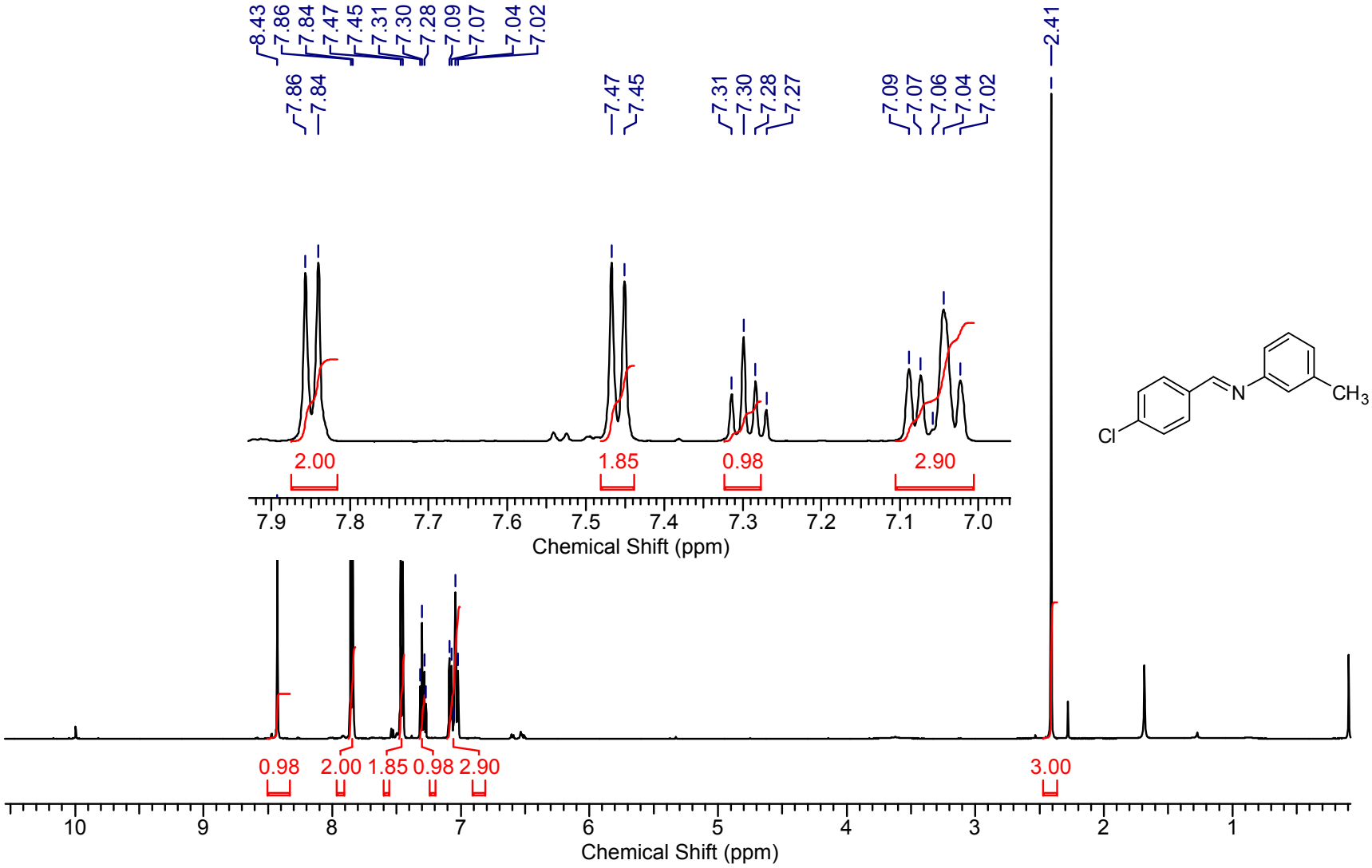

Supplementary Figure 1. ^{1}H NMR of **3aa**

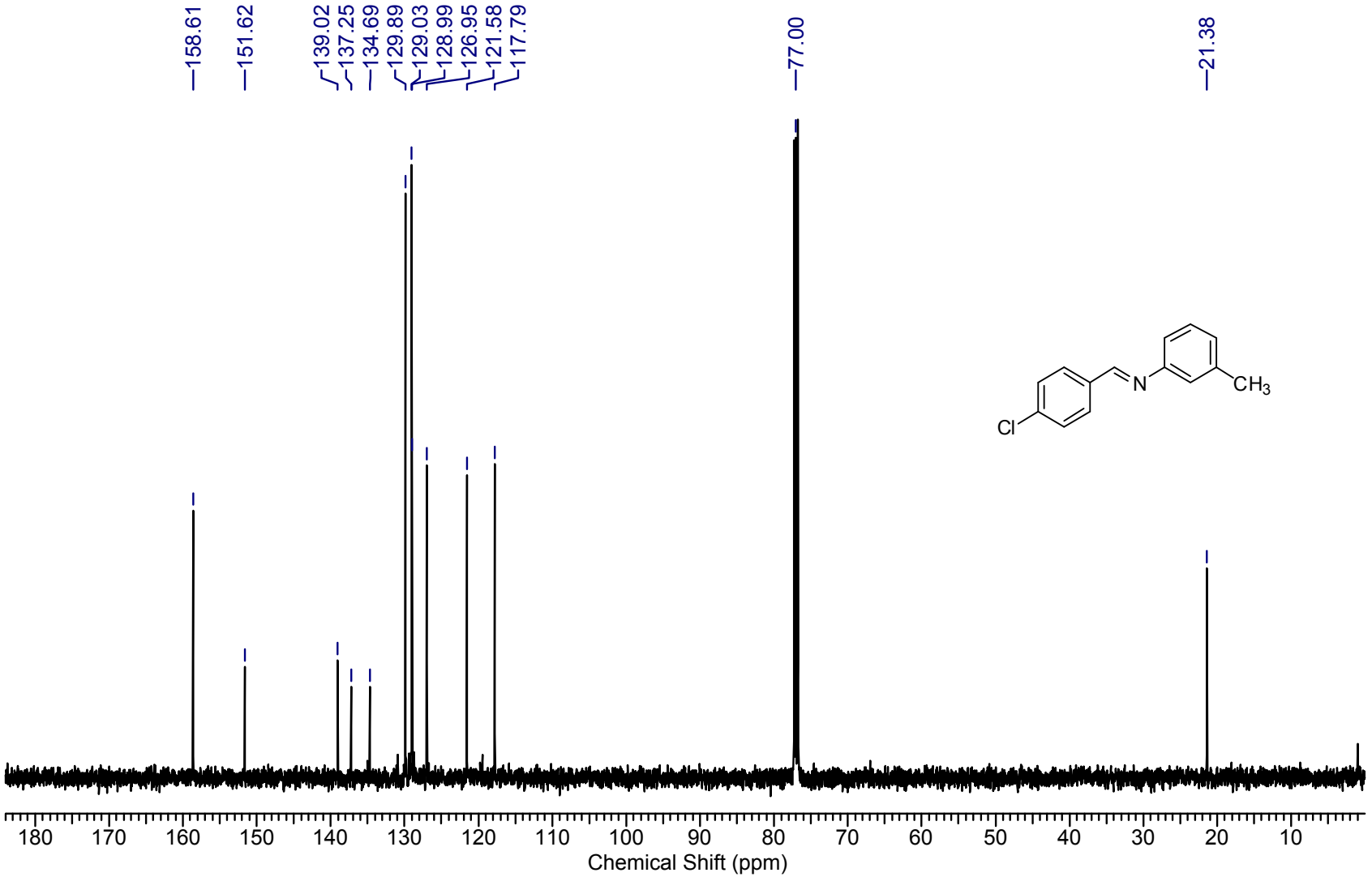

Supplementary Figure 2. ^{13}C NMR of **3aa**

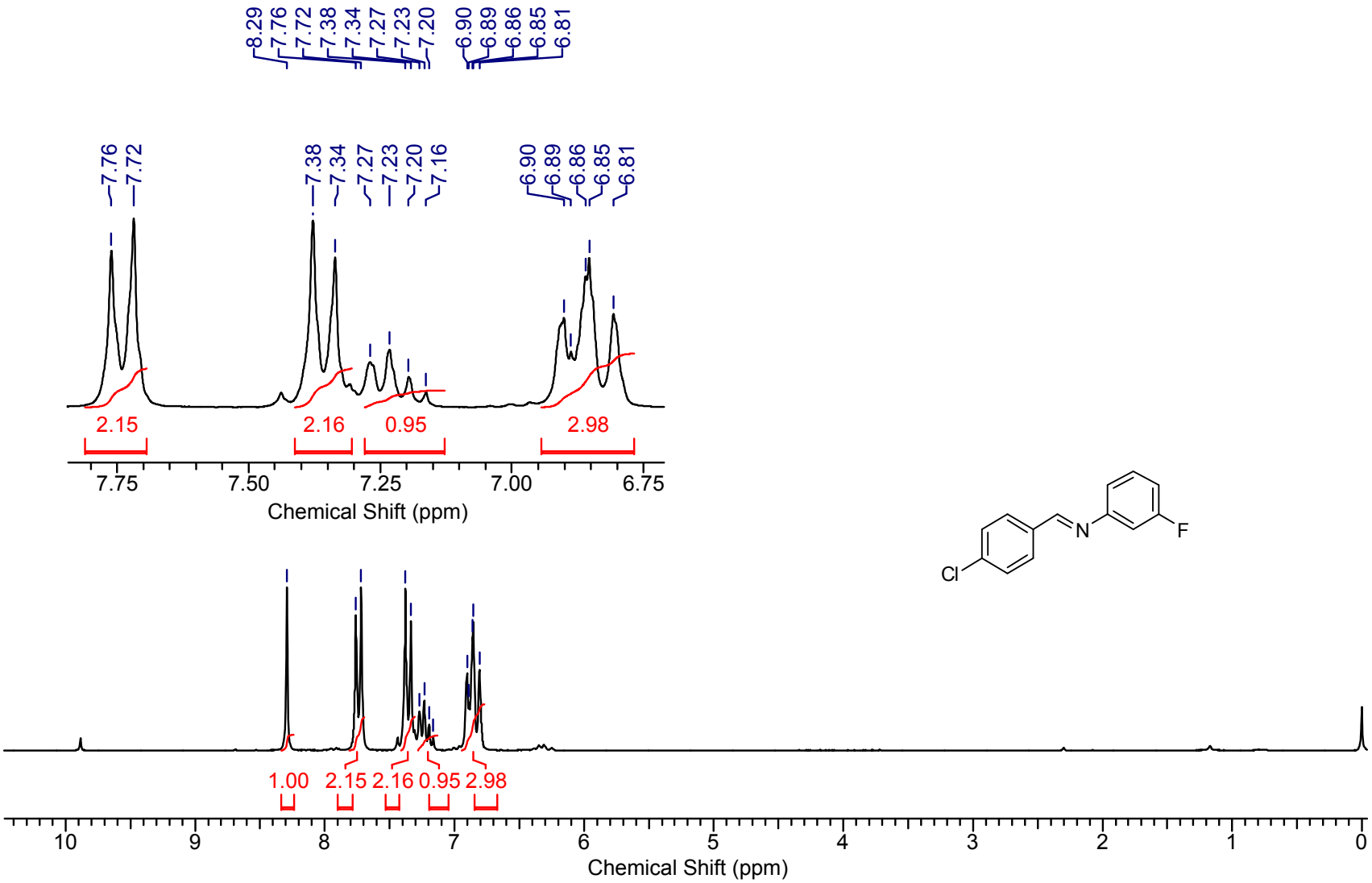

Supplementary Figure 3. ^{1}H NMR of **3ab**

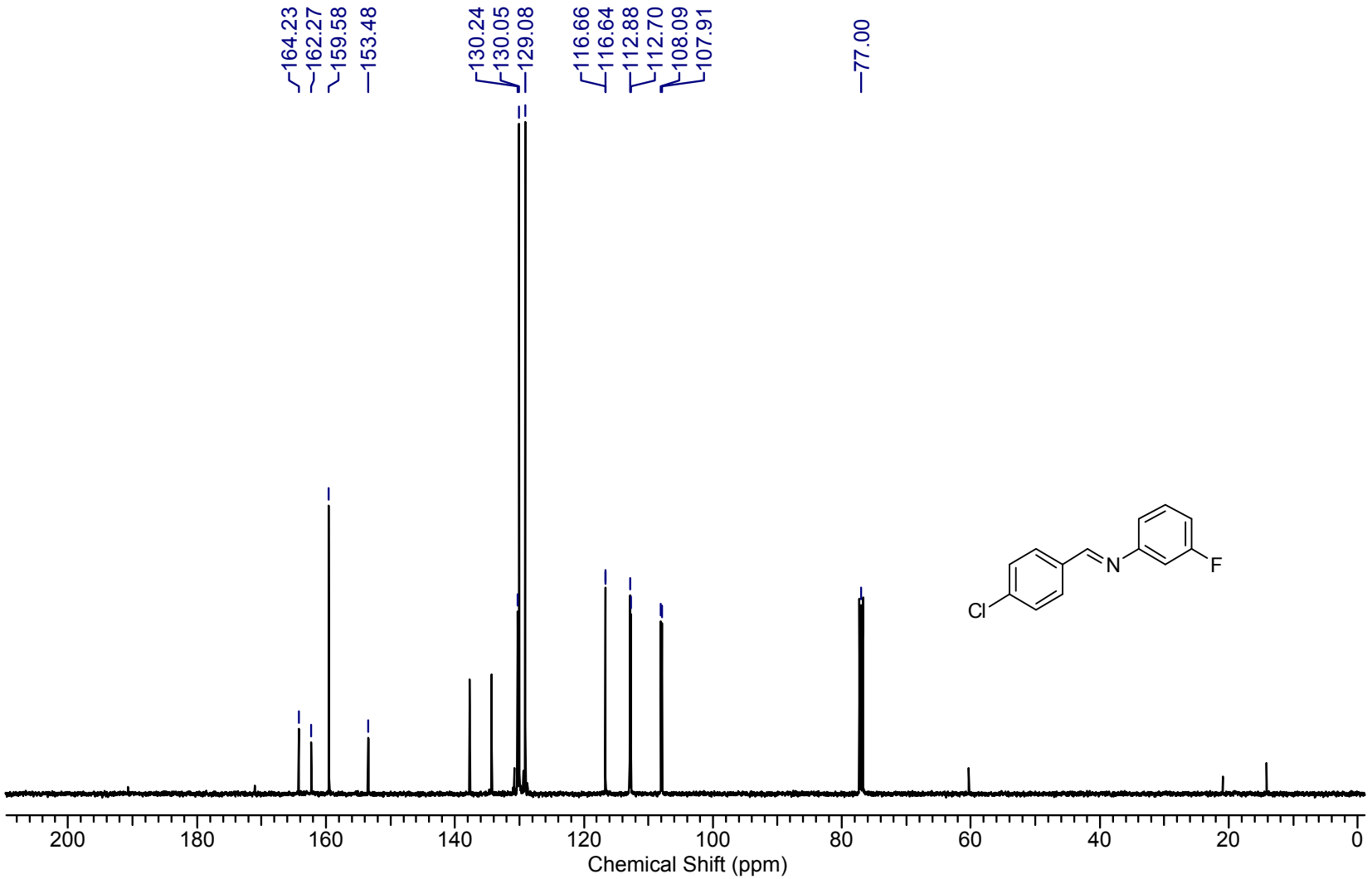

Supplementary Figure 4. ^{13}C NMR of **3ab**

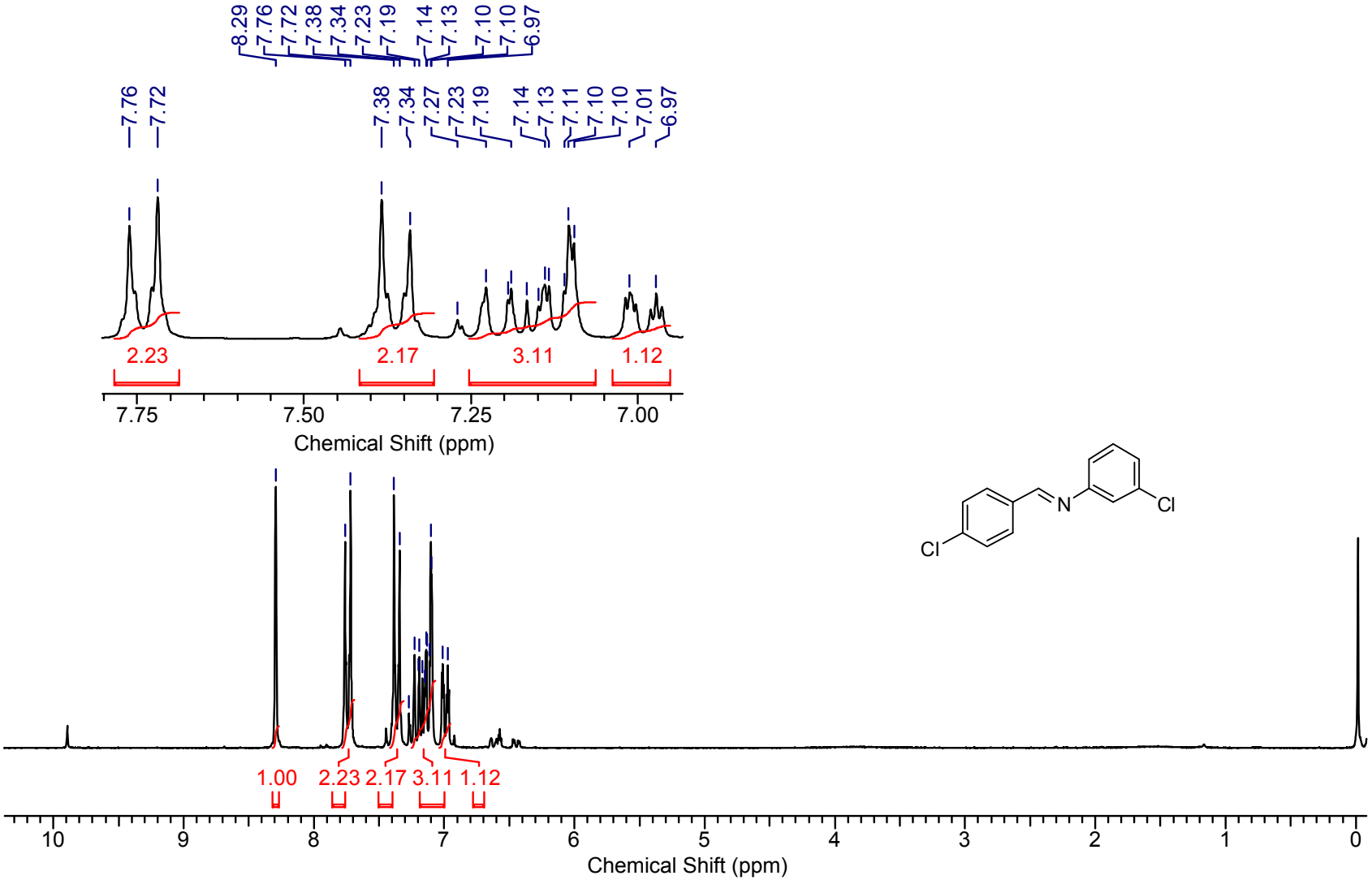

Supplementary Figure 5. ^{1}H NMR of **3ac**

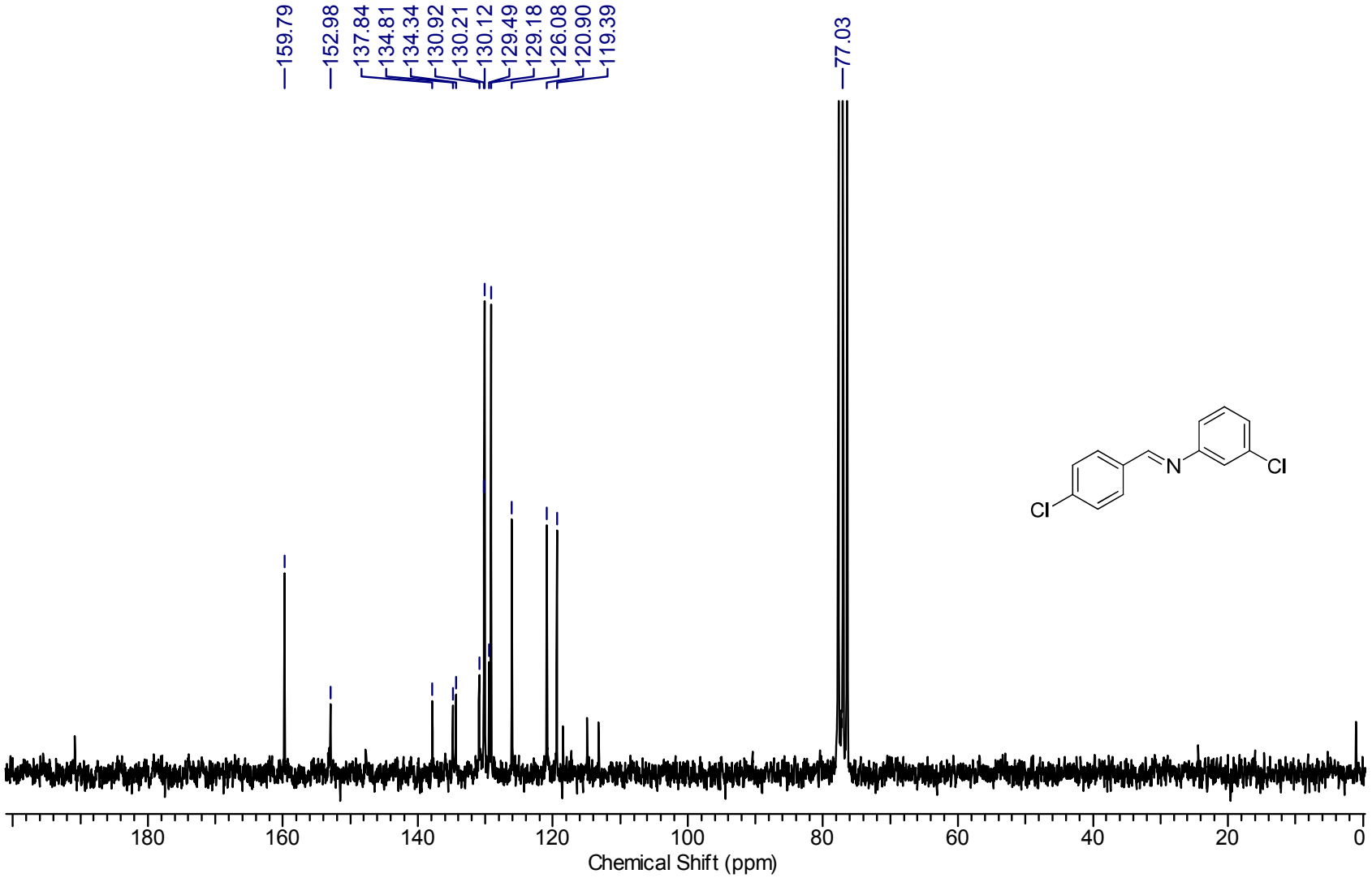

Supplementary Figure 6. ^{13}C NMR of **3ac**

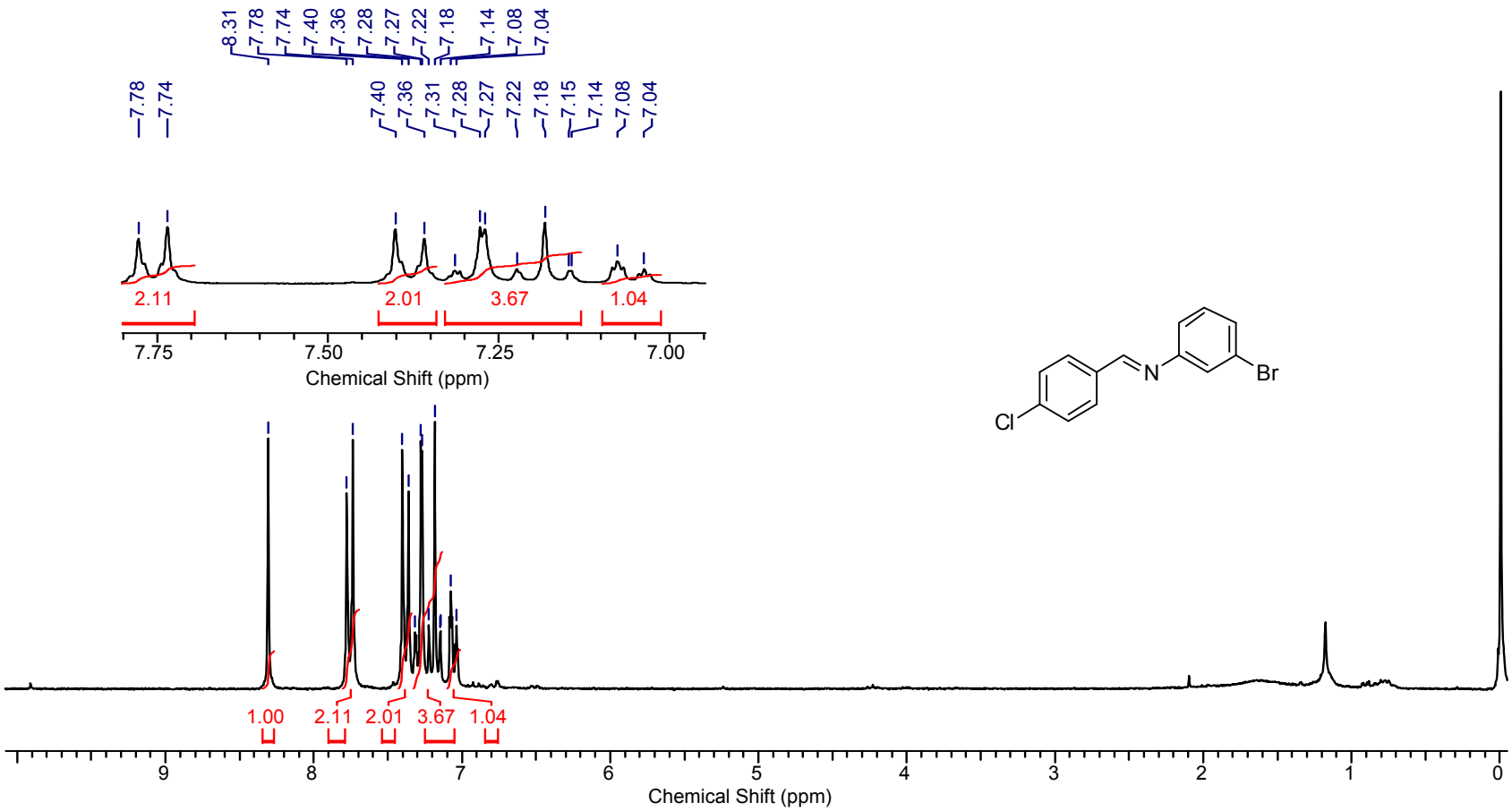

Supplementary Figure 7. ^{1}H NMR of **3ad**

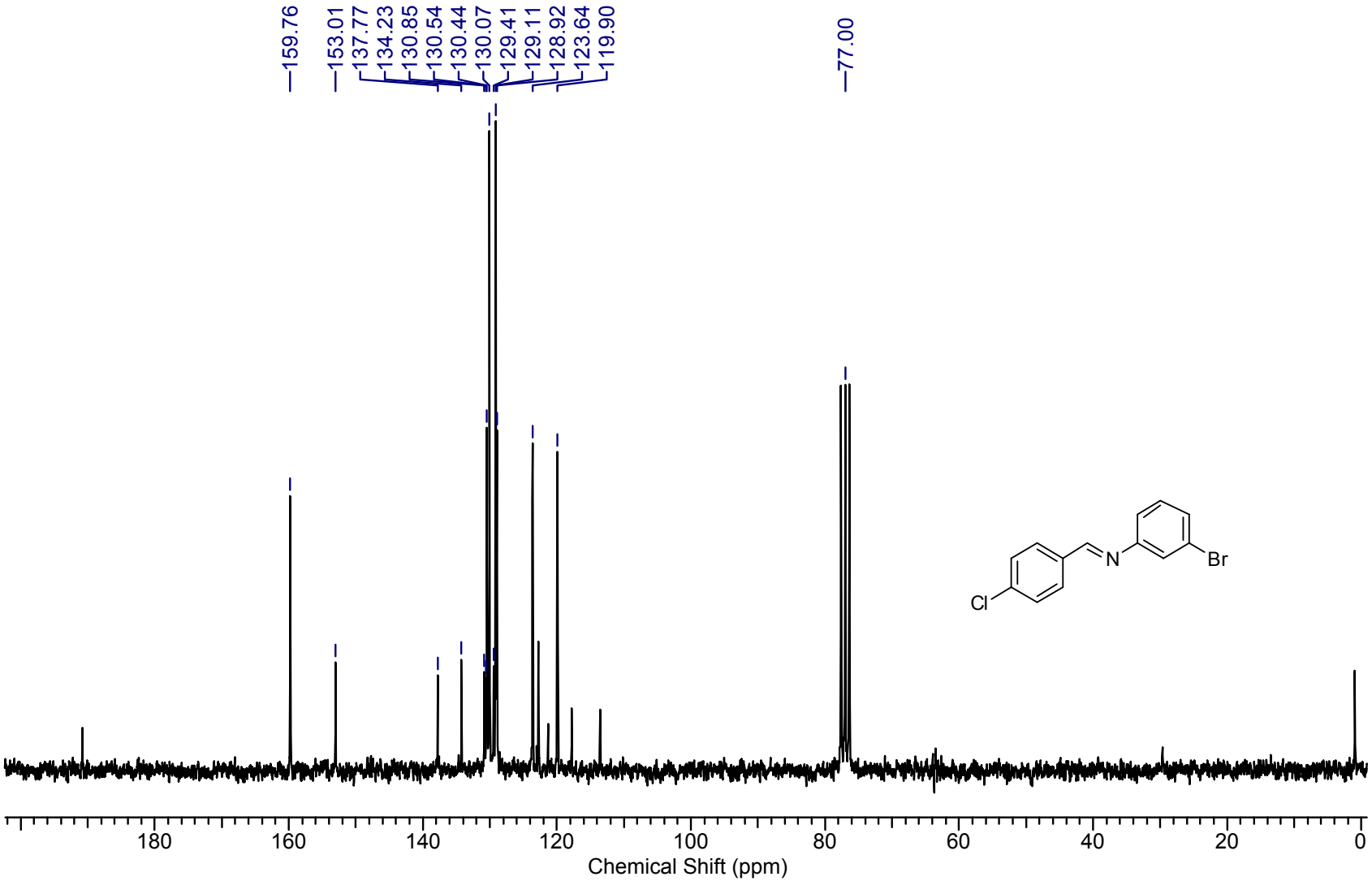

Supplementary Figure 8. ^{13}C NMR of **3ad**

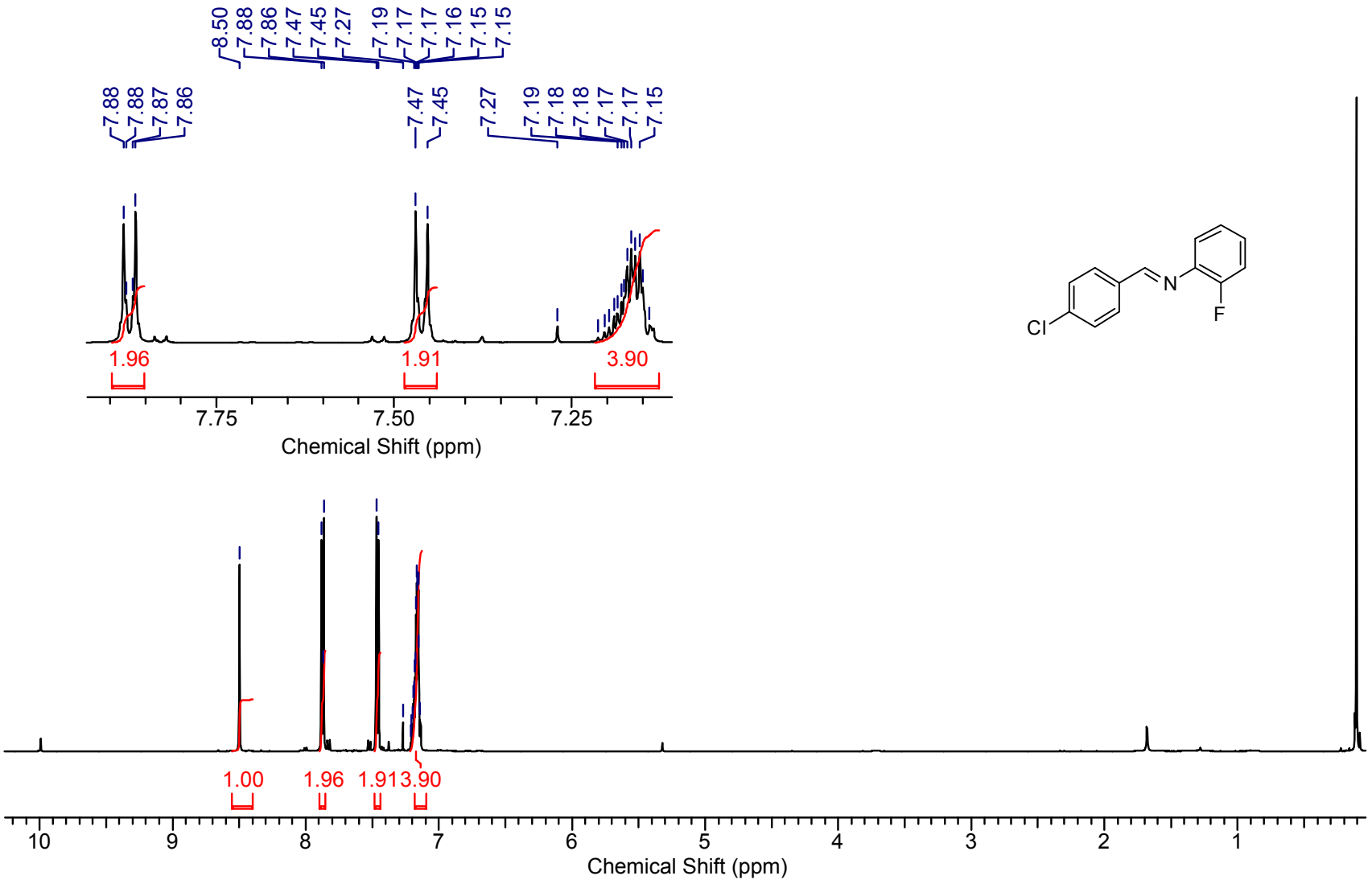

Supplementary Figure 9. ^{1}H NMR of **3ae**

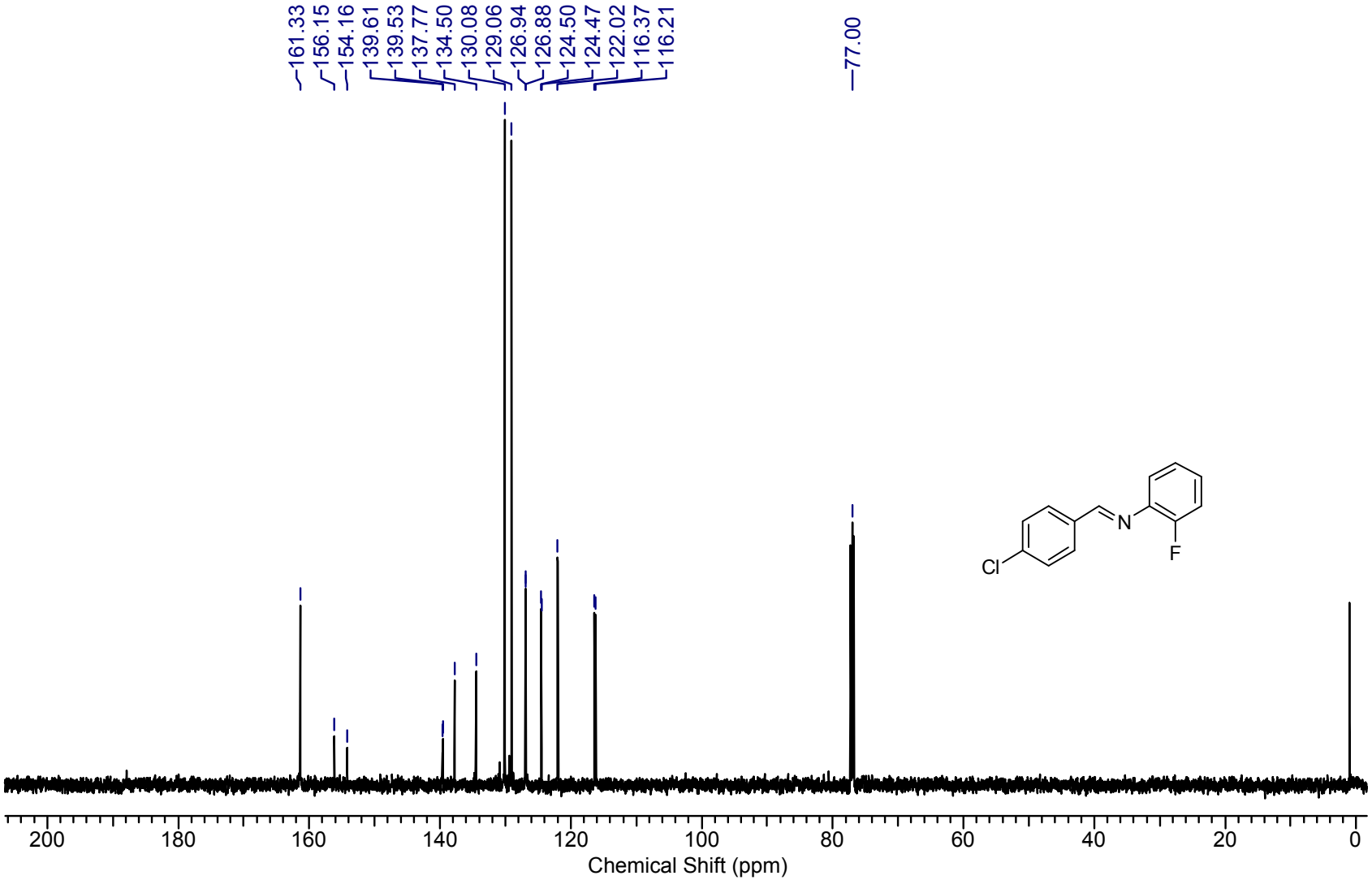

Supplementary Figure 10. ^{13}C NMR of **3ae**

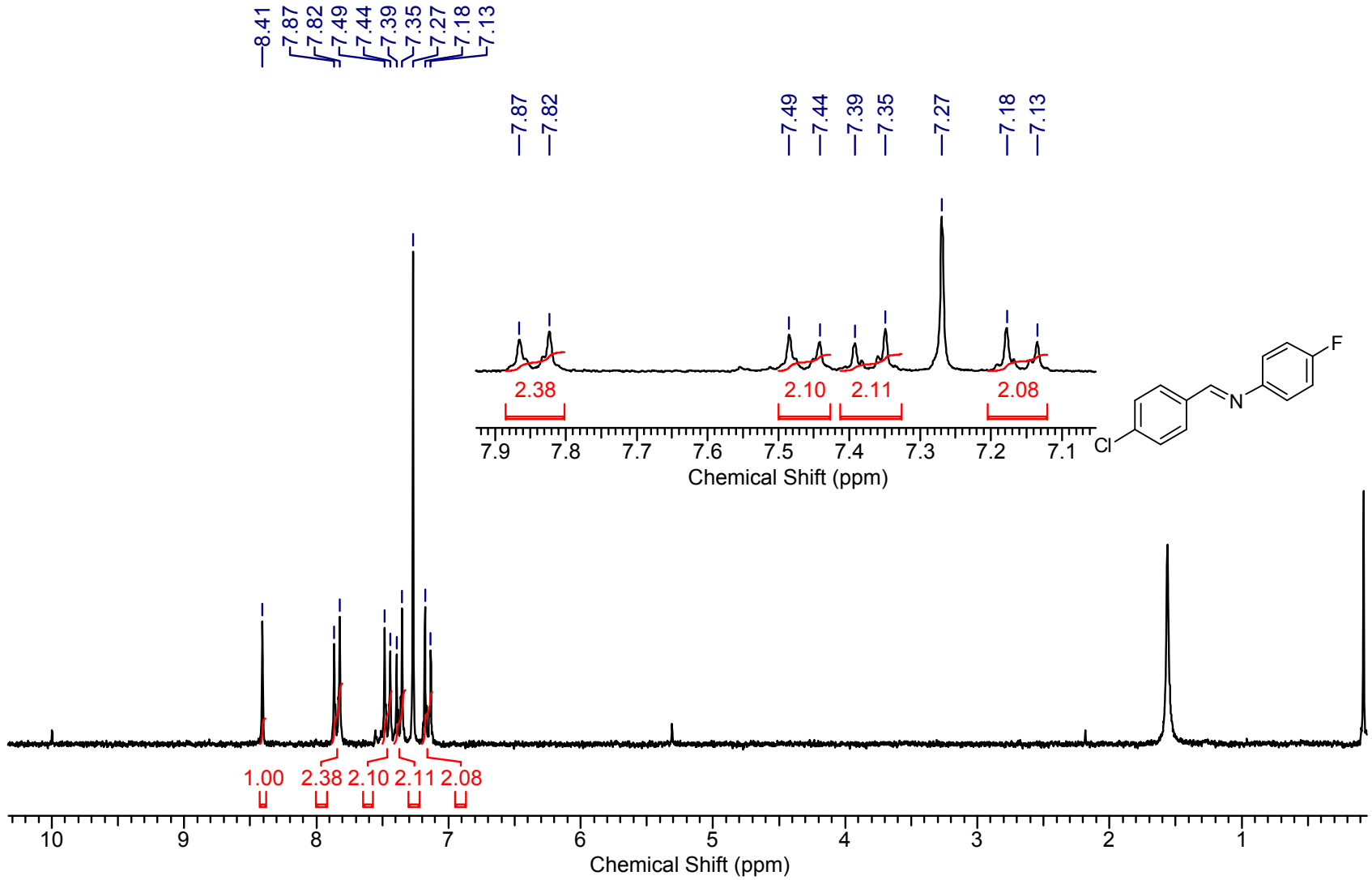

Supplementary Figure 11. ^{1}H NMR of **3af**

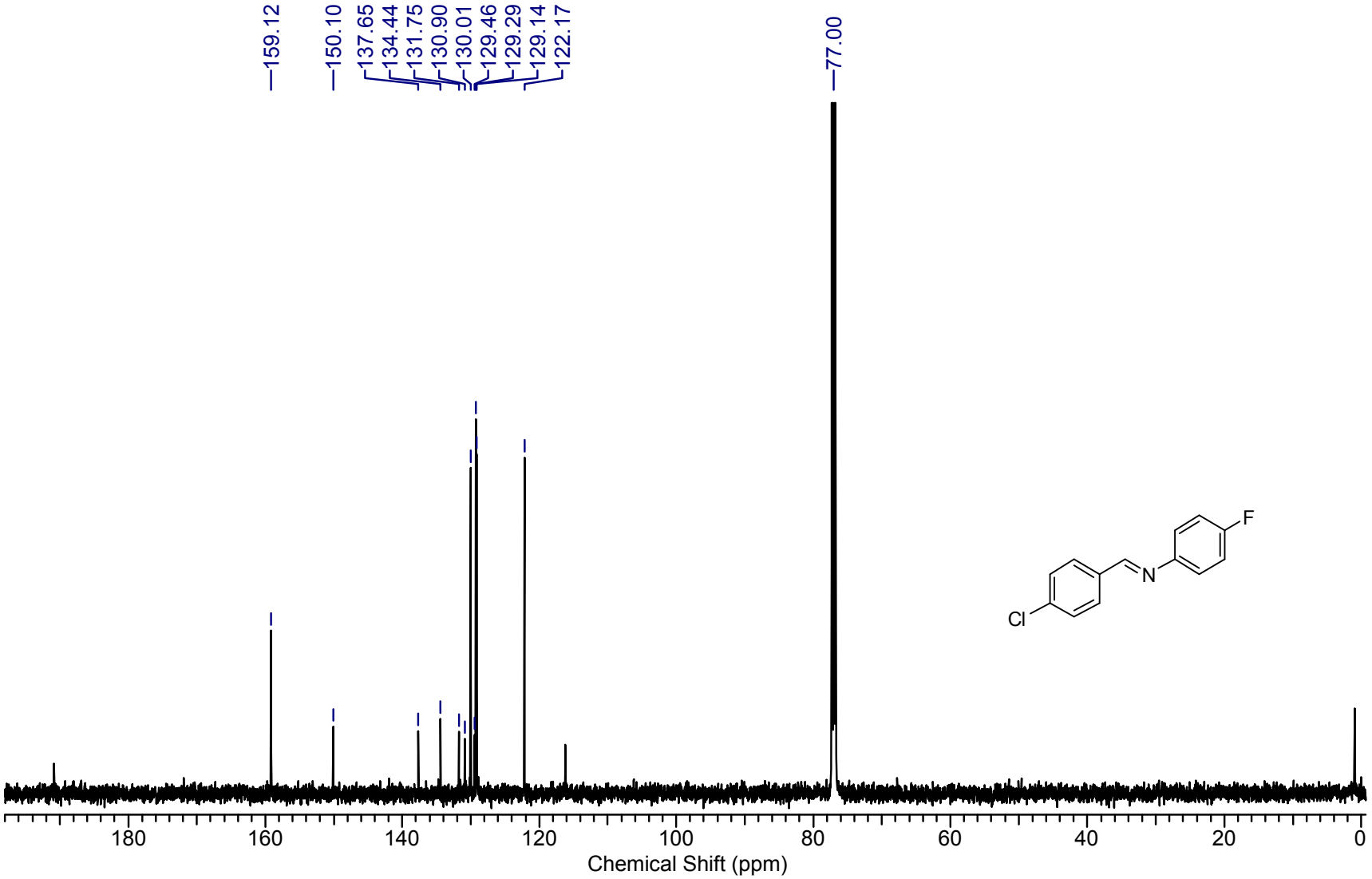

Supplementary Figure 12. ^{13}C NMR of **3af**

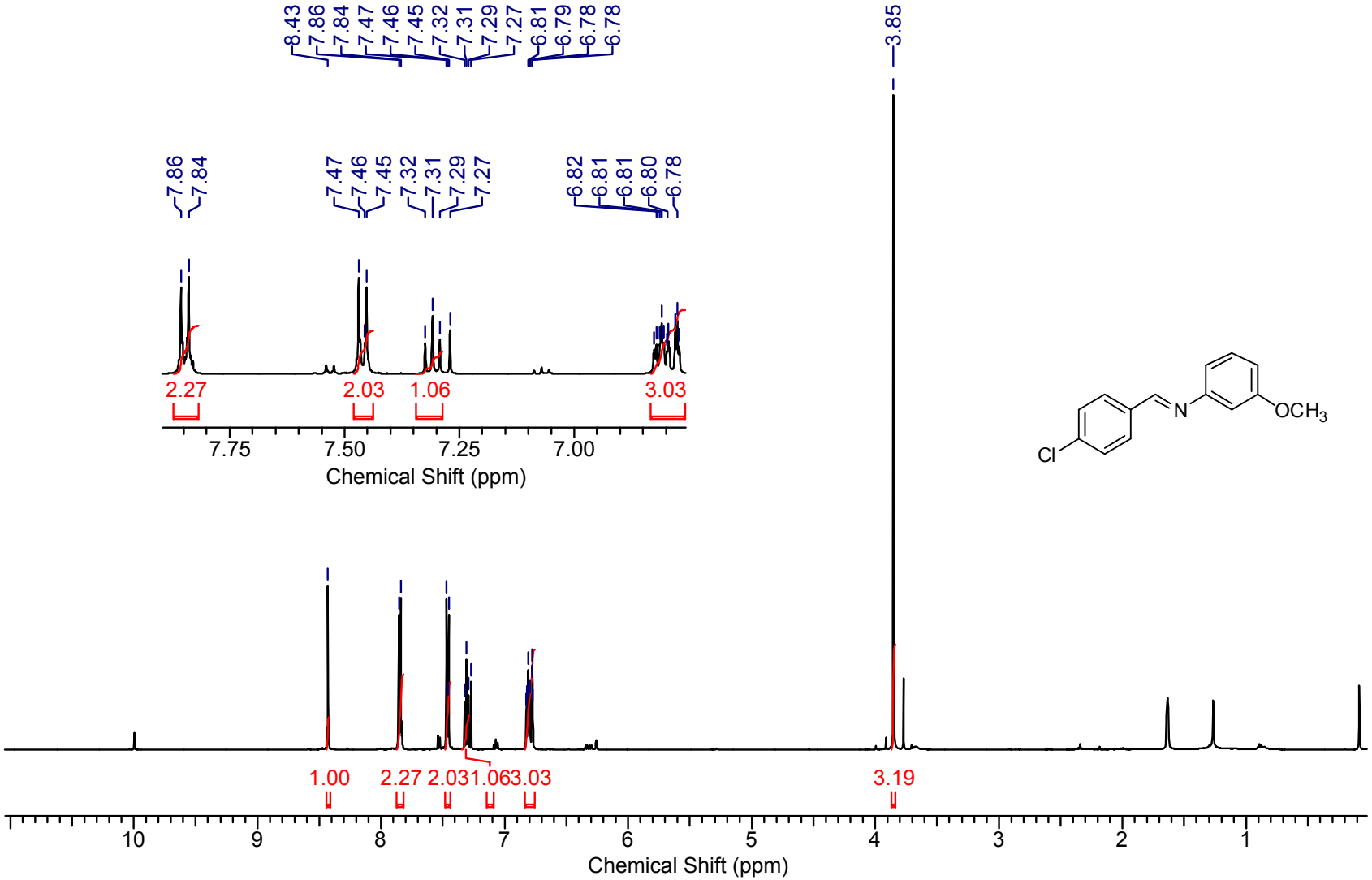

Supplementary Figure 13. ^{1}H NMR of **3ag**

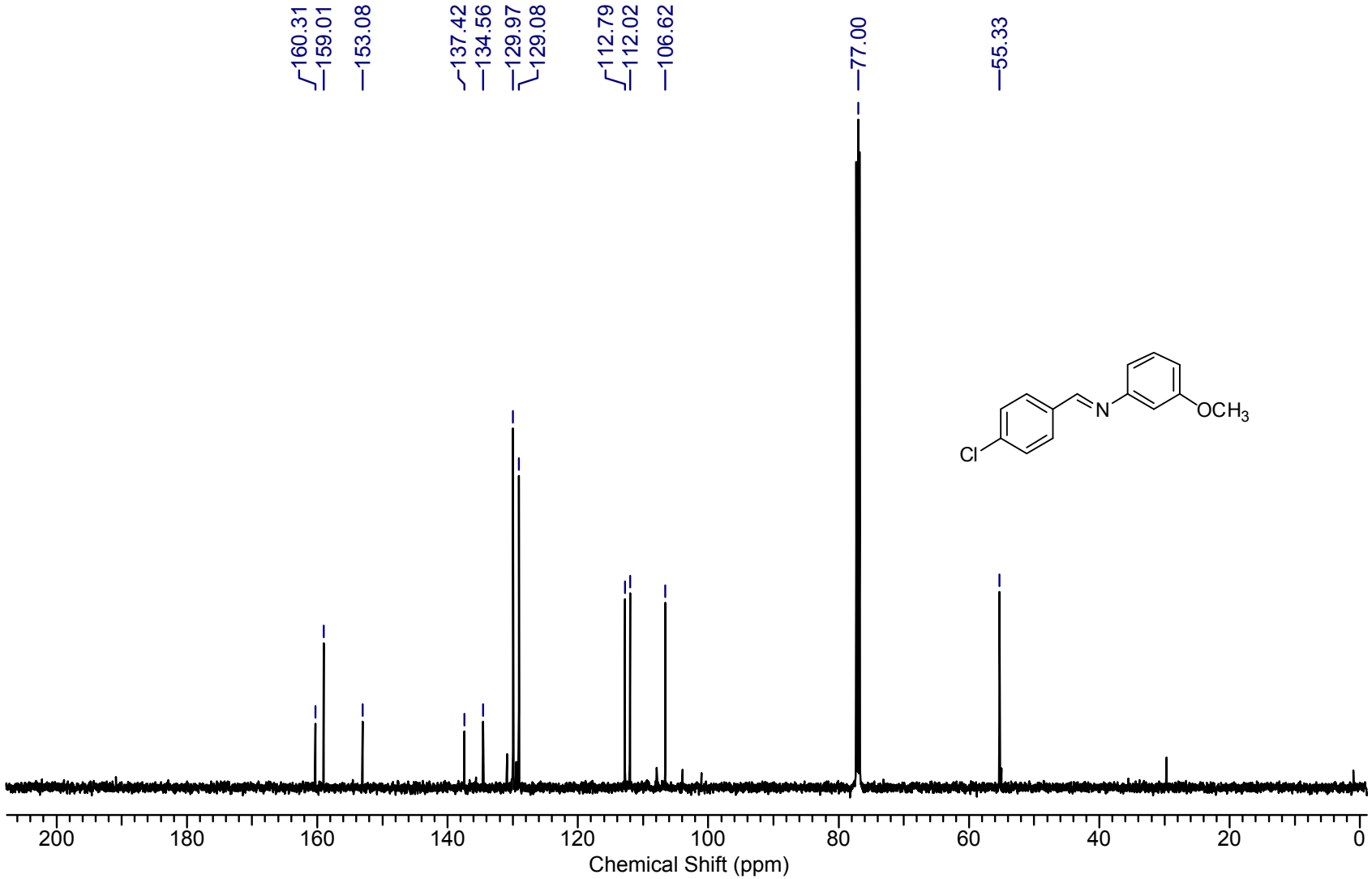

Supplementary Figure 14. ^{13}C NMR of **3ag**

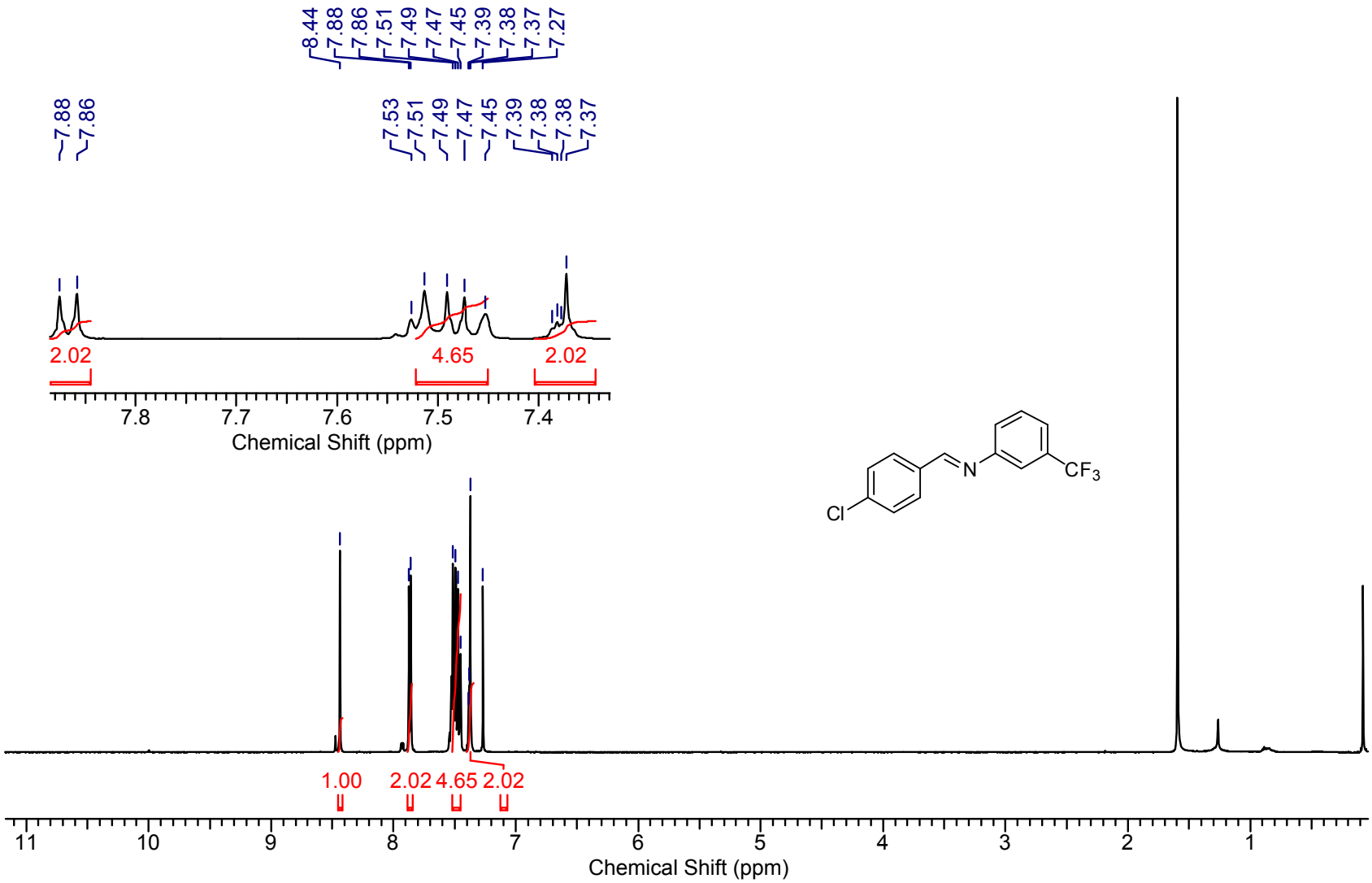

Supplementary Figure 15. ^{1}H NMR of **3ah**

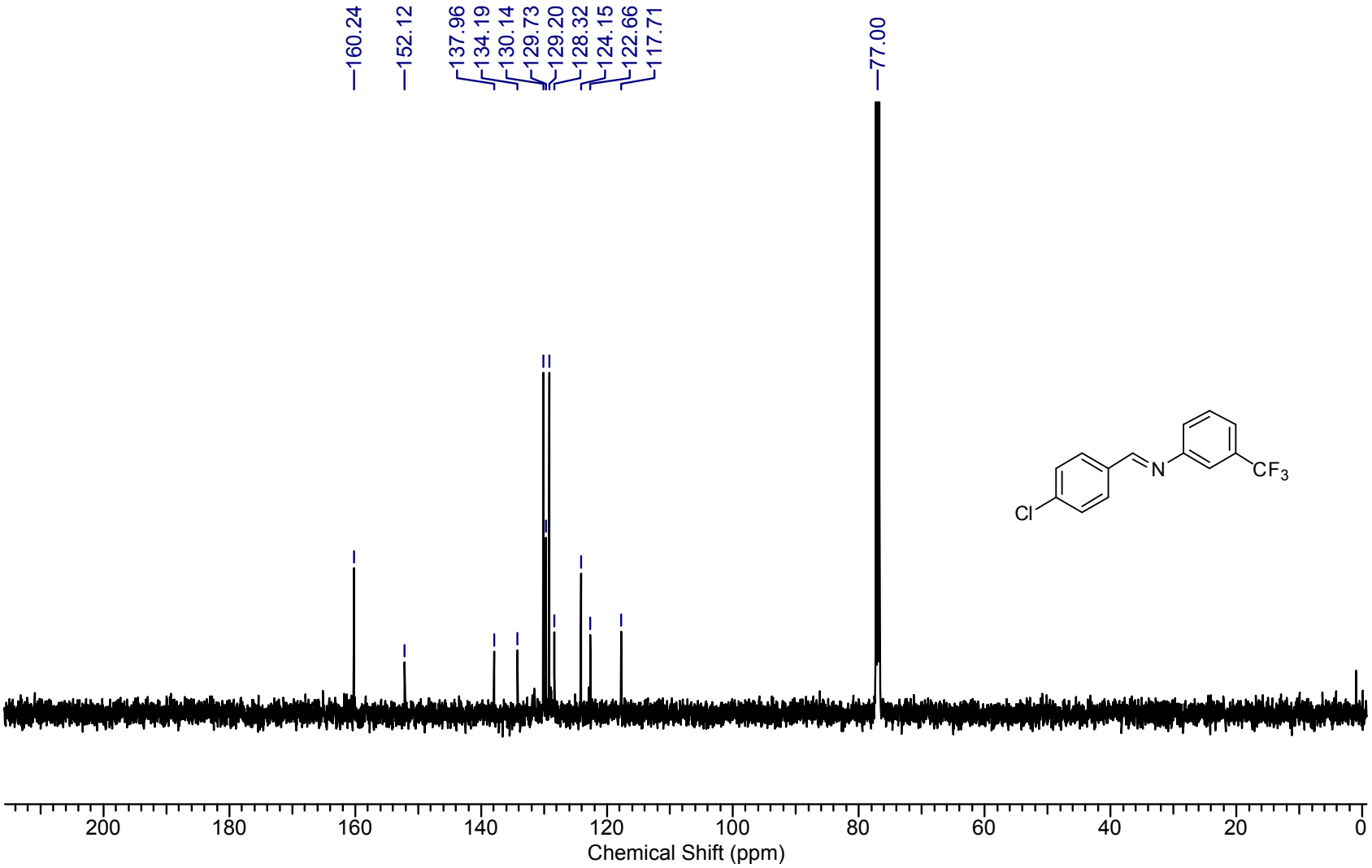

Supplementary Figure 16. ^{13}C NMR of **3ah**

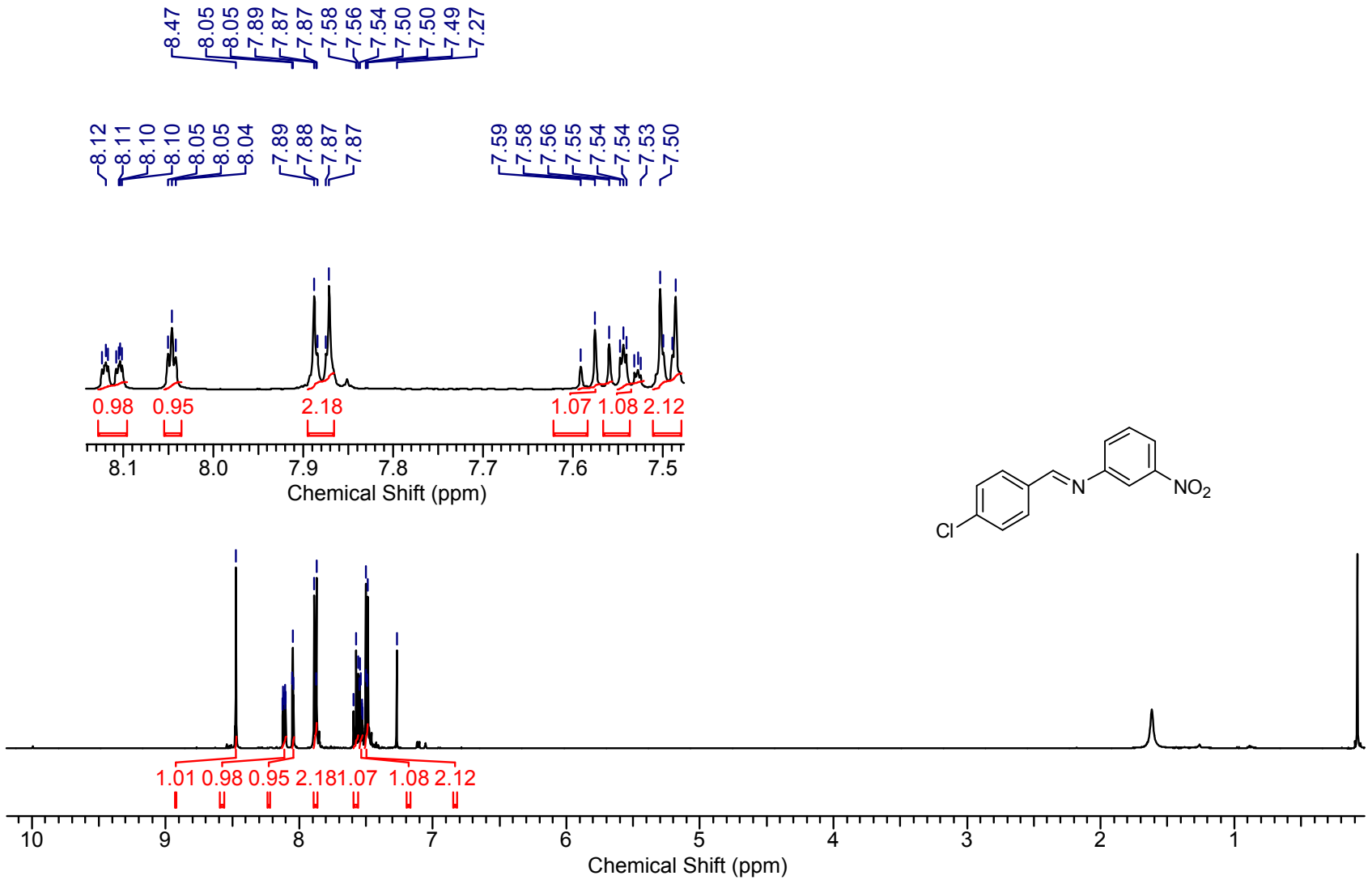

Supplementary Figure 17. ^{1}H NMR of **3ai**

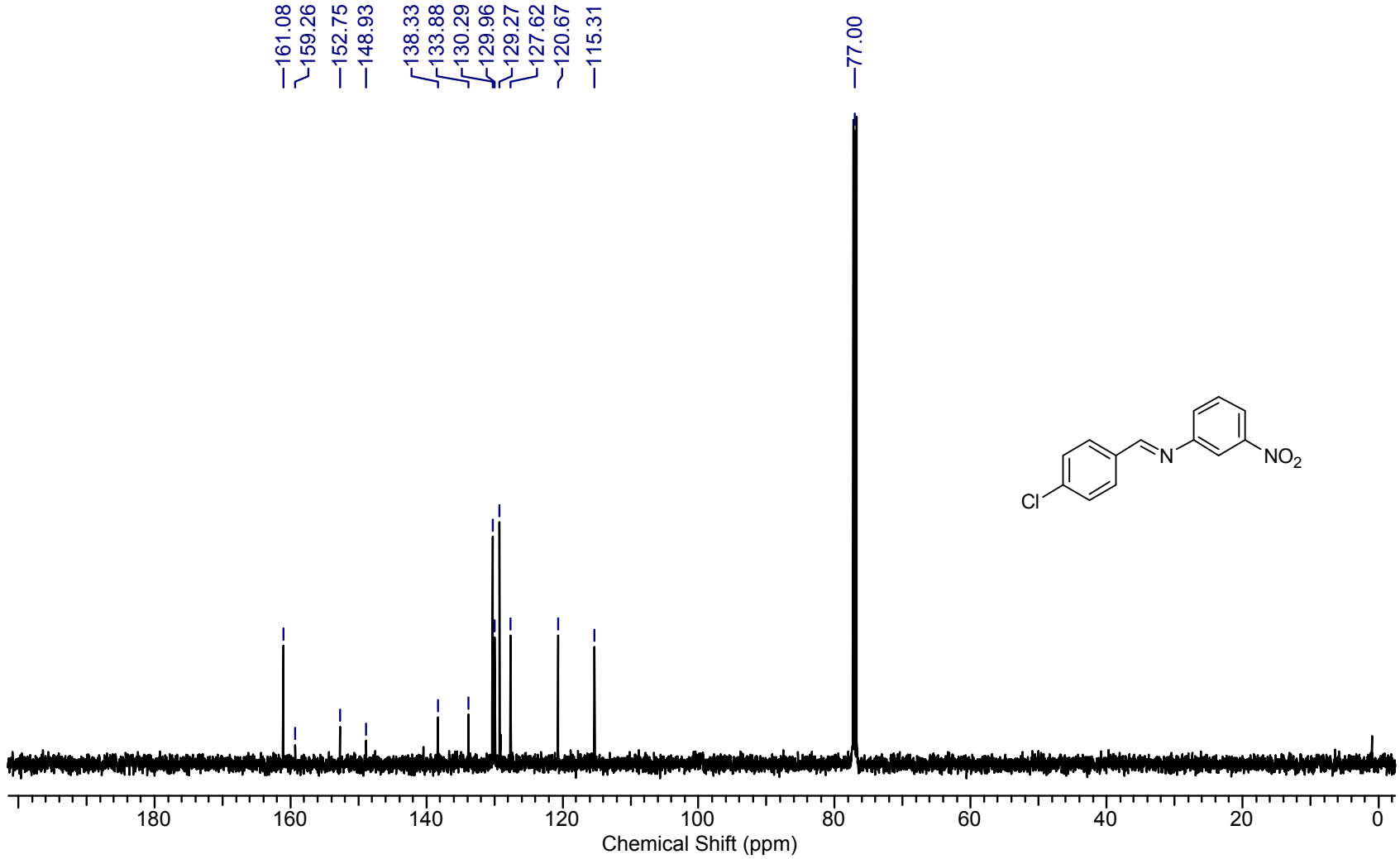

Supplementary Figure 18. ^{13}C NMR of **3ai**

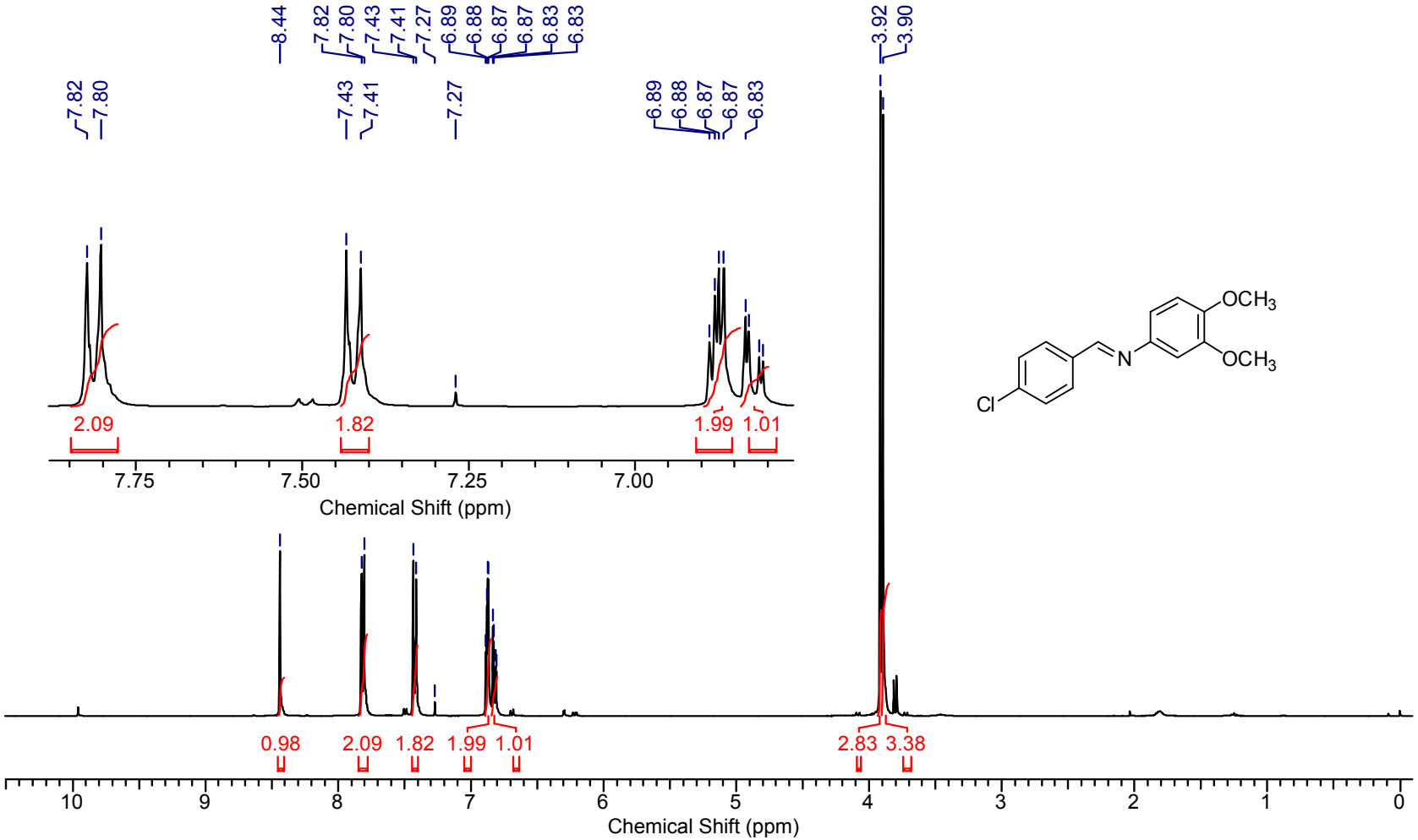

Supplementary Figure 19. ^{1}H NMR of **3aj**

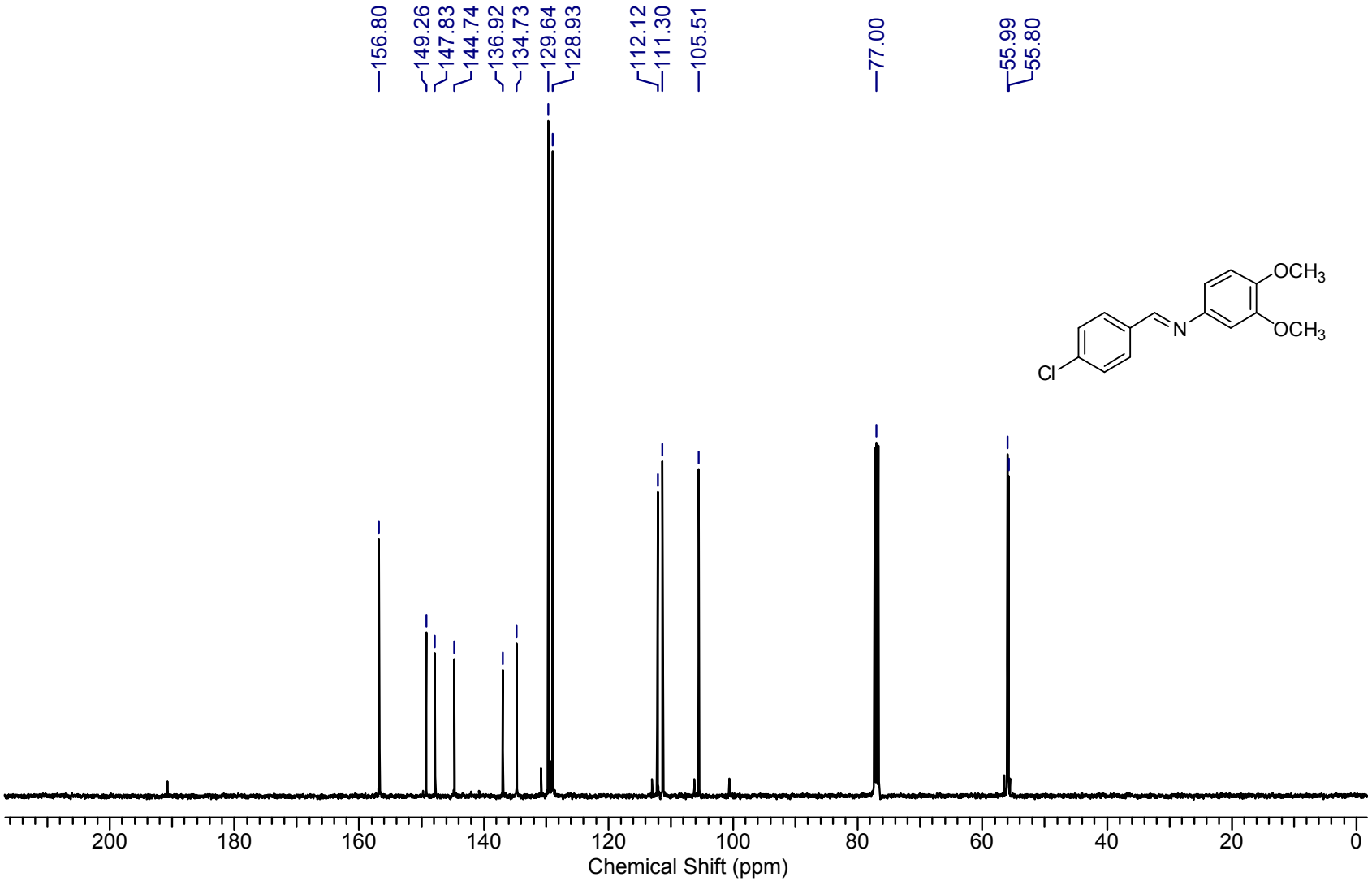

Supplementary Figure 20. ^{13}C NMR of **3aj**

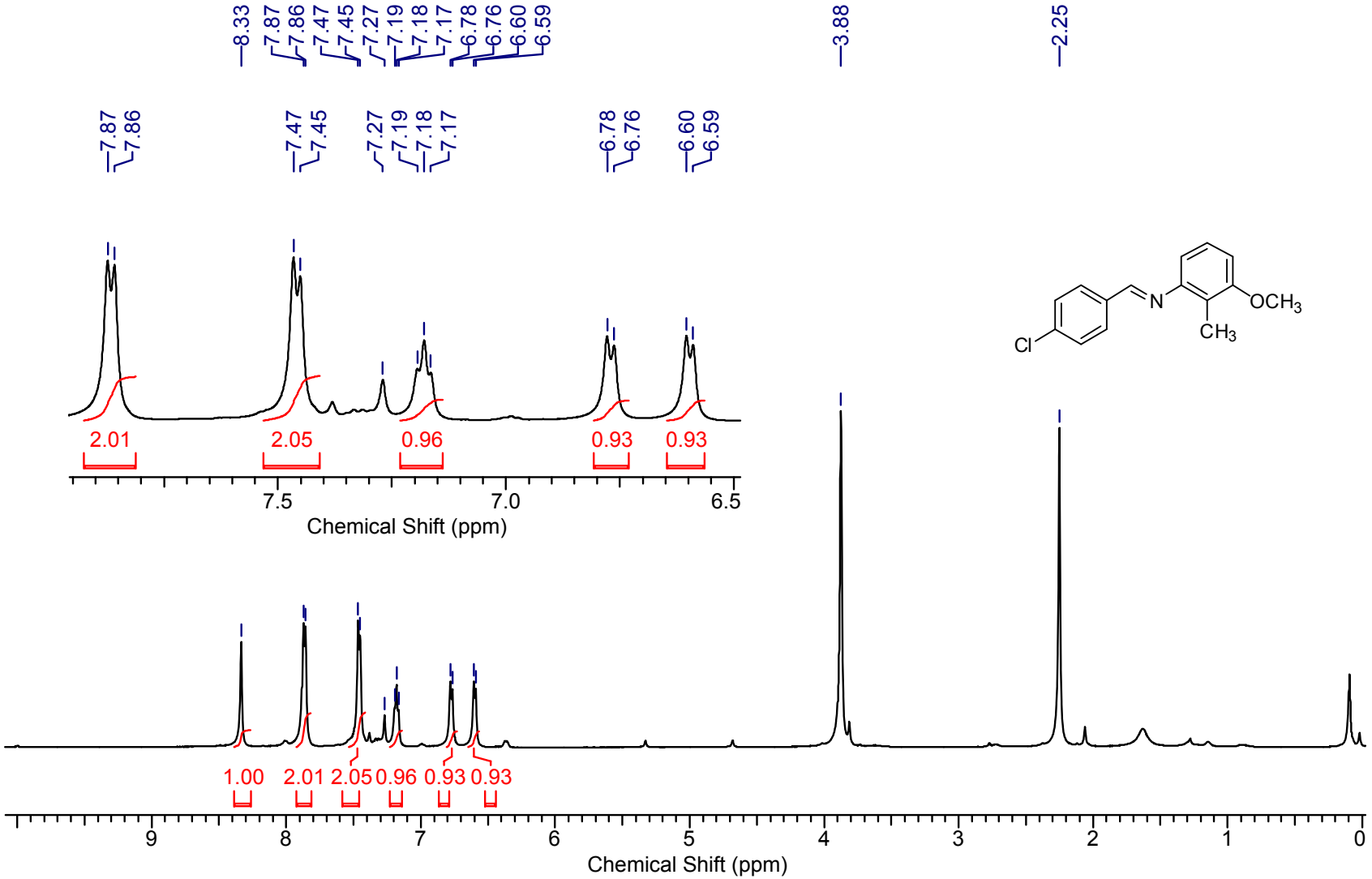

Supplementary Figure 21. ^{1}H NMR of **3ak**

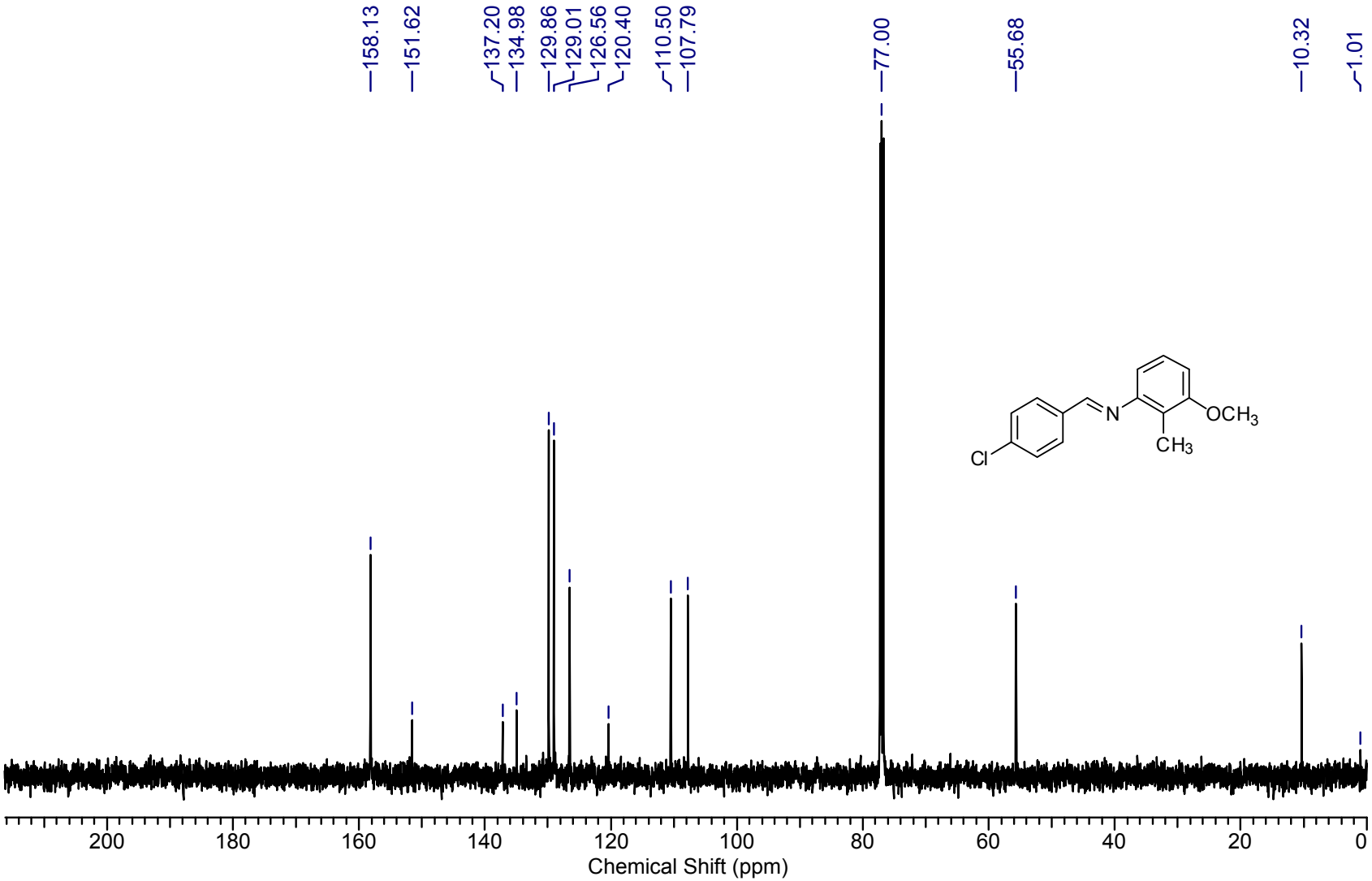

Supplementary Figure 22. ^{13}C NMR of **3ak**

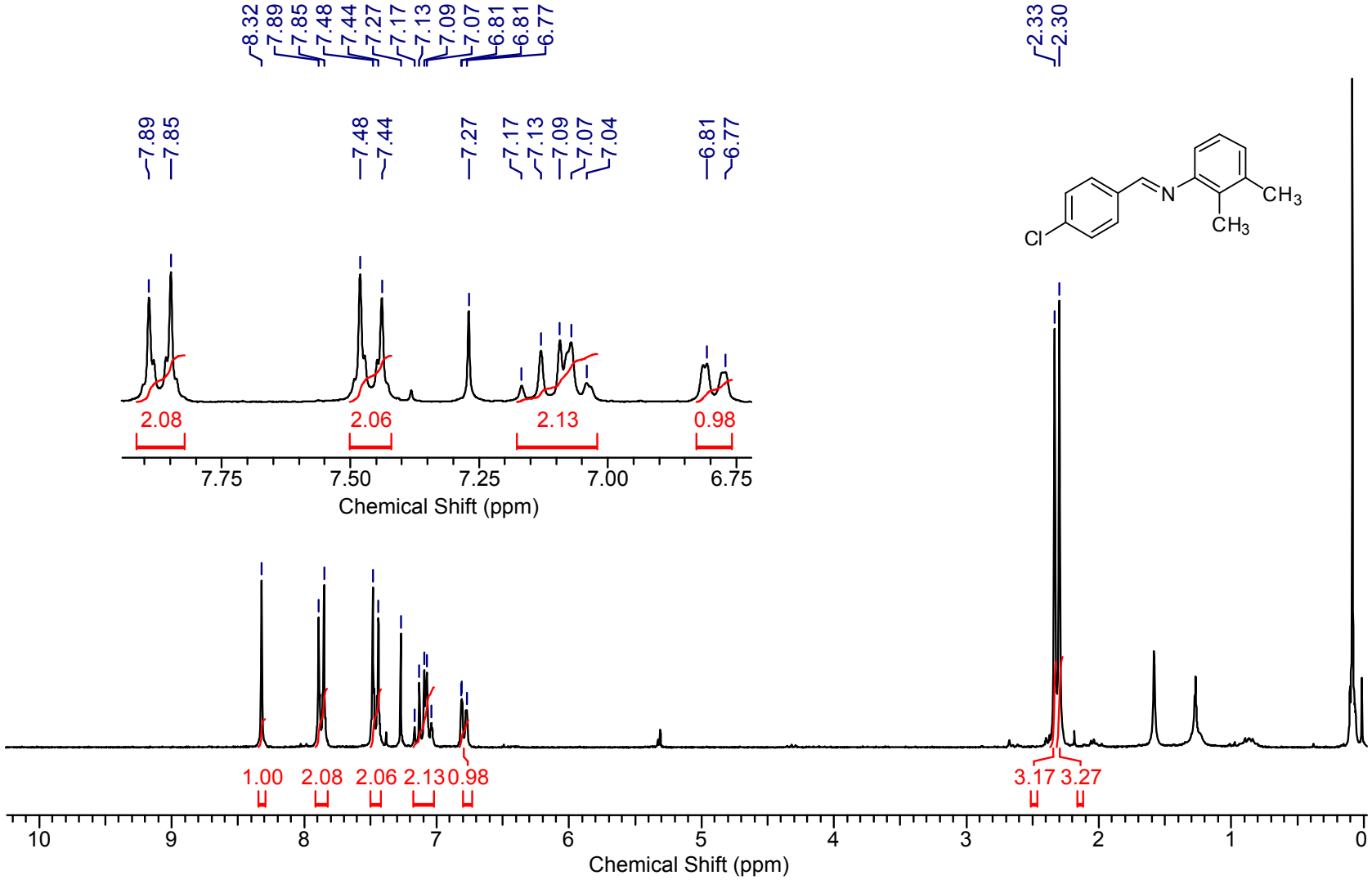

Supplementary Figure 23. ^{1}H NMR of **3al**

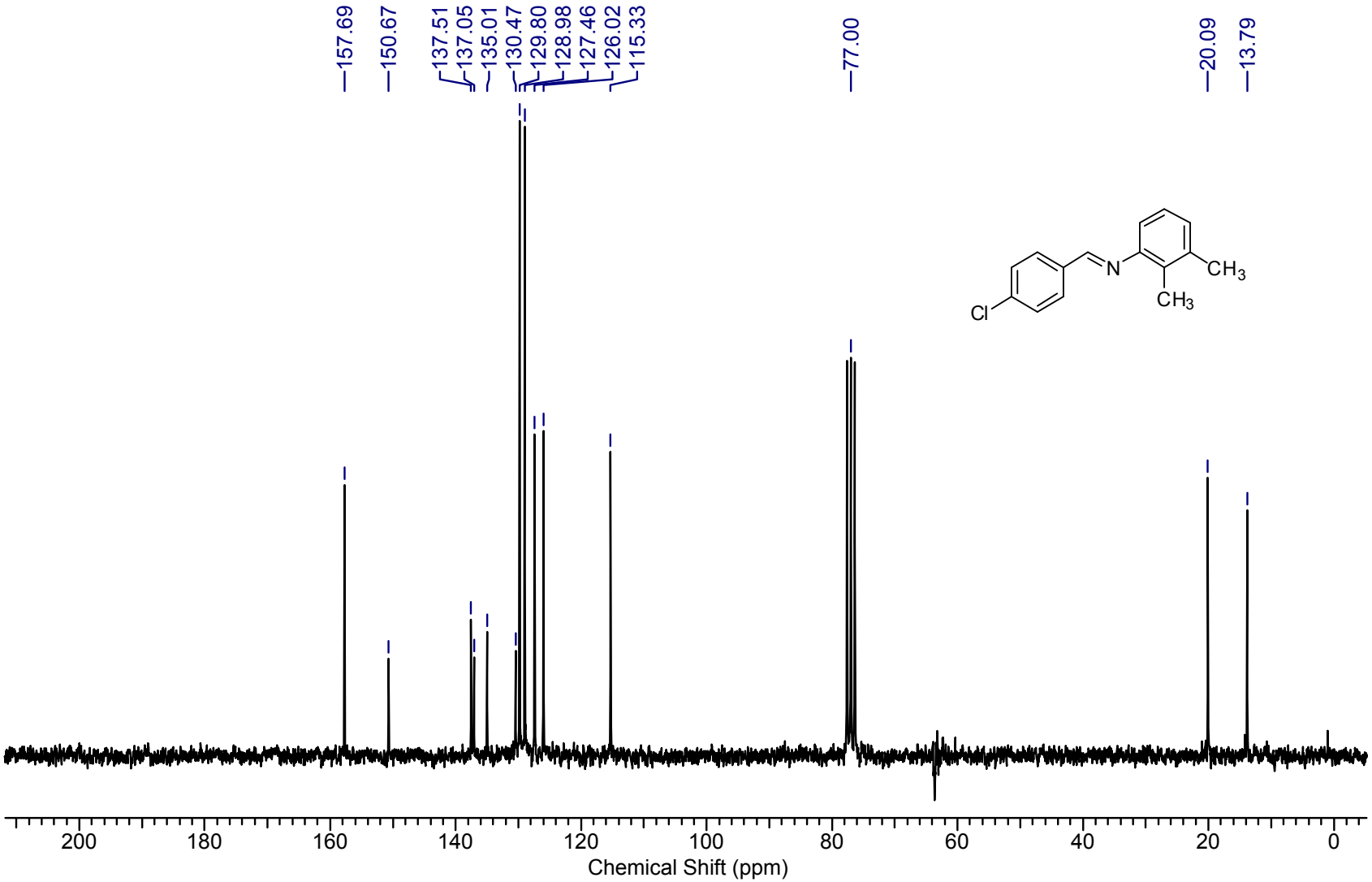

Supplementary Figure 24. ^{13}C NMR of **3al**

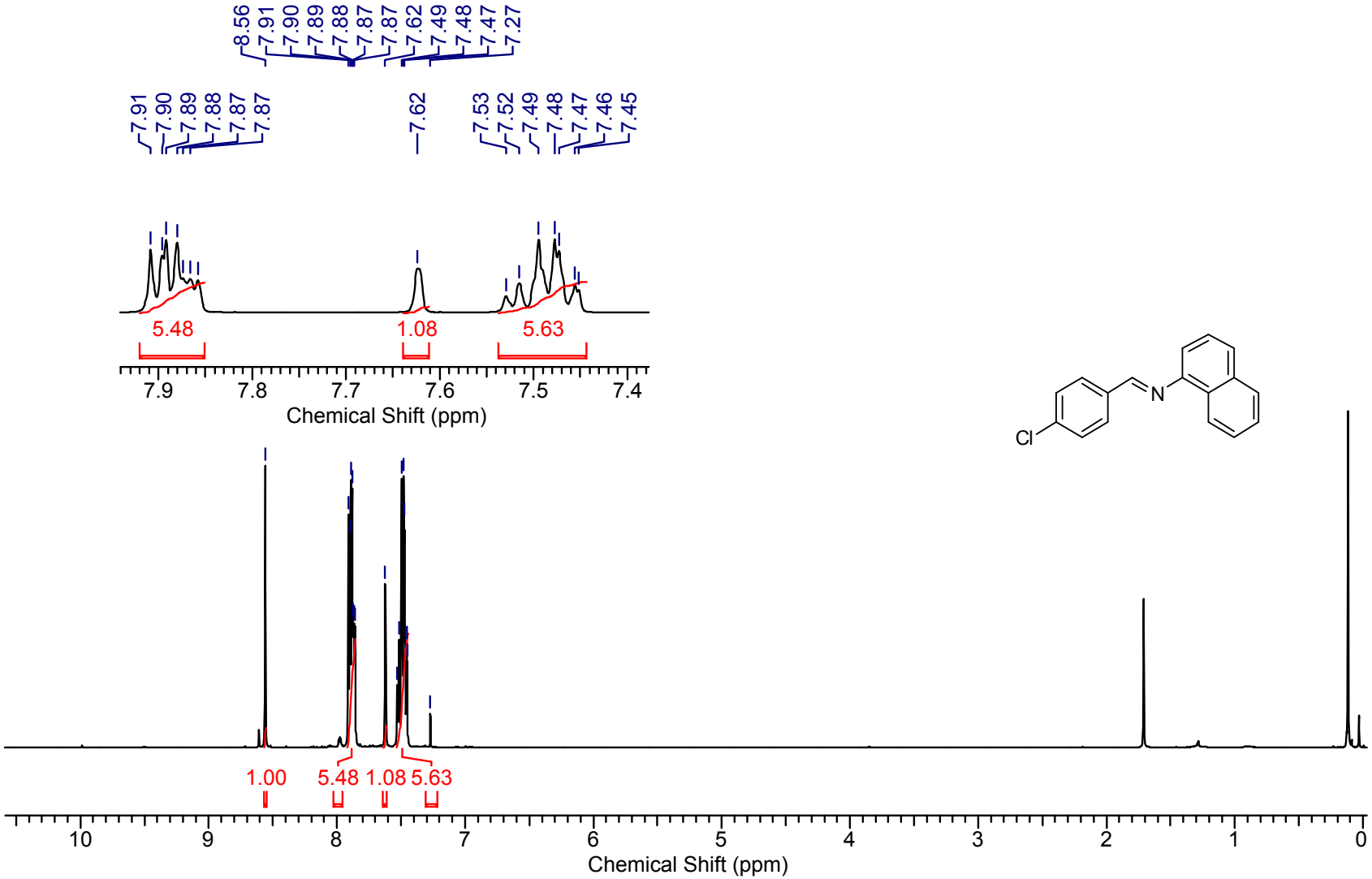

Supplementary Figure 25. ^{1}H NMR of **3am**

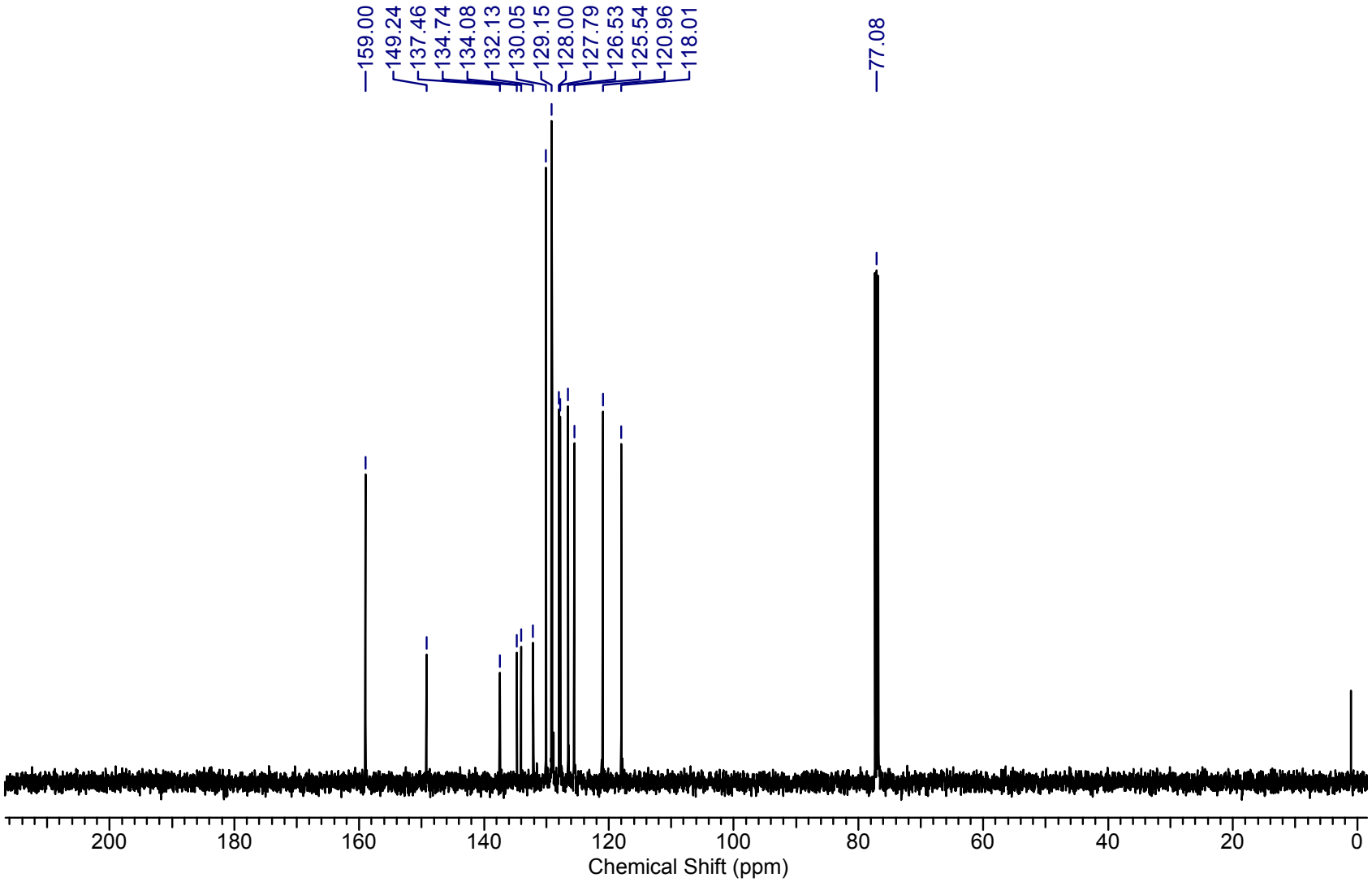

Supplementary Figure 26. ^{13}C NMR of **3am**

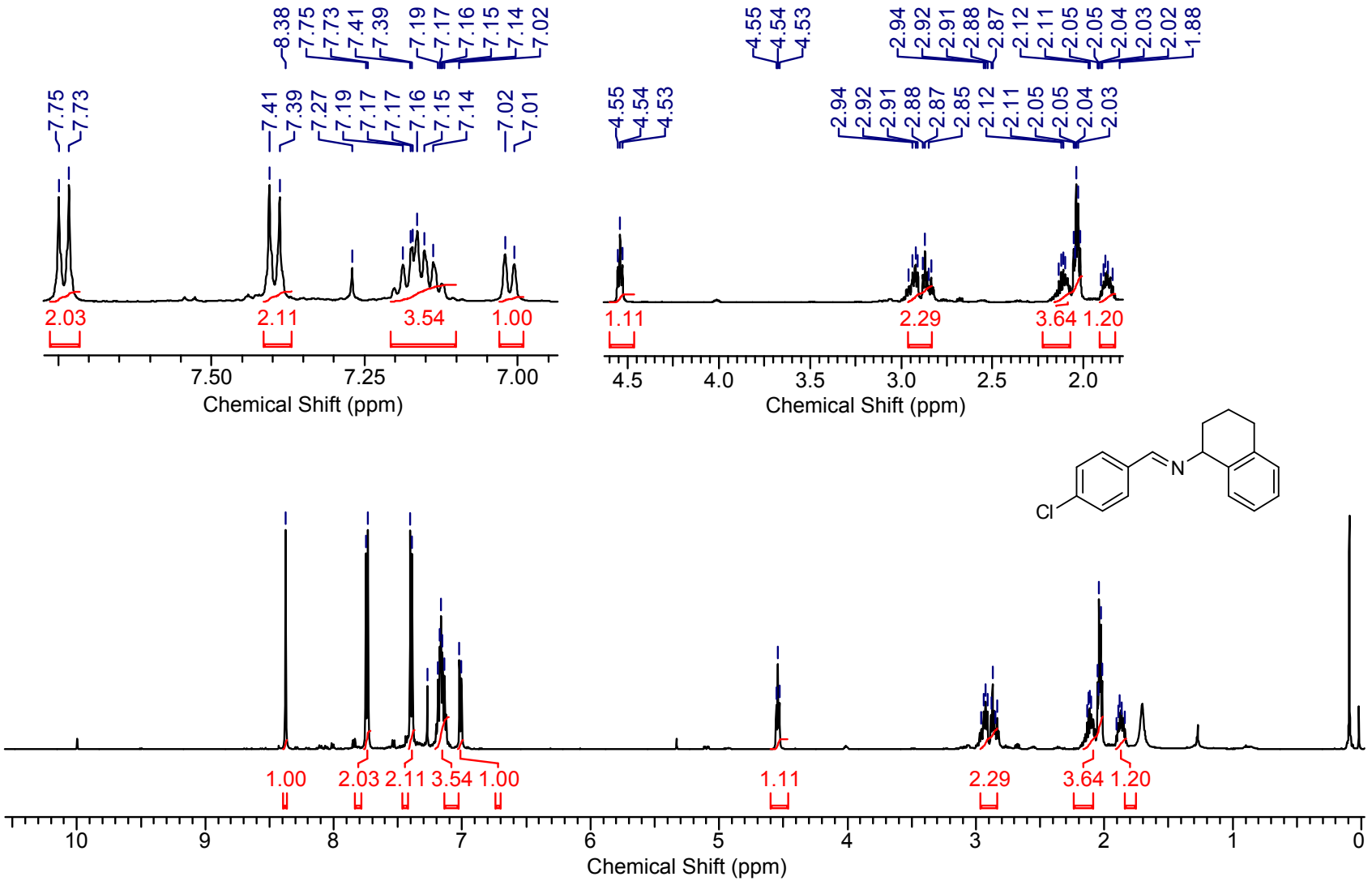

Supplementary Figure 27. ^{1}H NMR of **3an**

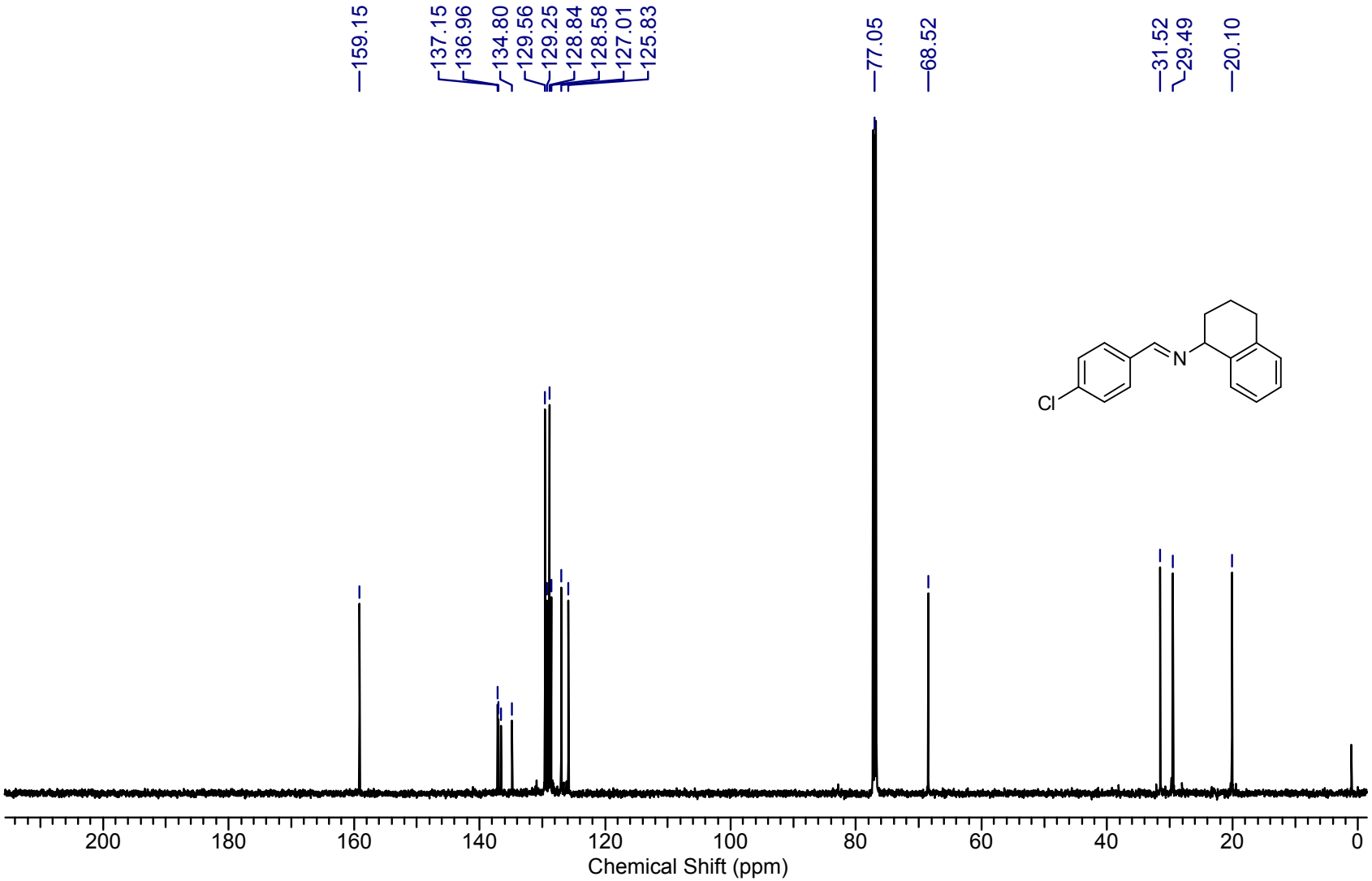

Supplementary Figure 28. ^{13}C NMR of **3an**

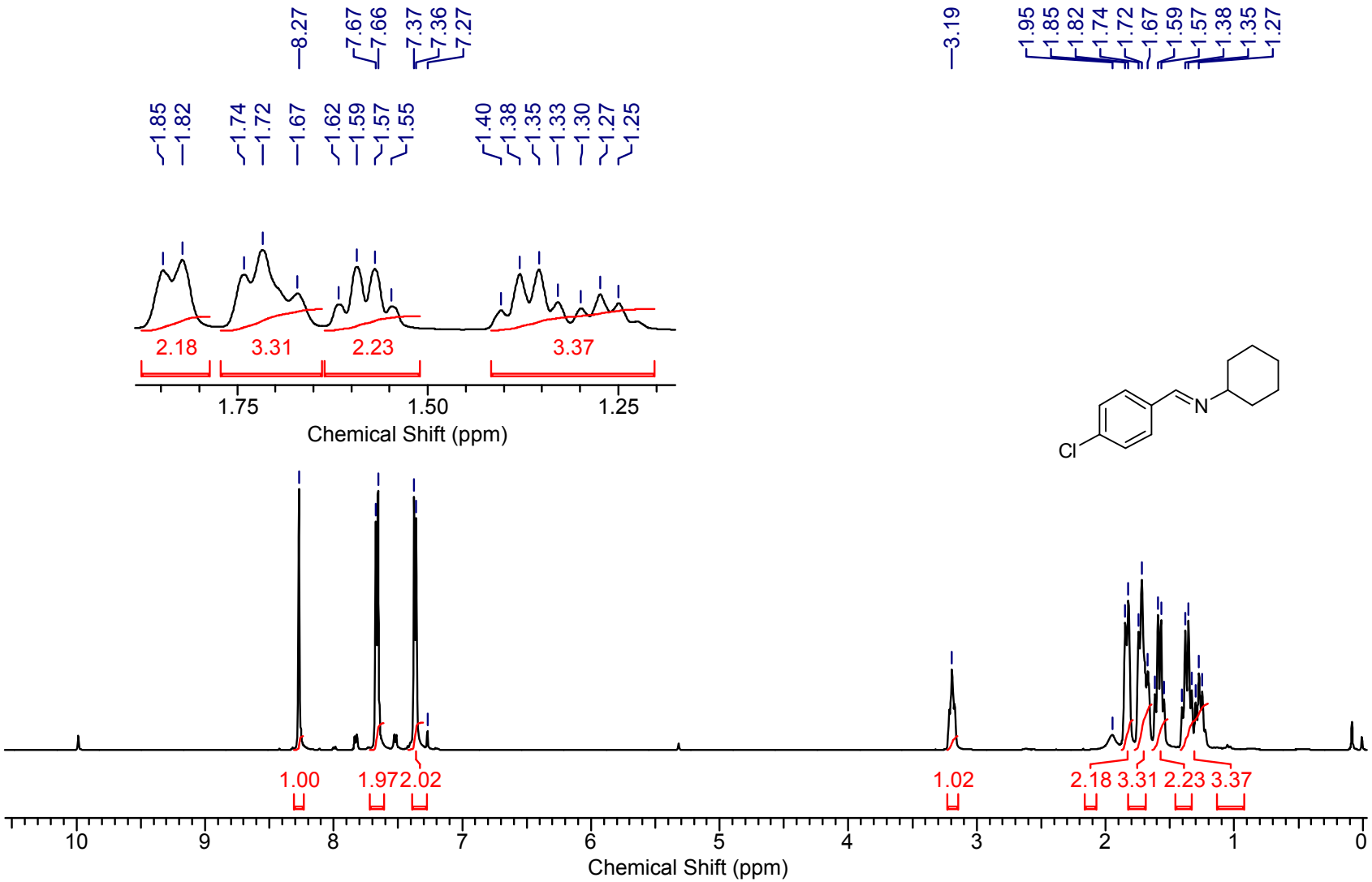

Supplementary Figure 29. ^{1}H NMR of **3ao**

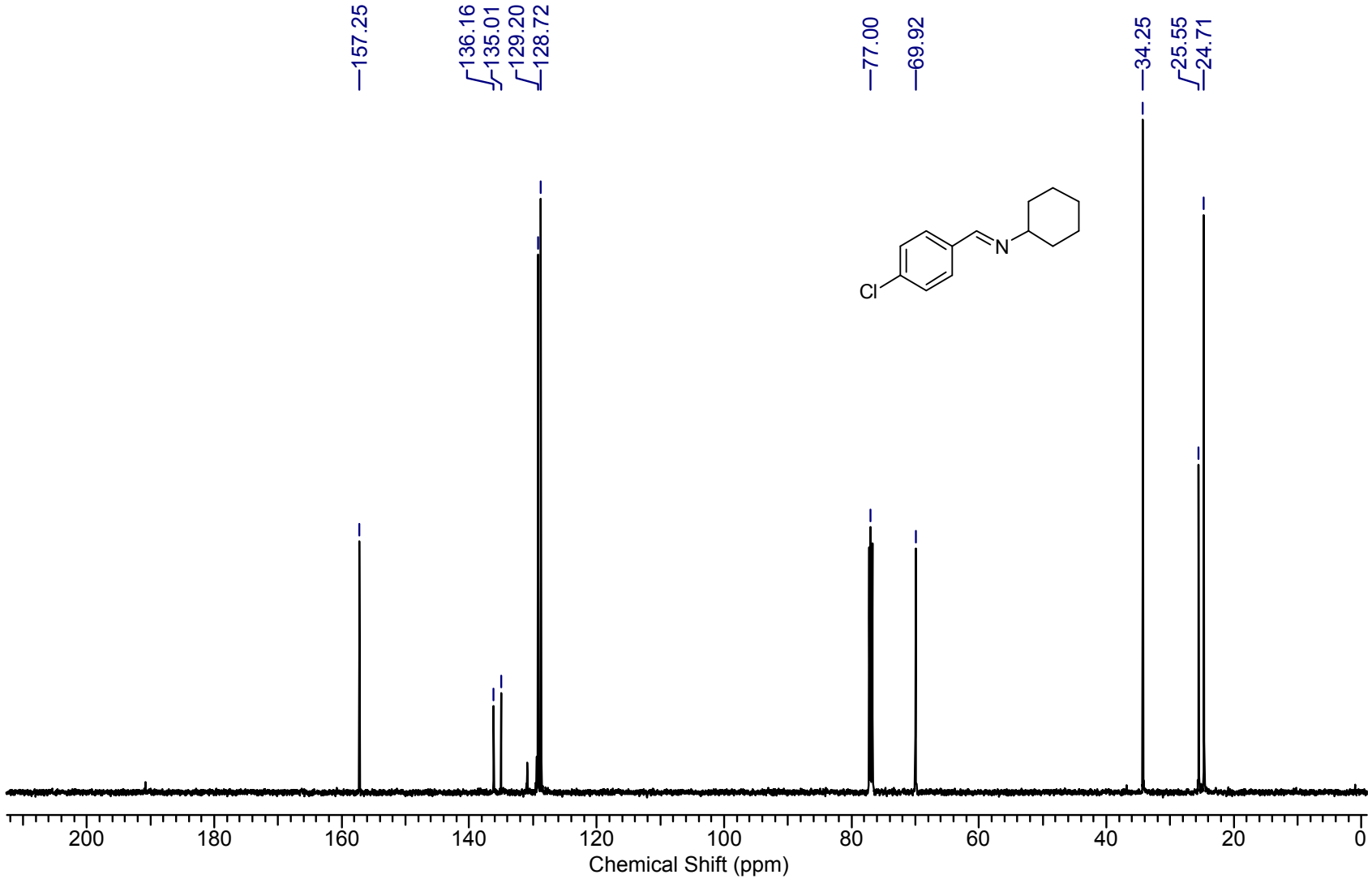

Supplementary Figure 30. ^{13}C NMR of **3ao**

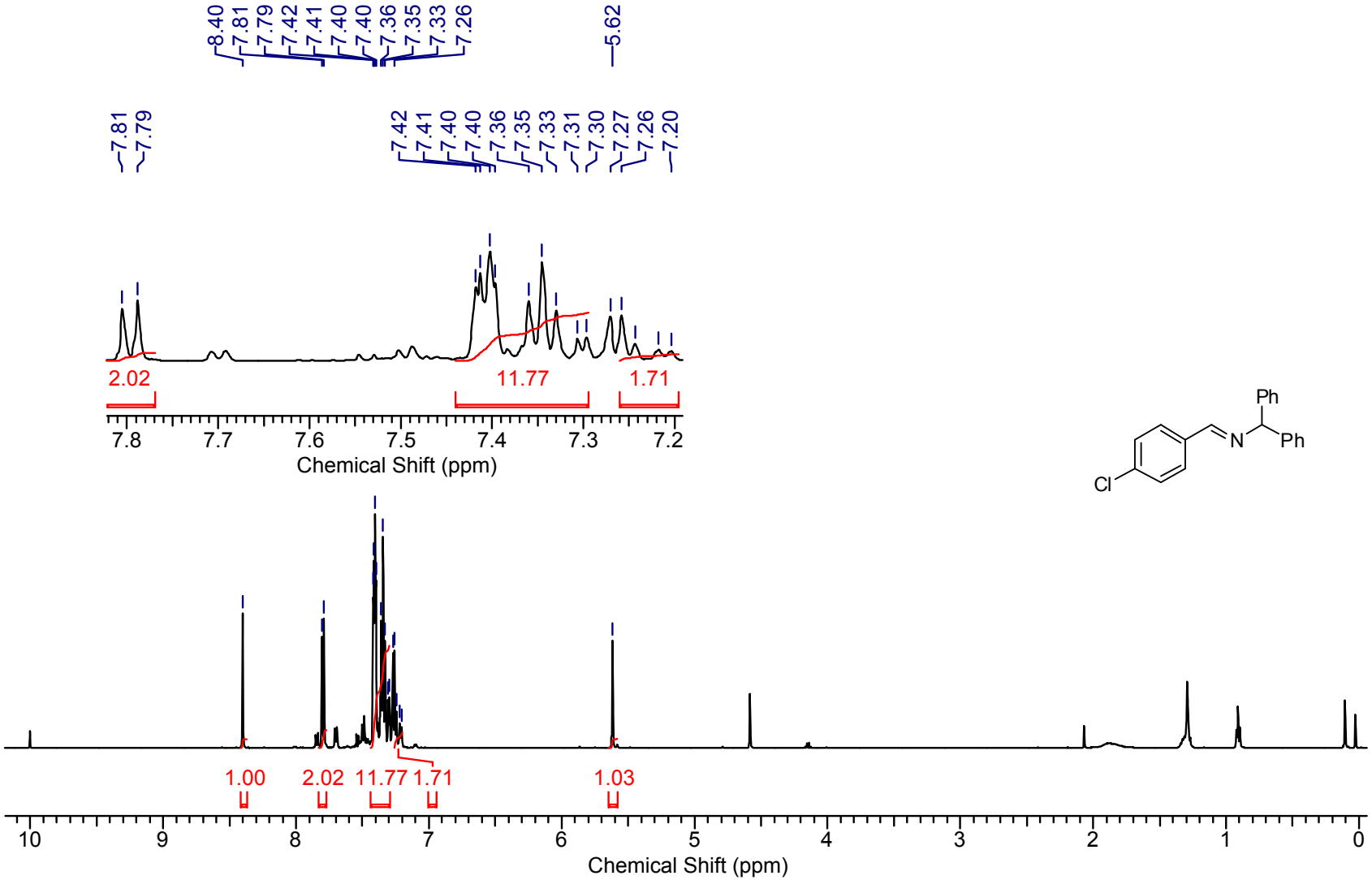

Supplementary Figure 31. ^{1}H NMR of **3aq**

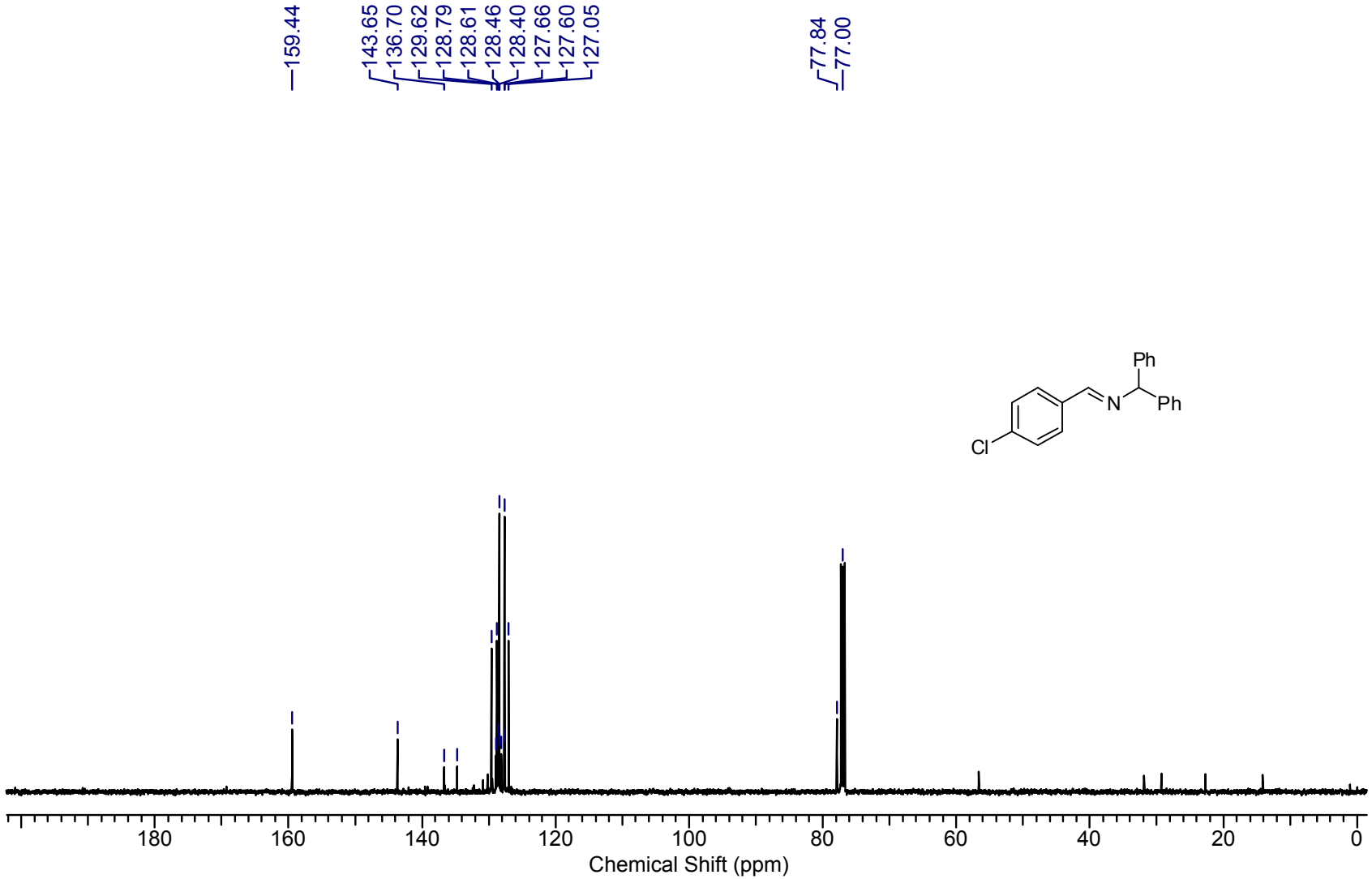

Supplementary Figure 32. ^{13}C NMR of **3aq**

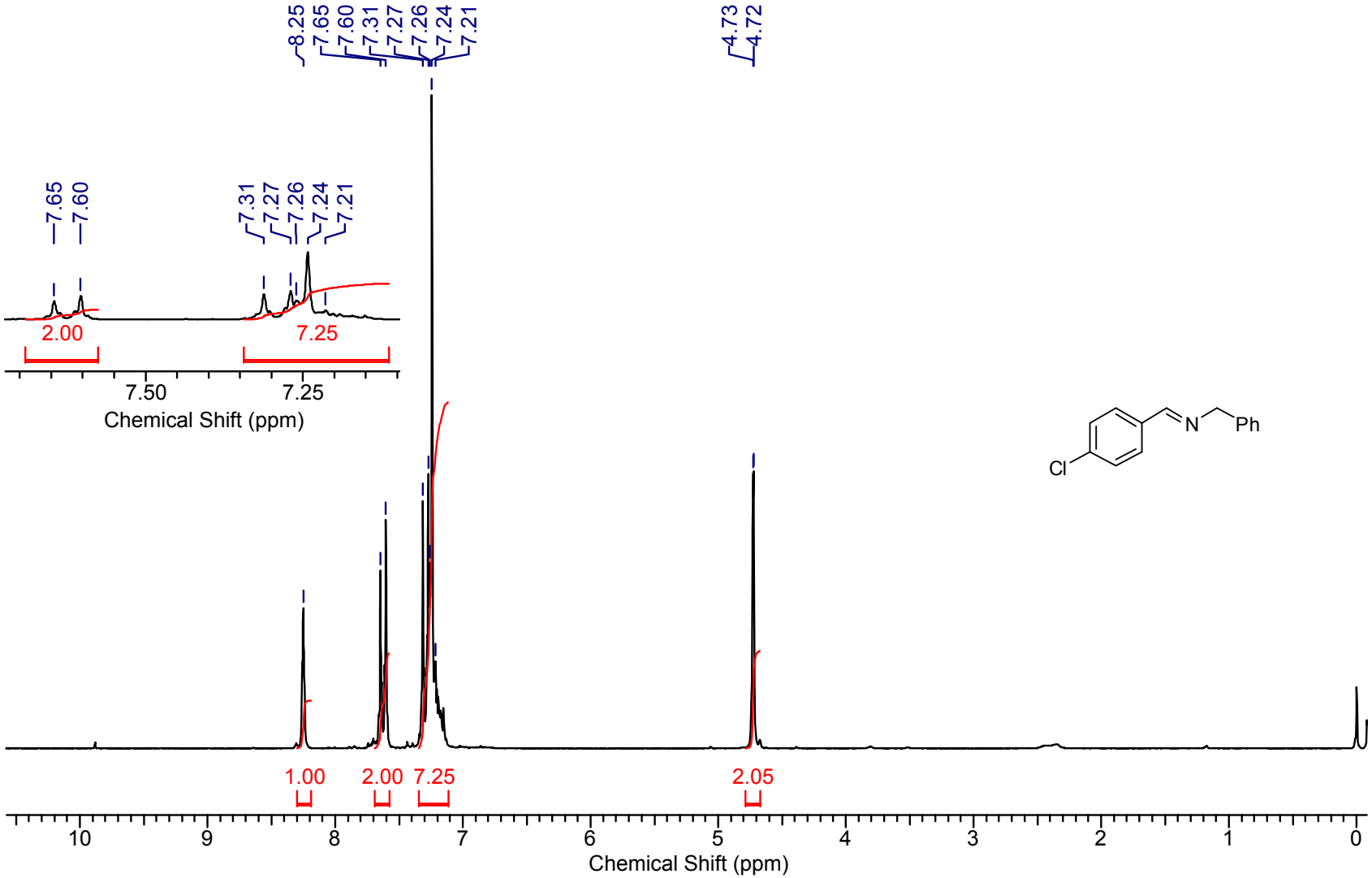

Supplementary Figure 33. ^{1}H NMR of **3ar**

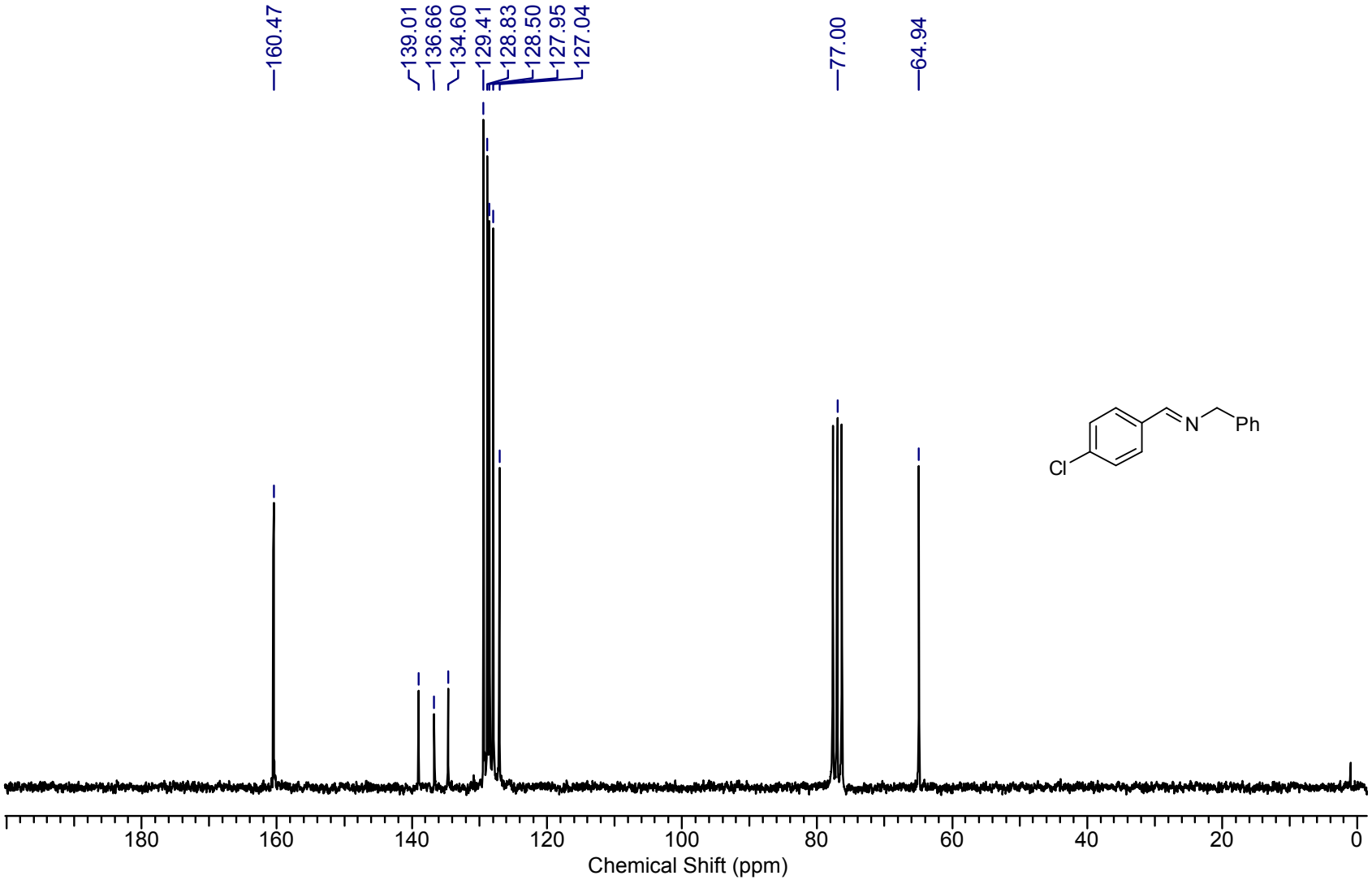

Supplementary Figure 34. ^{13}C NMR of **3ar**

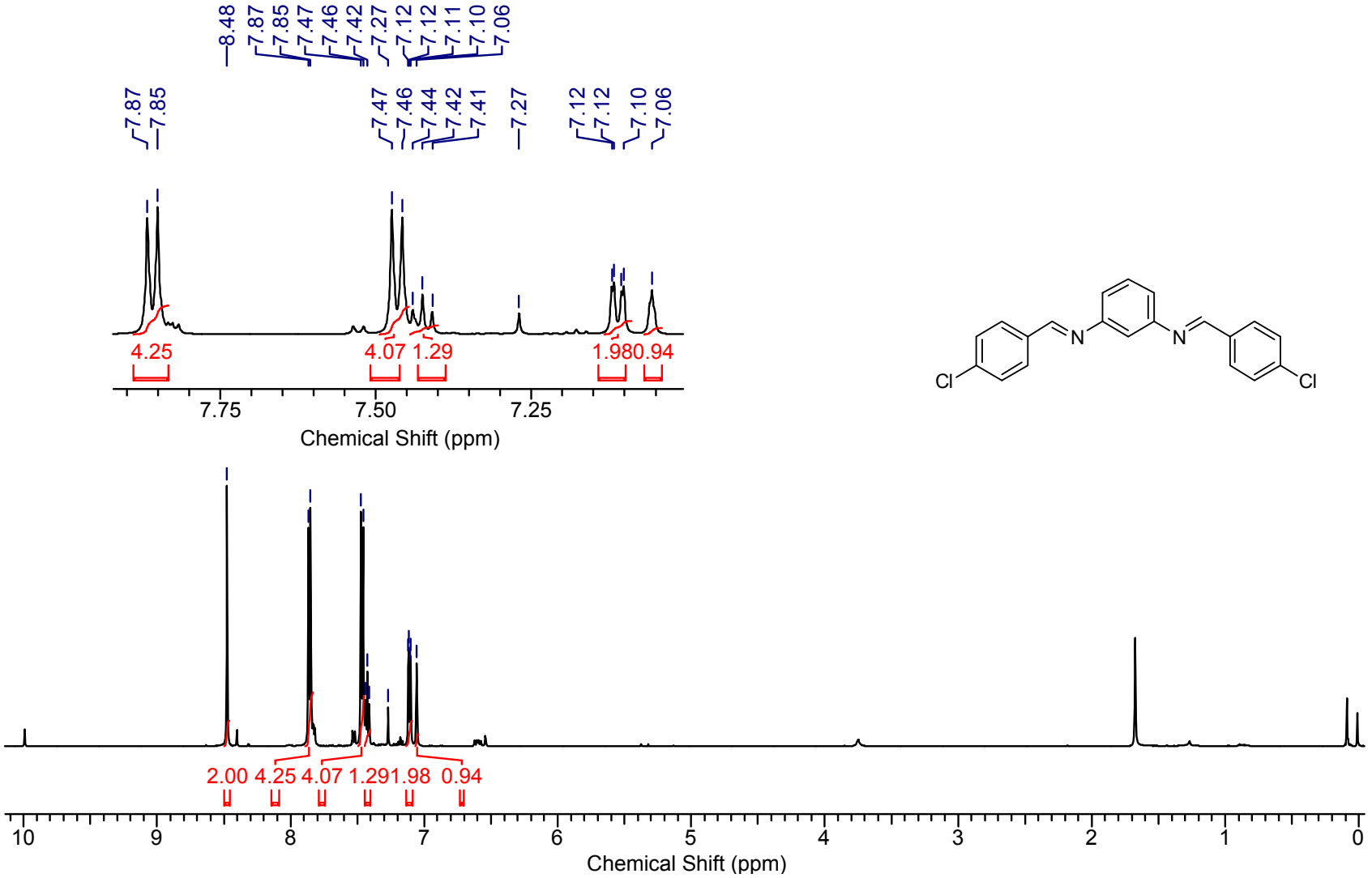

Supplementary Figure 35. ^{1}H NMR of **3as**

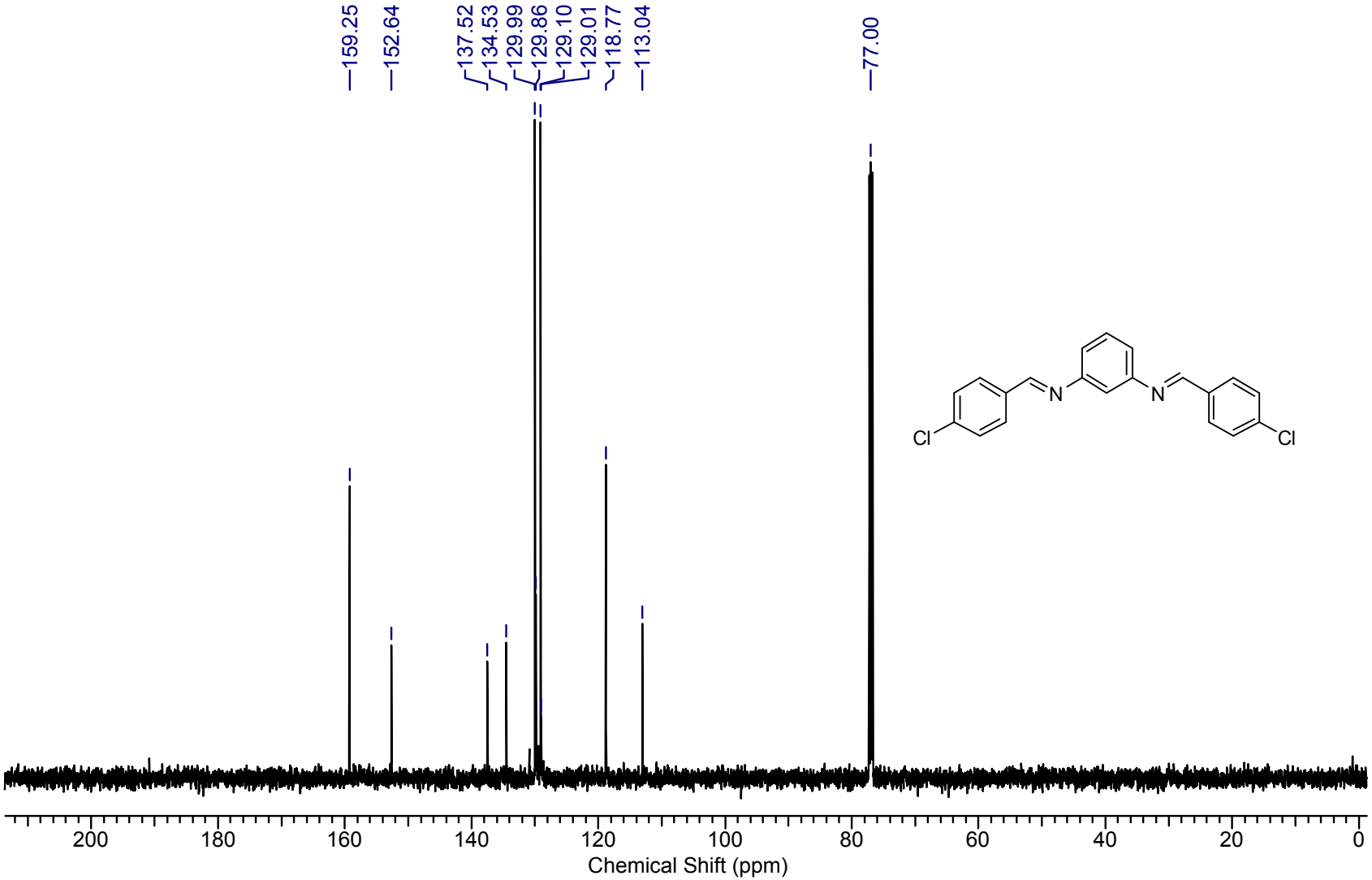

Supplementary Figure 36. ^{13}C NMR of **3as**

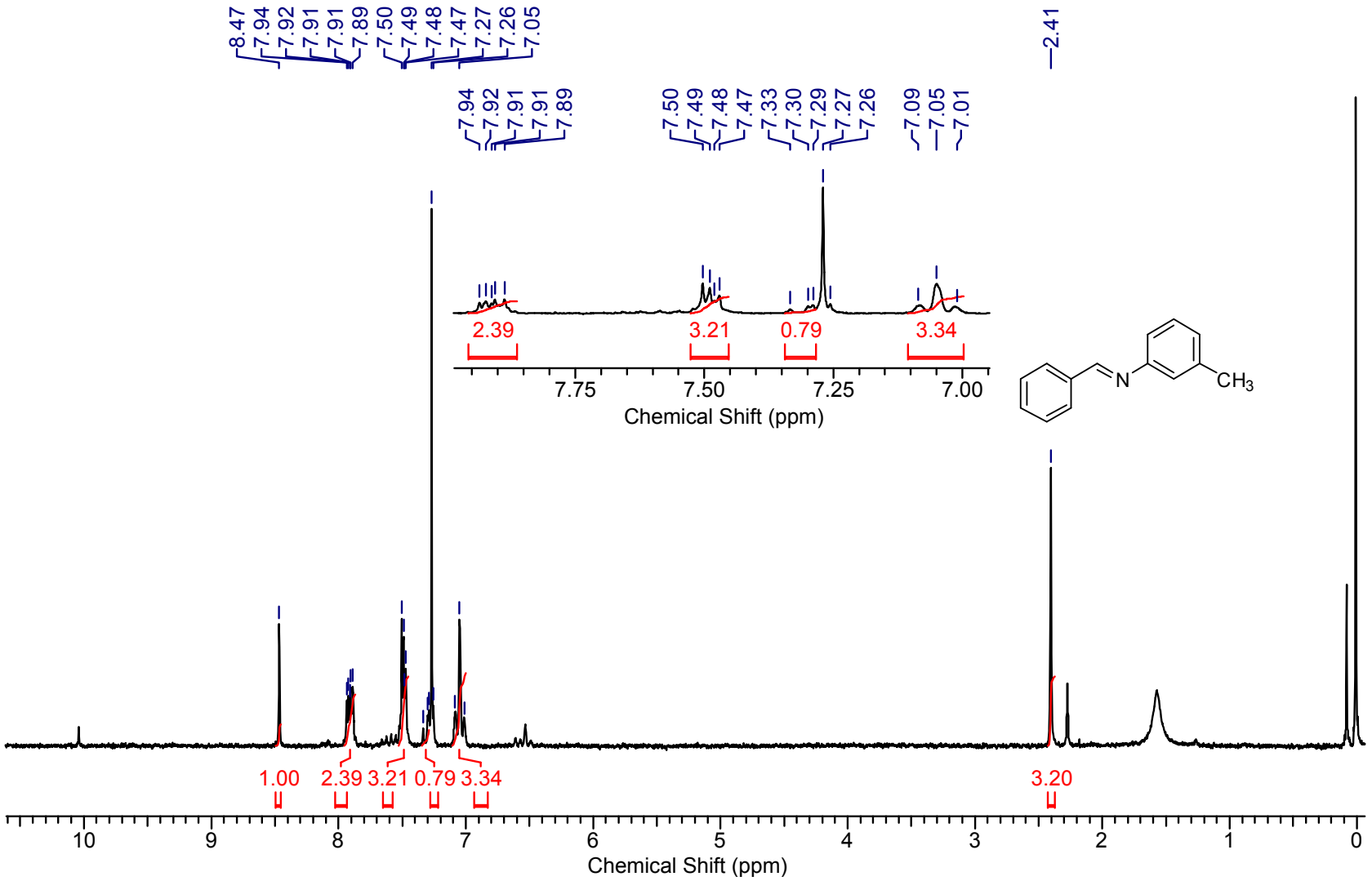

Supplementary Figure 37. ^{1}H NMR of **3ba**

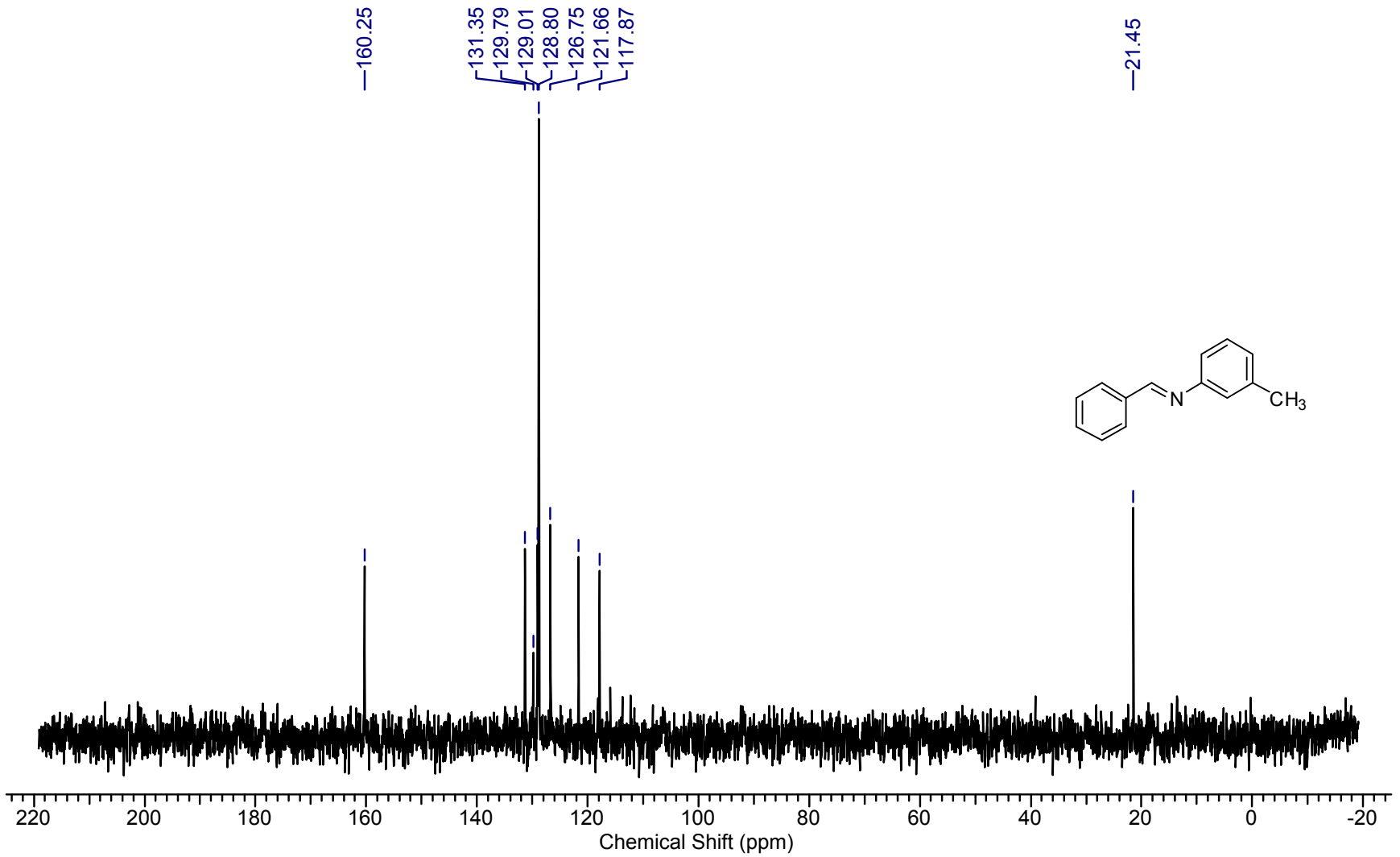

Supplementary Figure 38. ^{13}C NMR of **3ba**

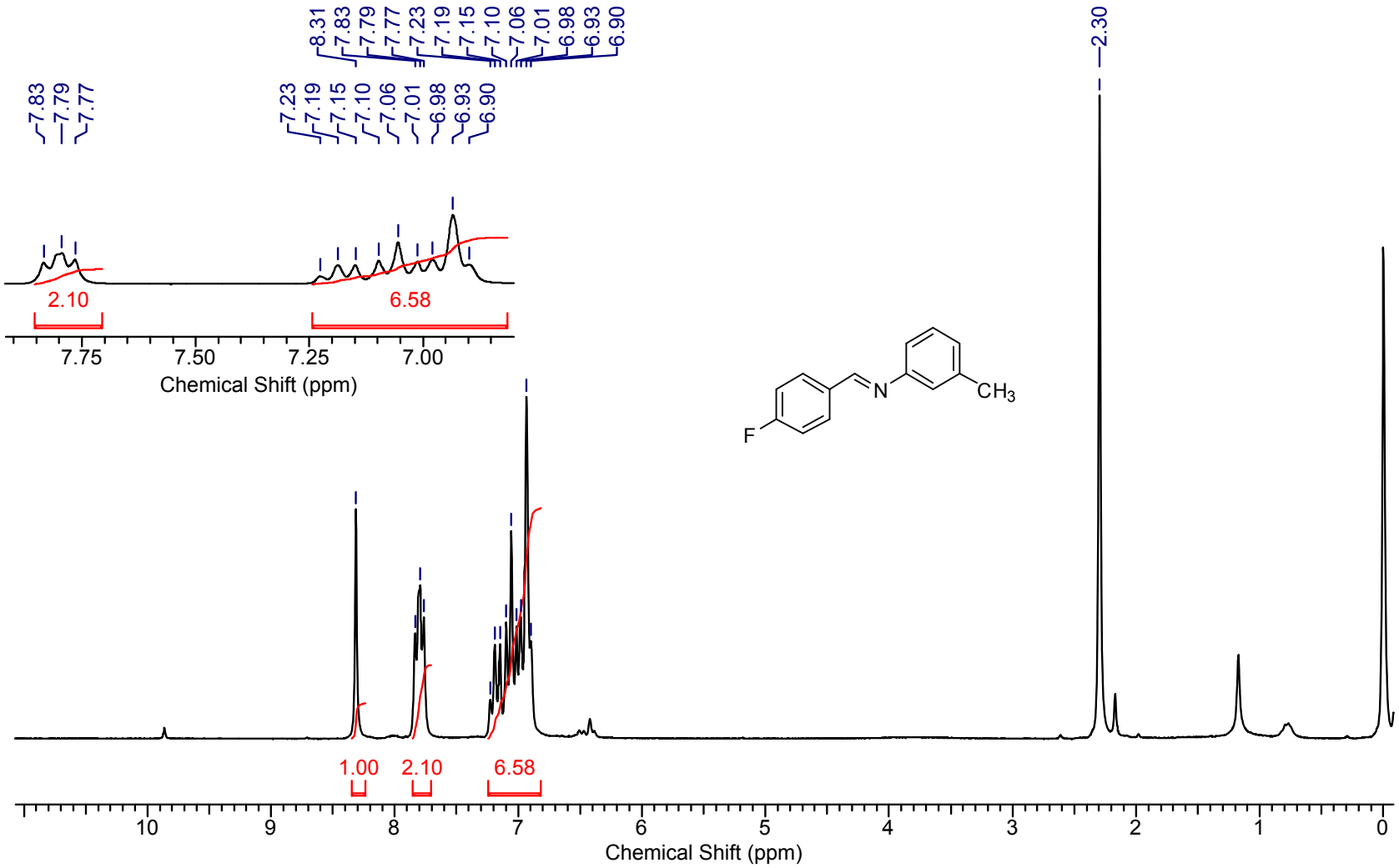

Supplementary Figure 39. ^{1}H NMR of **3bb**

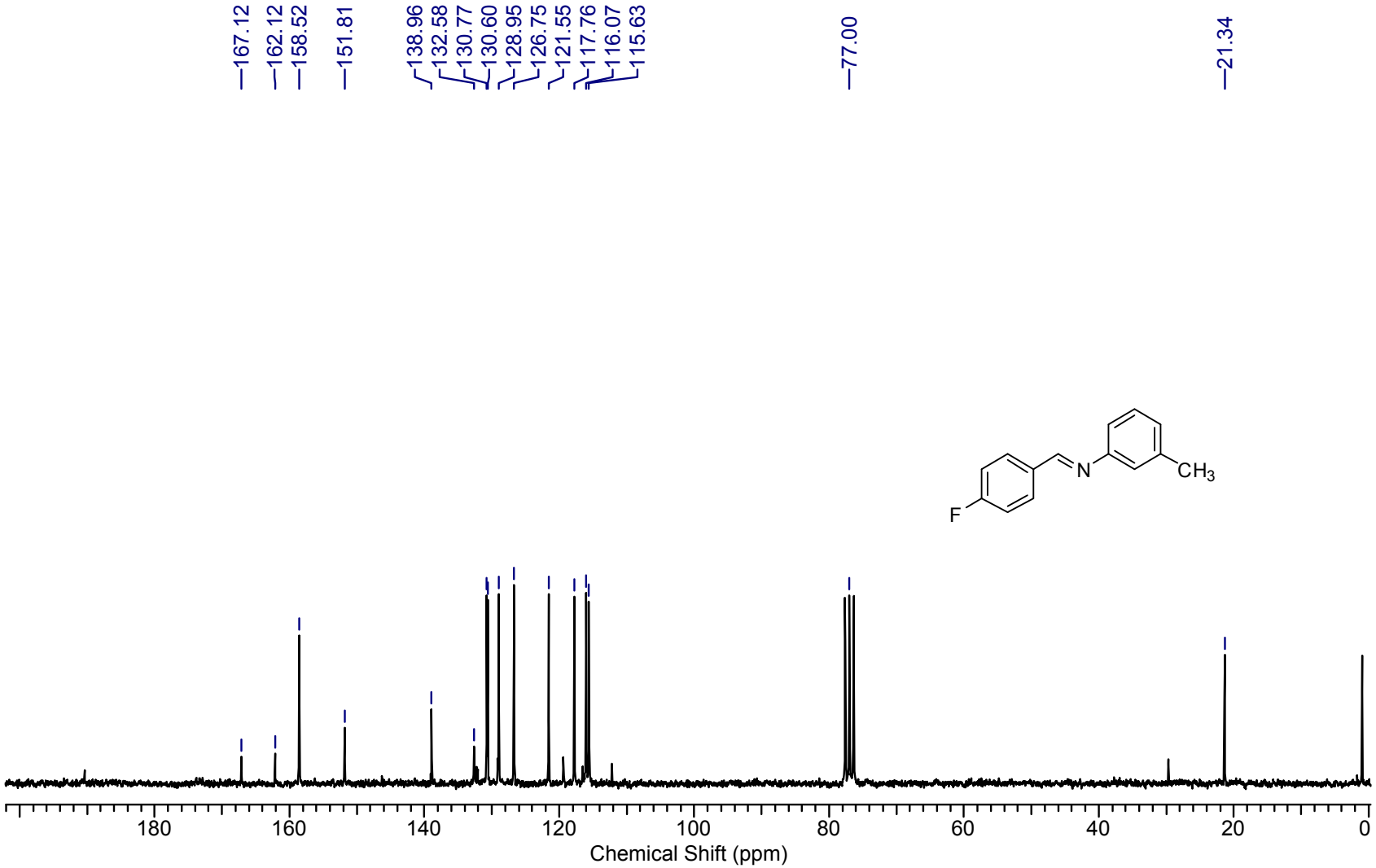

Supplementary Figure 40. ^{13}C NMR of **3bb**

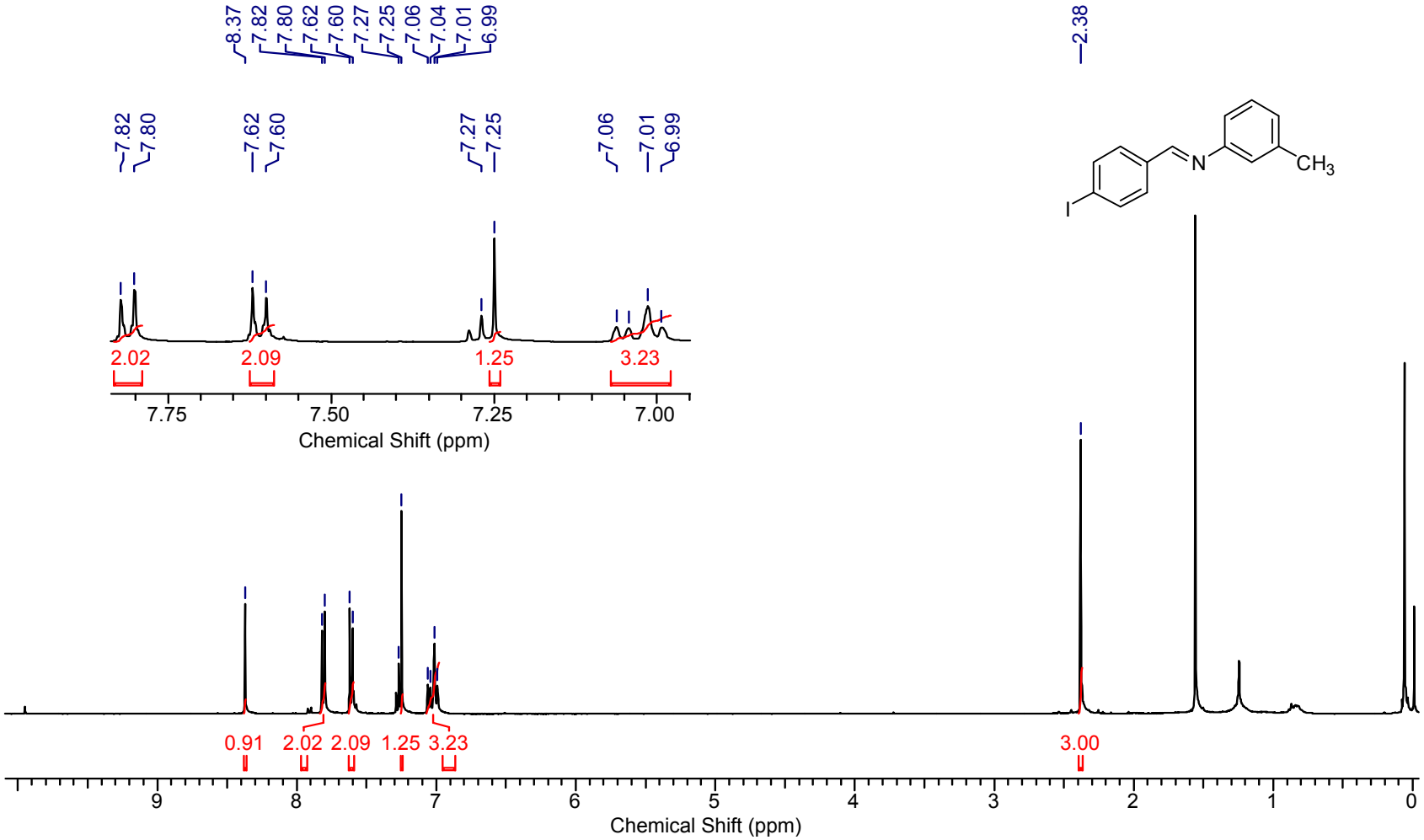

Supplementary Figure 41. ^{1}H NMR of **3bc**

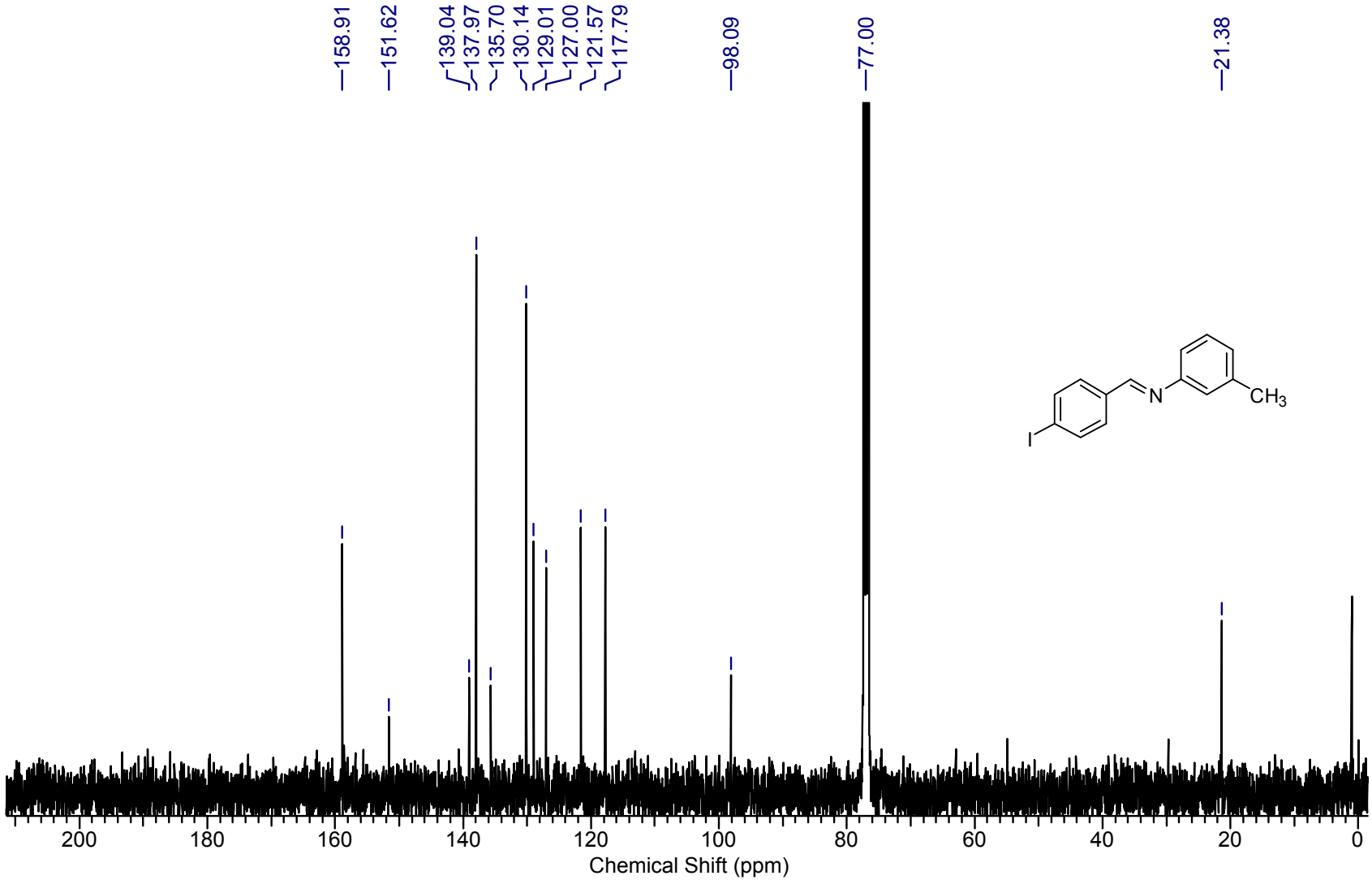

Supplementary Figure 42. ^{13}C NMR of **3bc**

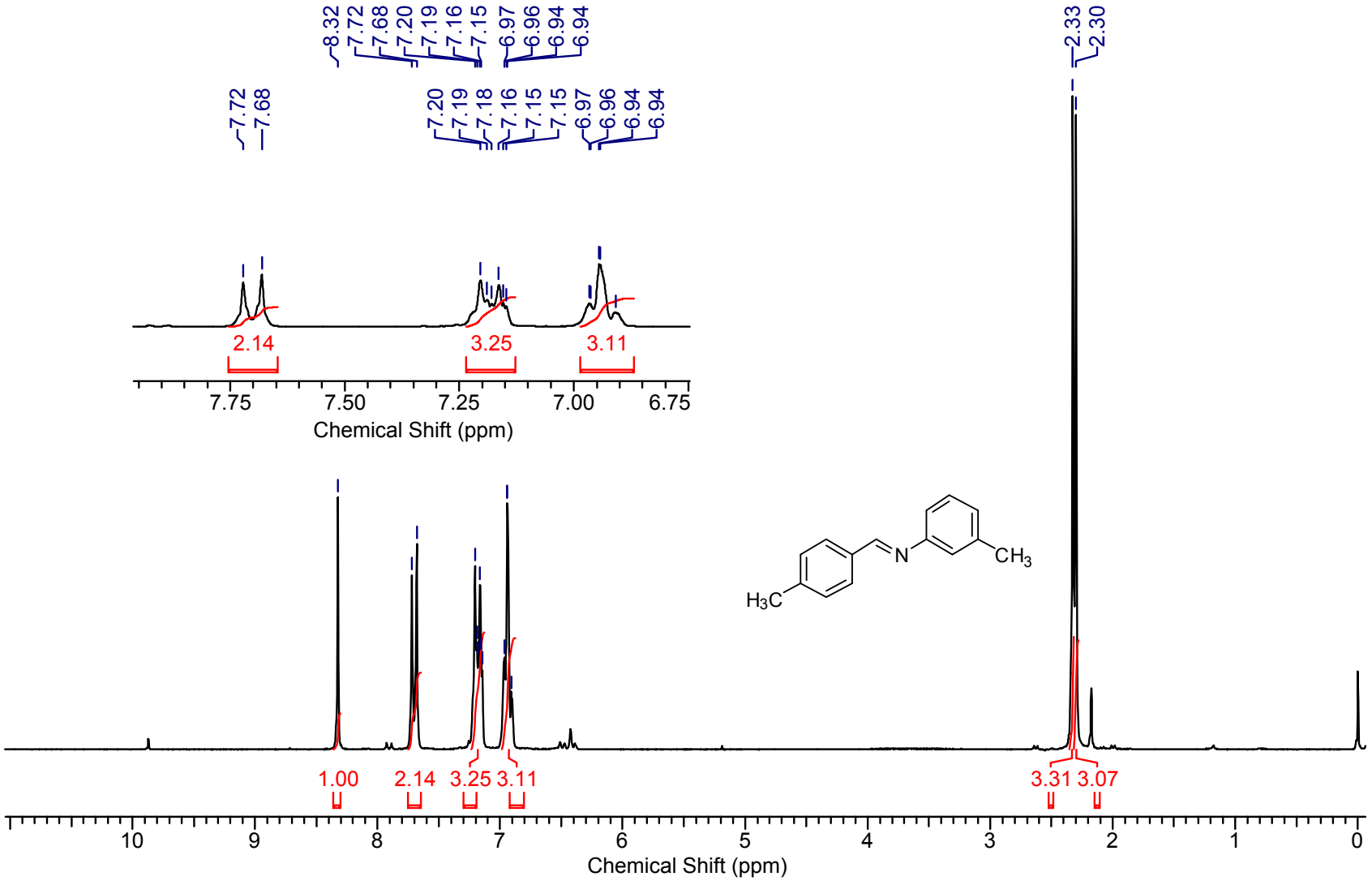

Supplementary Figure 43. ^{1}H NMR of **3bd**

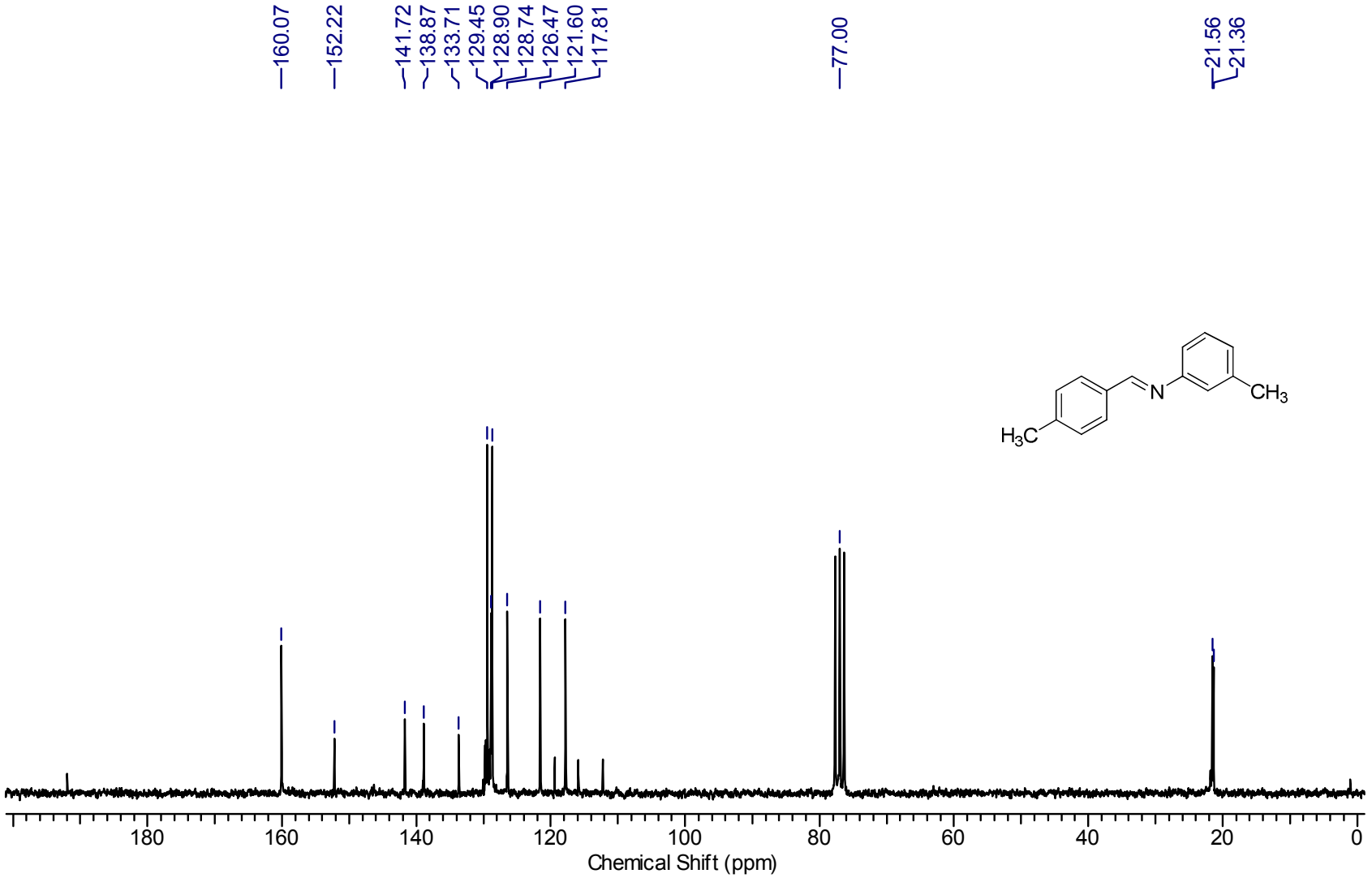

Supplementary Figure 44. ^{13}C NMR of **3bd**

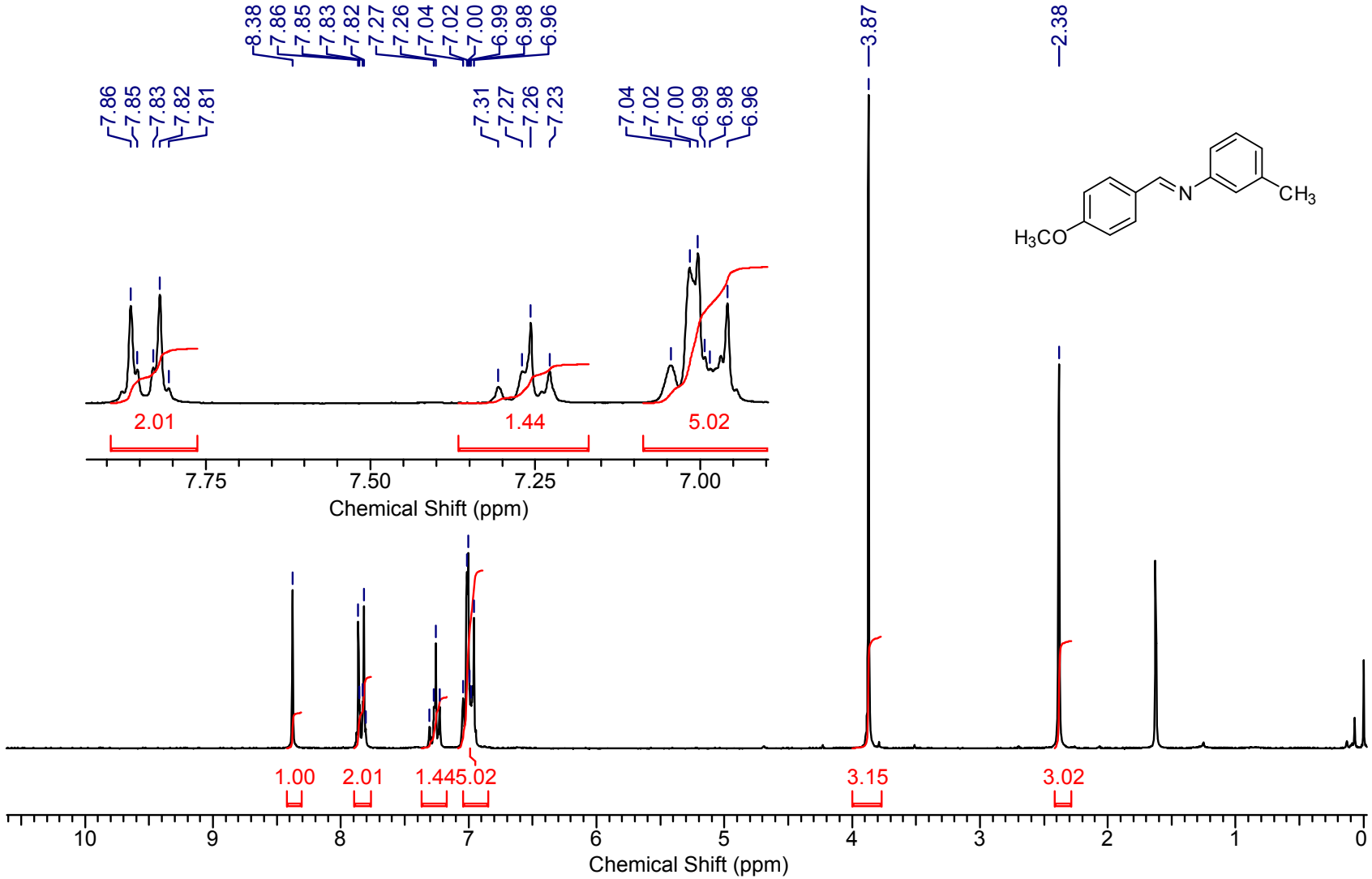

Supplementary Figure 45. ^{1}H NMR of **3be**

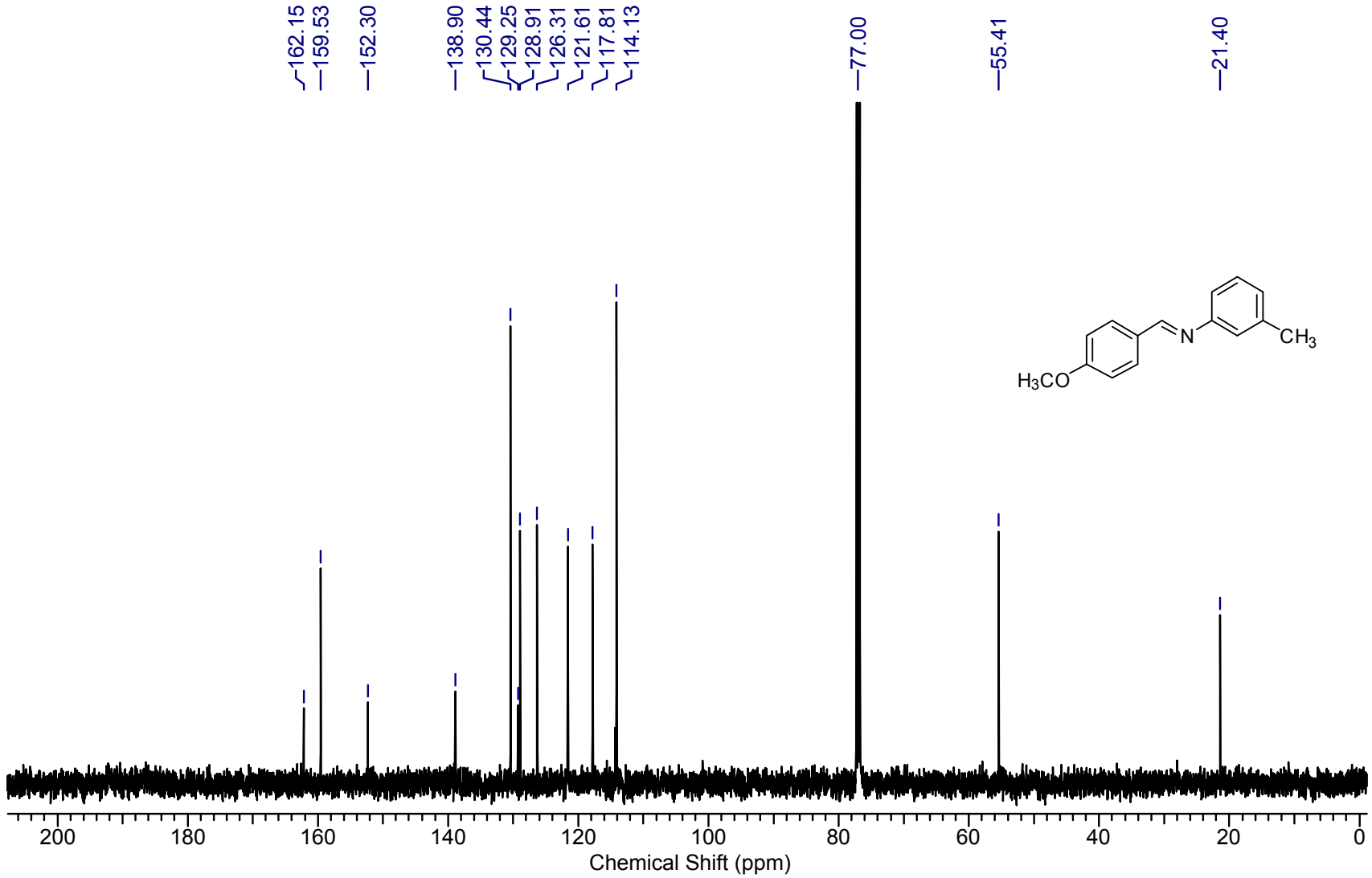

Supplementary Figure 46. ^{13}C NMR of **3be**

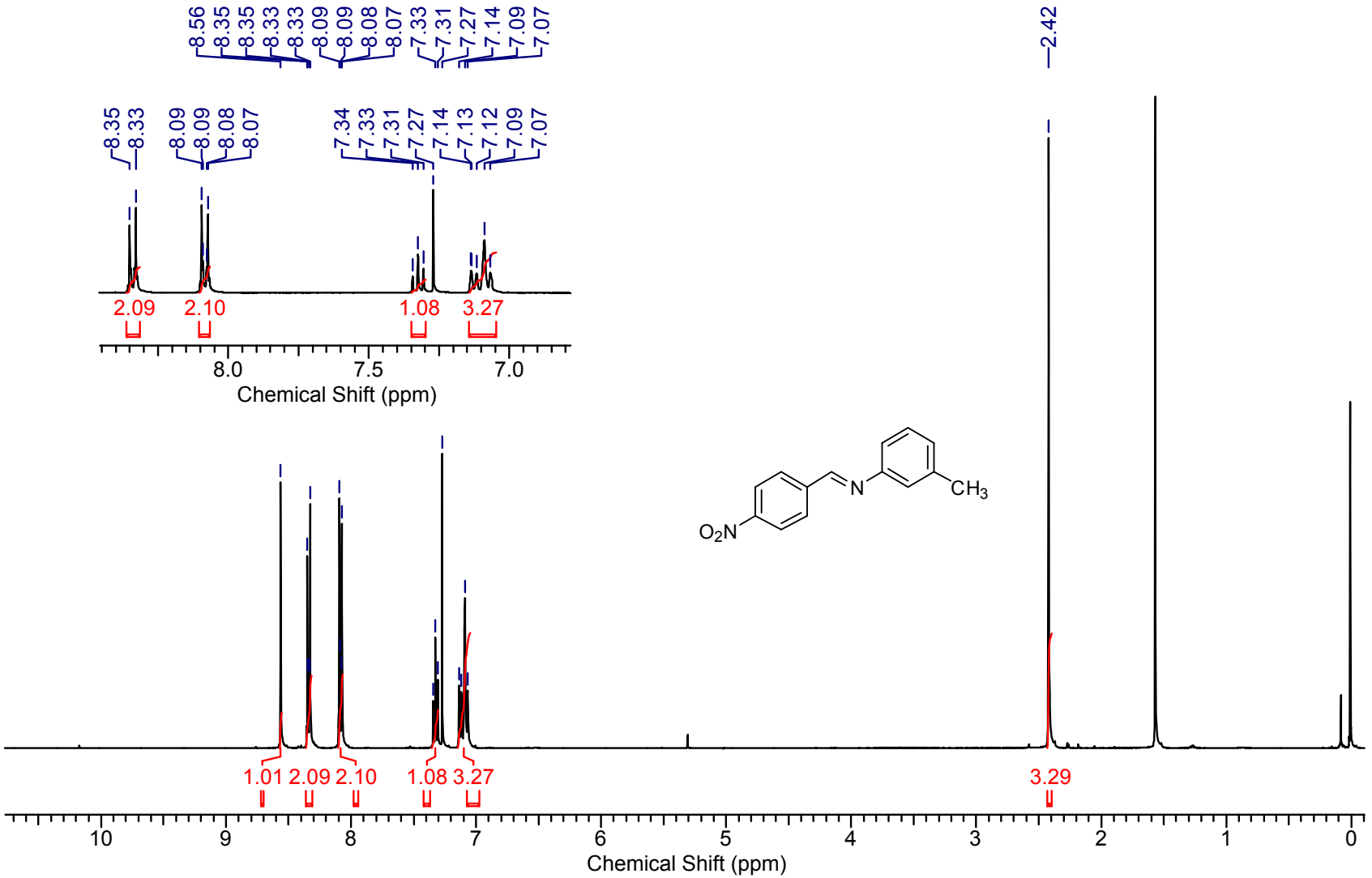

Supplementary Figure 47. ^{1}H NMR of **3bf**

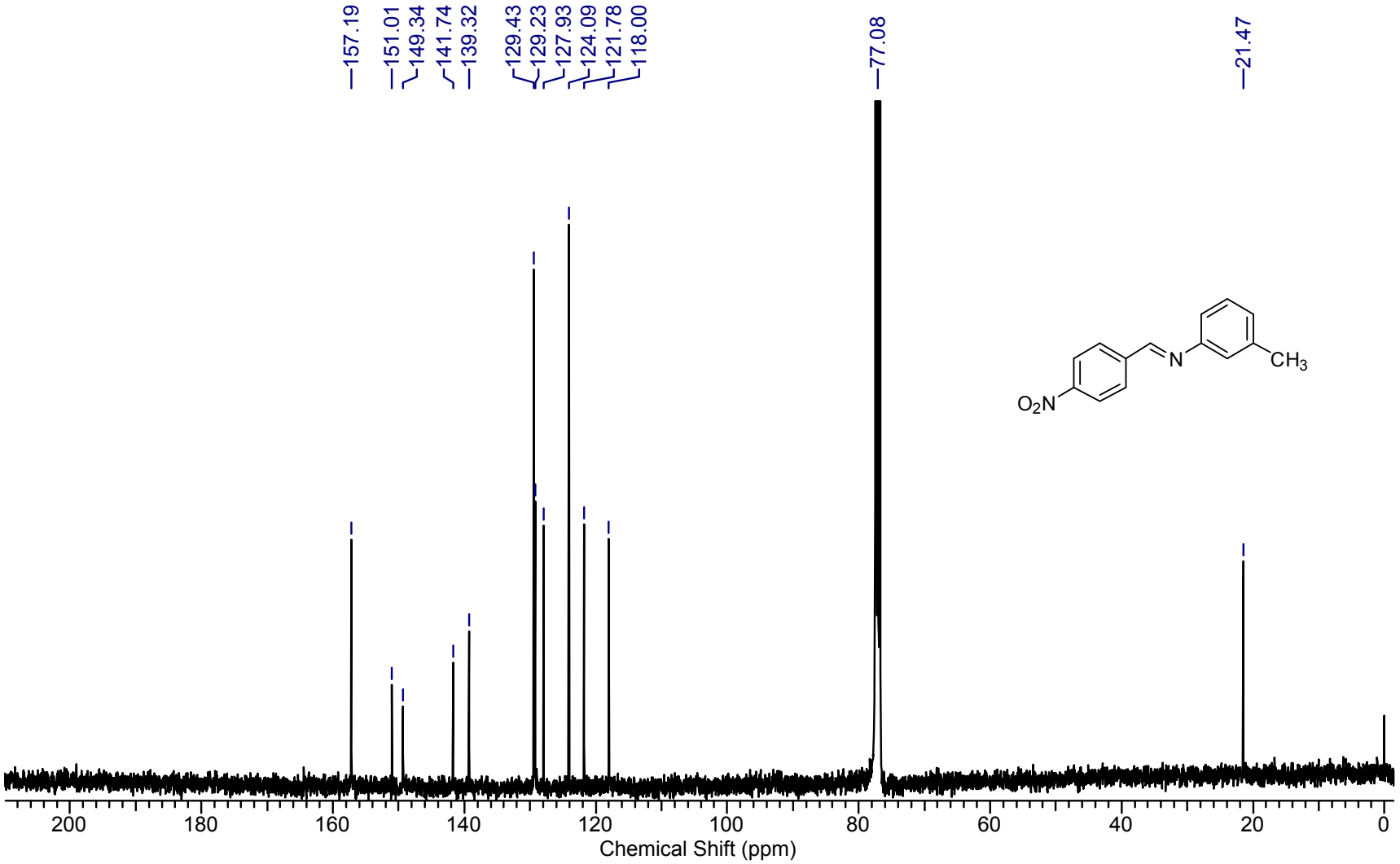

Supplementary Figure 48. ^{13}C NMR of **3bf**

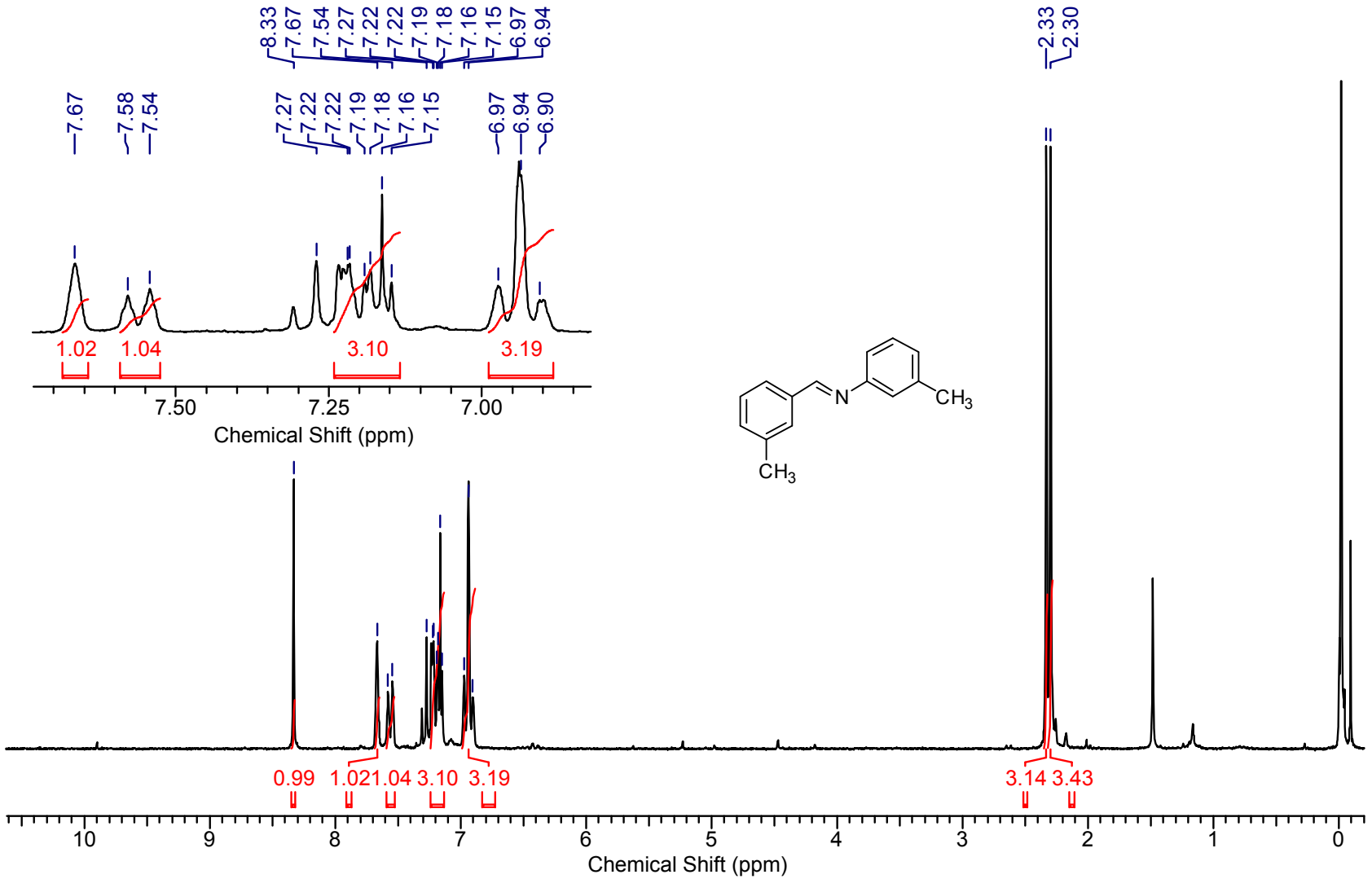

Supplementary Figure 49. ^{1}H NMR of **3bg**

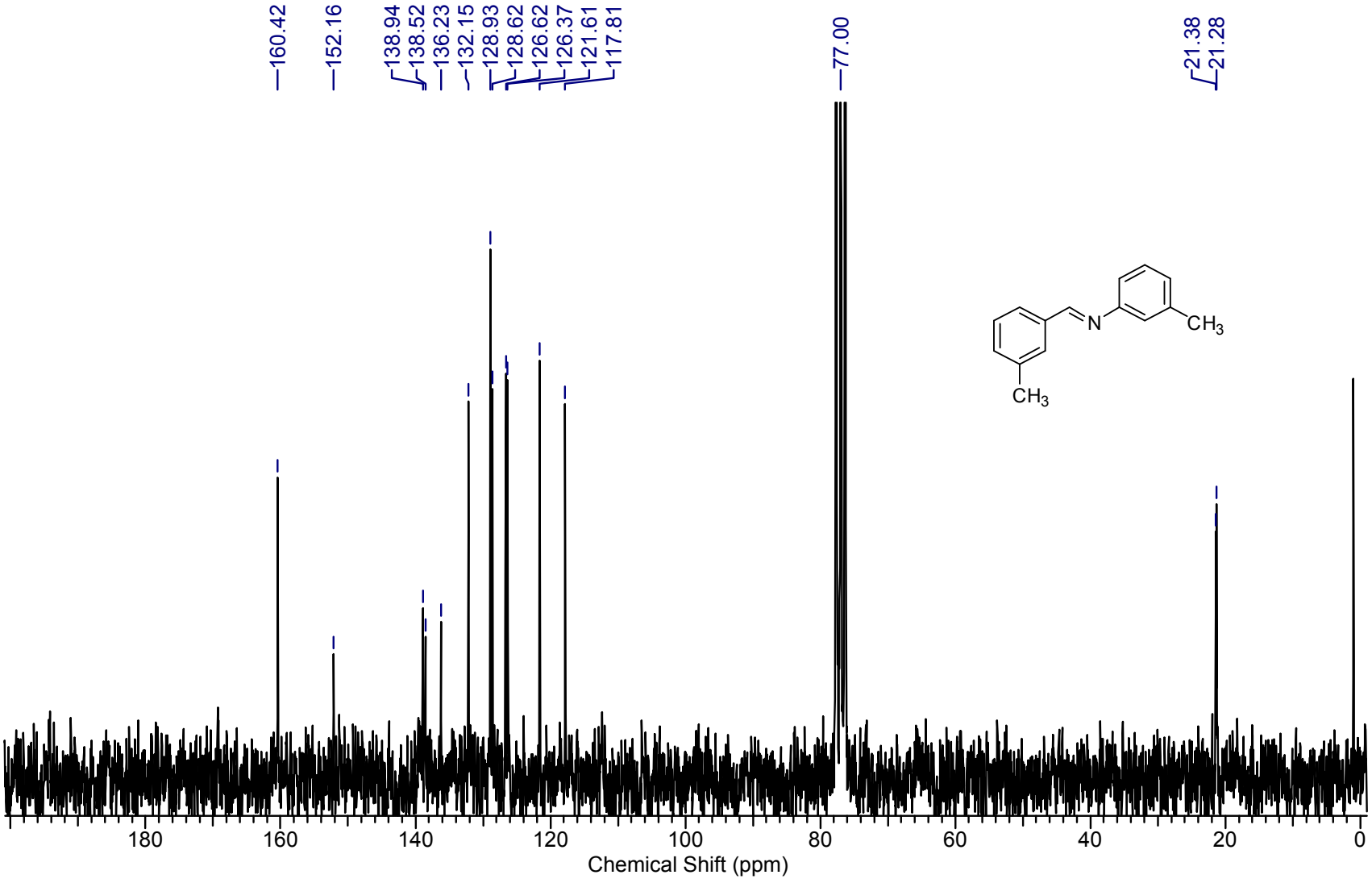

Supplementary Figure 50. ^{13}C NMR of **3bg**

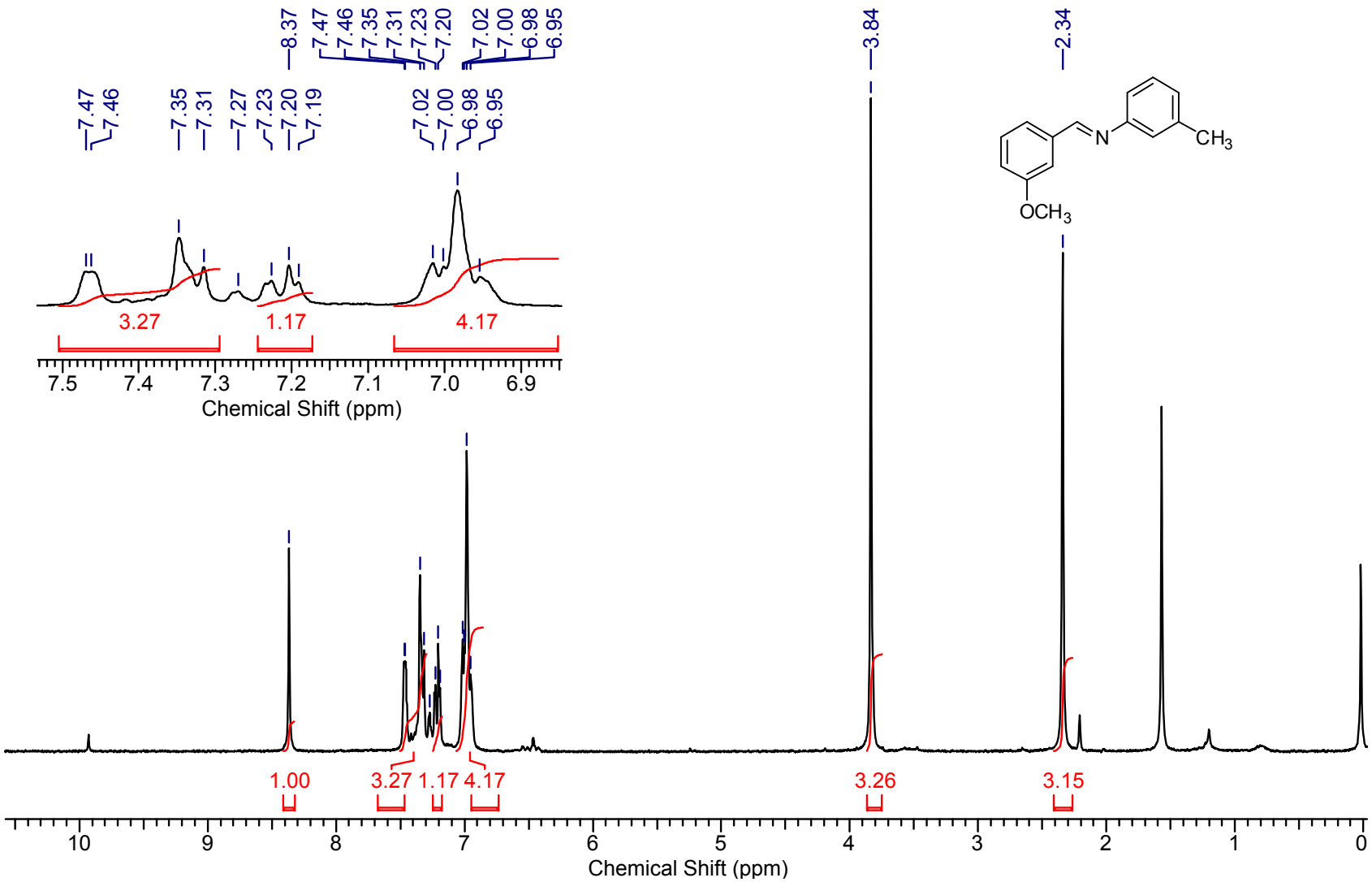

Supplementary Figure 51. ^{1}H NMR of **3bh**

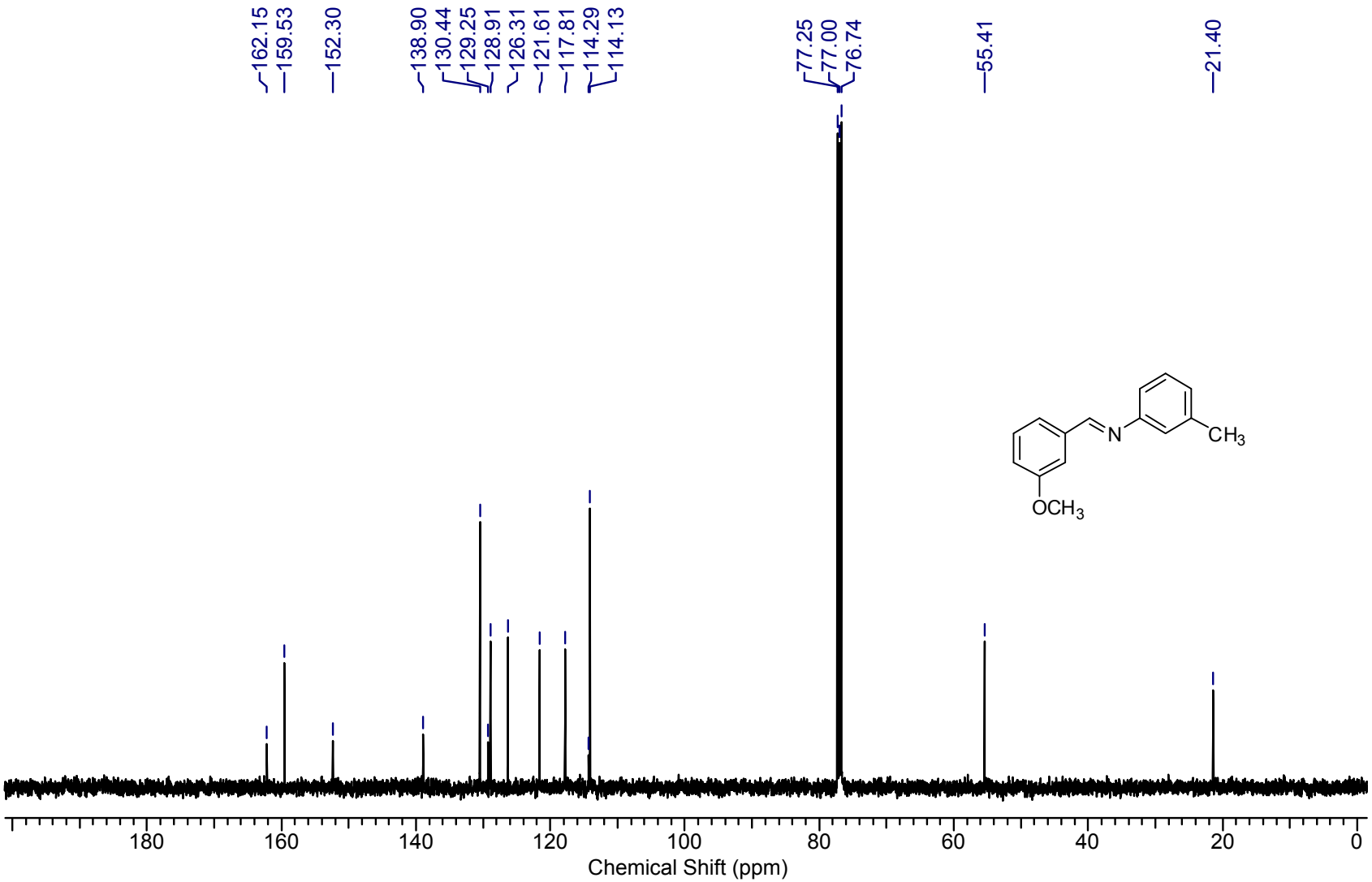

Supplementary Figure 52. ^{13}C NMR of **3bh**

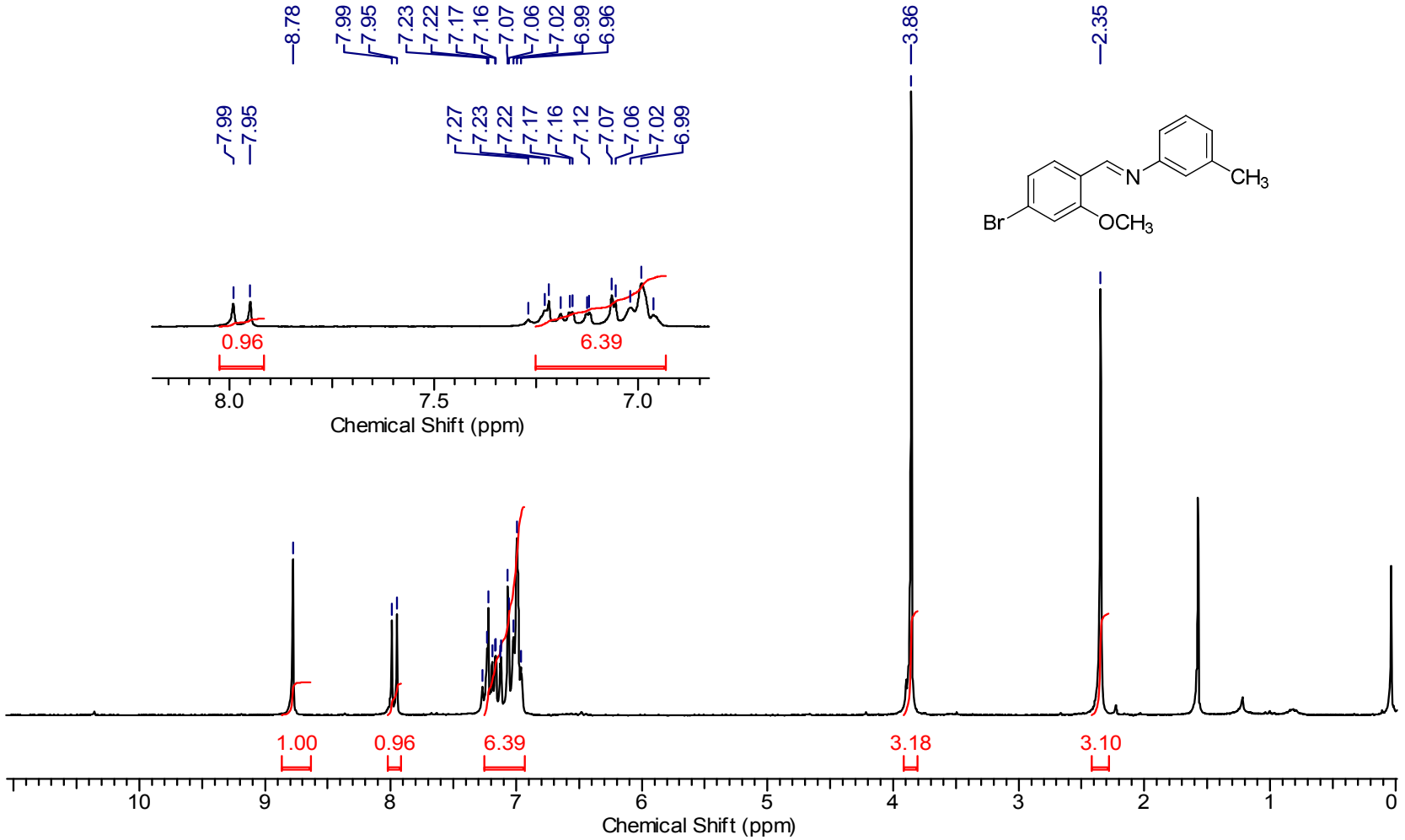

Supplementary Figure 53. ^{1}H NMR of **3bi**

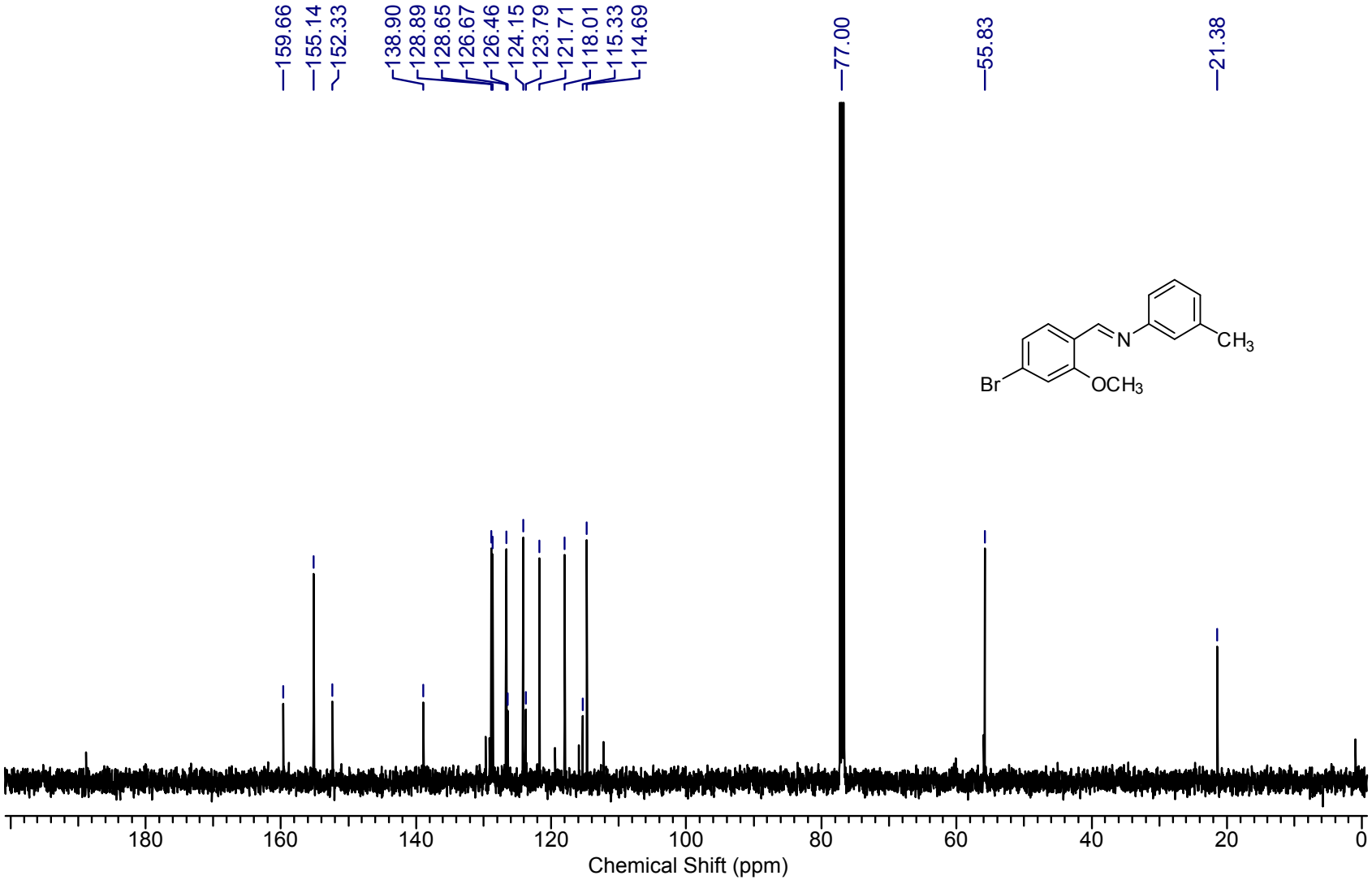

Supplementary Figure 54. ^{13}C NMR of **3bi**

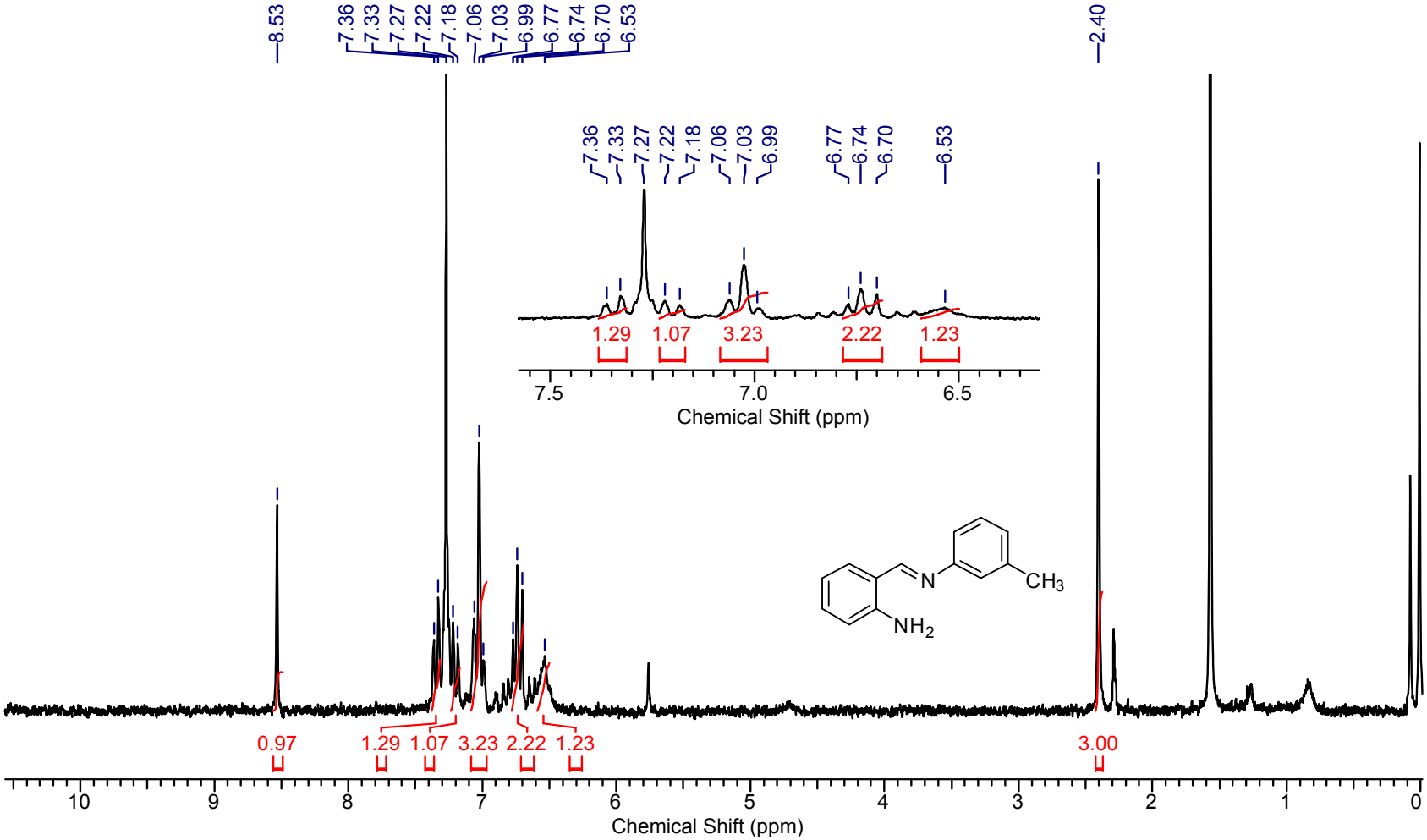

Supplementary Figure 55. ^{1}H NMR of

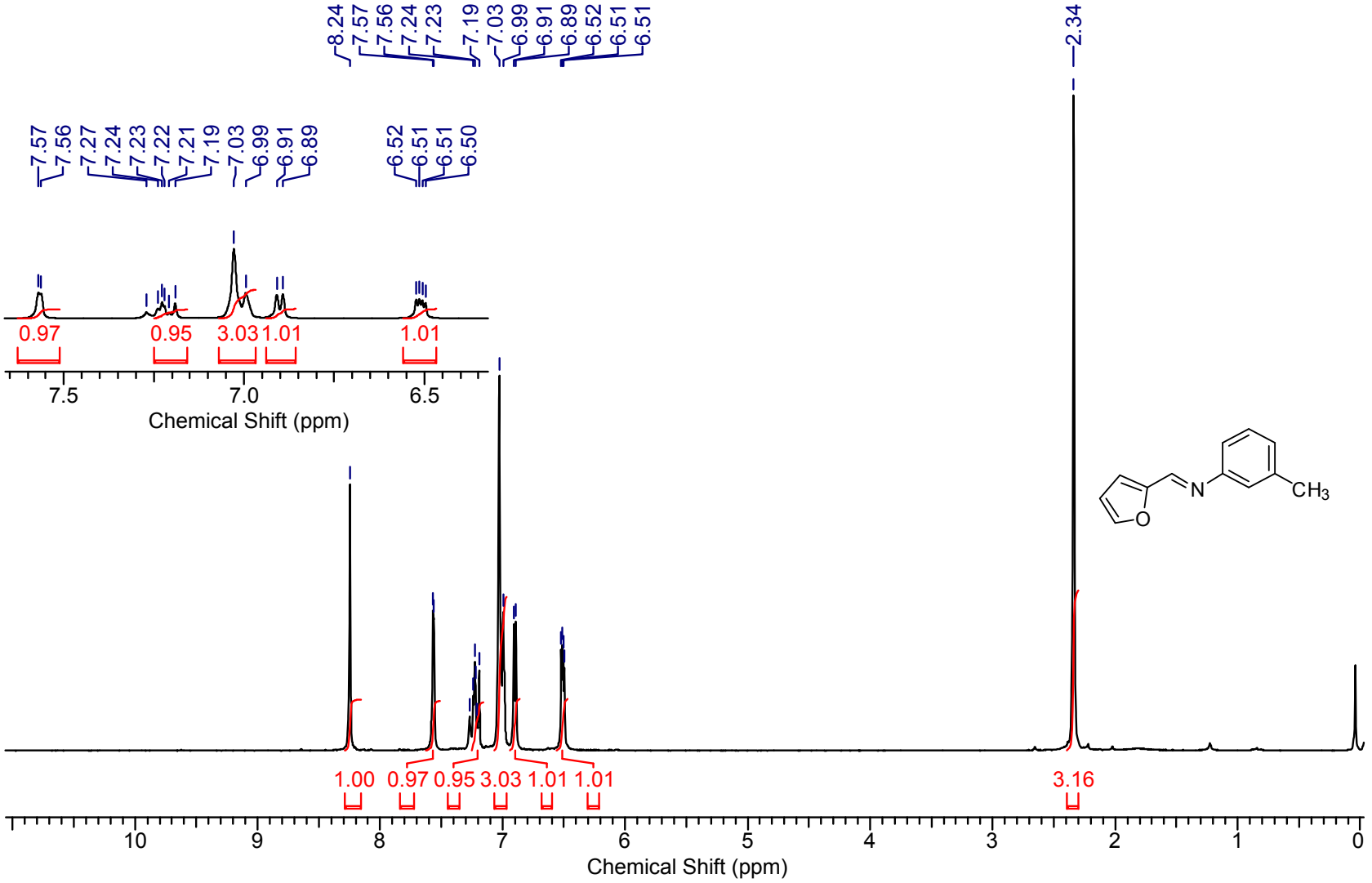

Supplementary Figure 56. ^{1}H NMR of **3bk**

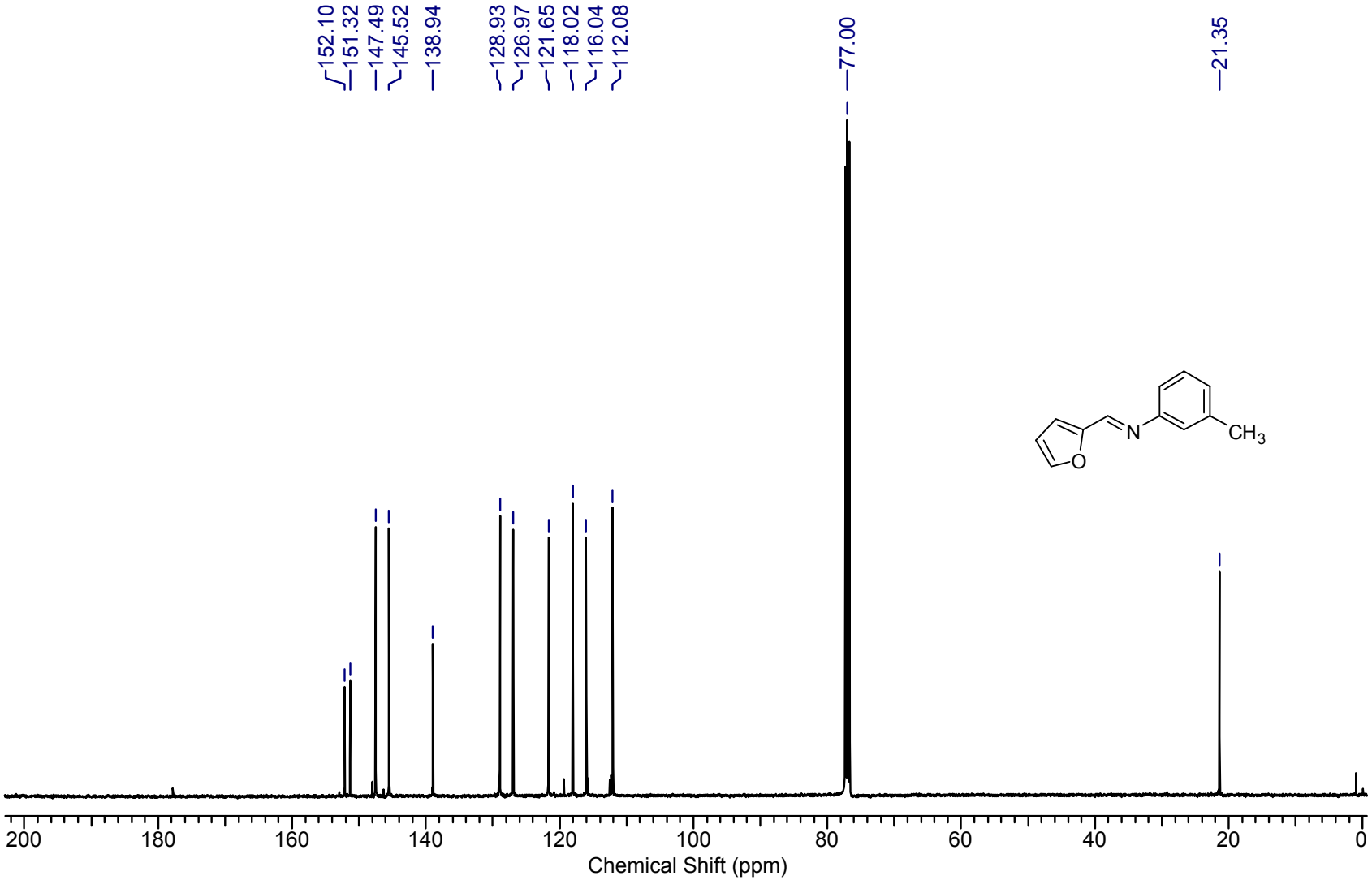

Supplementary Figure 57. ^{13}C NMR of **3bk**

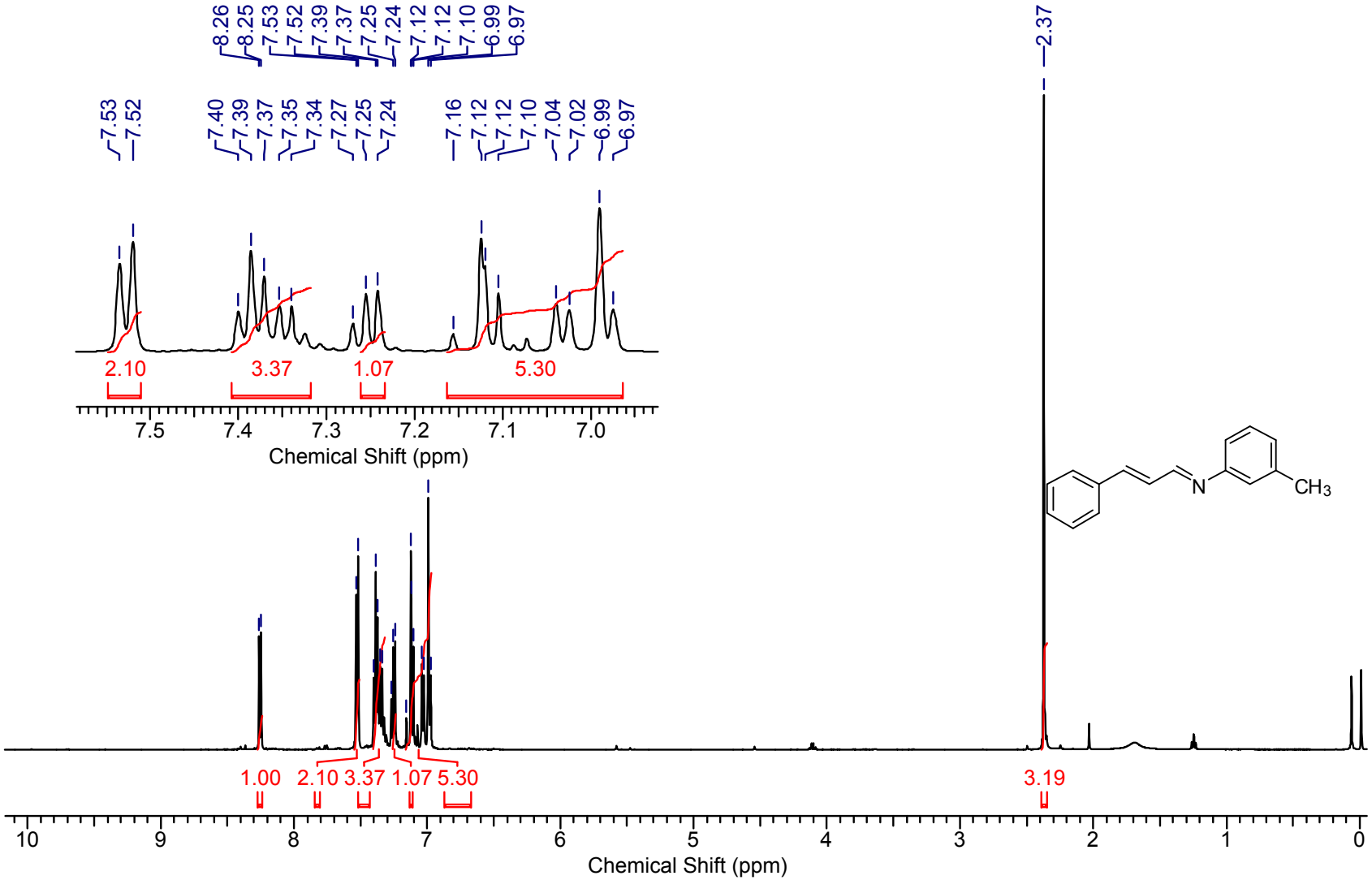

Supplementary Figure 58. ^{1}H NMR of **3bl**

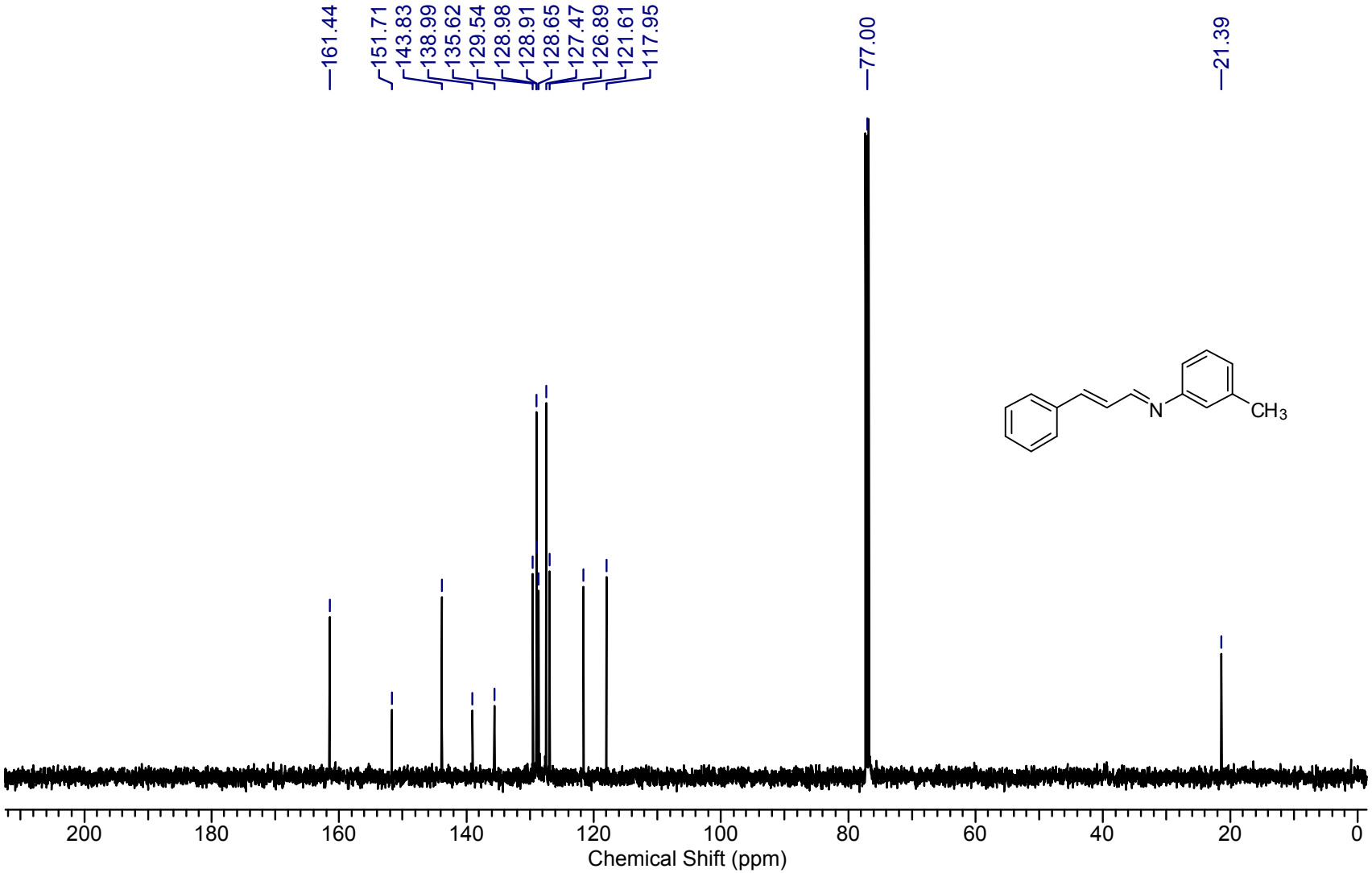

Supplementary Figure 59. 13C NMR of **3bl**

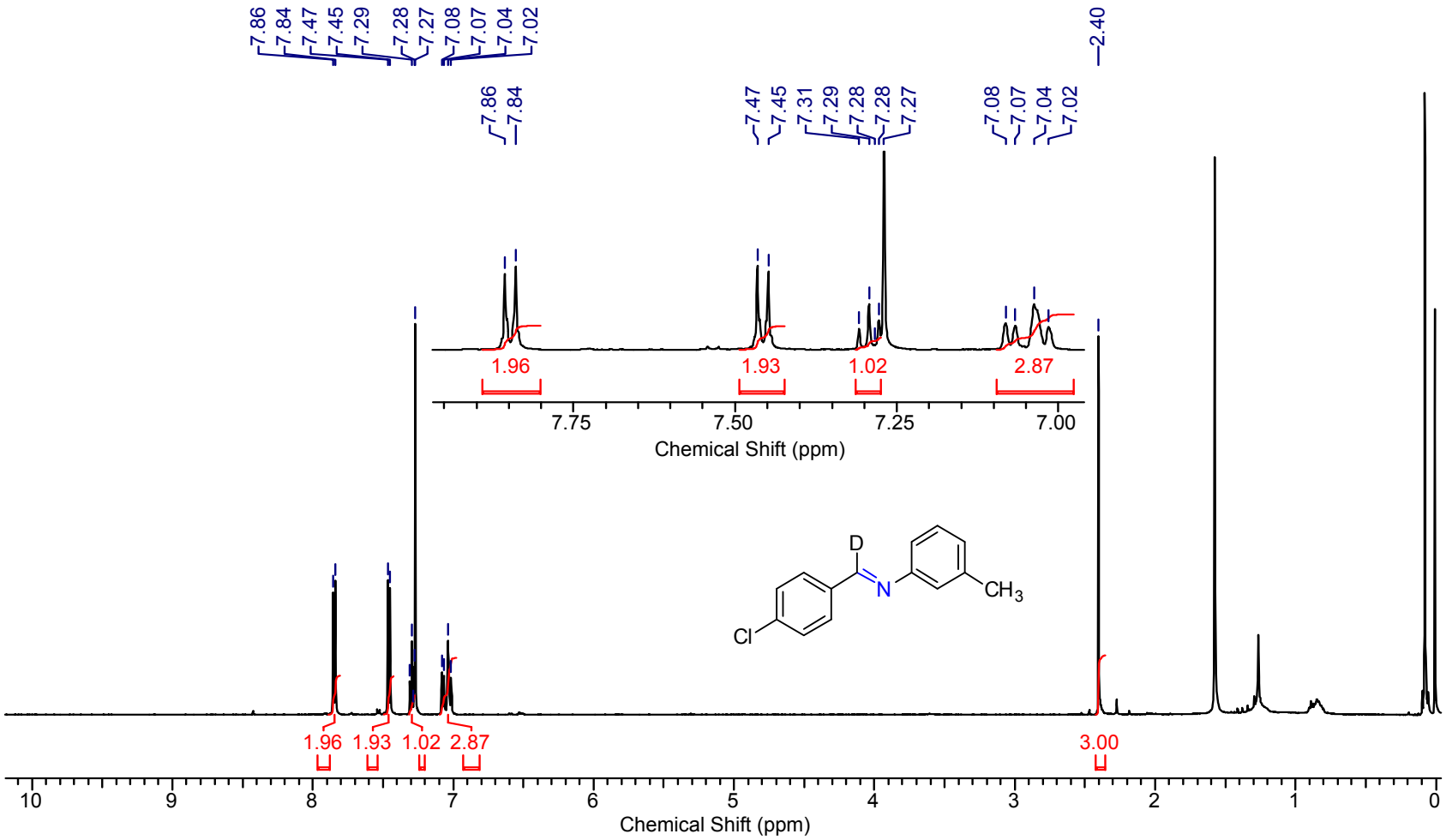

Supplementary Figure 60. ^{1}H NMR of **3aa-*d***